

# Sobolev Calibration of Imperfect Computer Models

Qingwen Zhang

Division of Emerging Interdisciplinary Areas,  
The Hong Kong University of Science and Technology

Wenjia Wang \*

Data Science and Analytics Thrust,  
The Hong Kong University of Science and Technology (Guangzhou)  
Department of Mathematics,  
The Hong Kong University of Science and Technology

## Abstract

Calibration refers to the statistical estimation of unknown model parameters in computer experiments, such that computer experiments can match underlying physical systems. This work develops a new calibration method for imperfect computer models, Sobolev calibration, which can rule out calibration parameters that generate overfitting calibrated functions. We prove that the Sobolev calibration enjoys desired theoretical properties including fast convergence rate, asymptotic normality and semiparametric efficiency. We also demonstrate an interesting property that the Sobolev calibration can bridge the gap between two influential methods:  $L_2$  calibration and Kennedy and O’Hagan’s calibration. In addition to exploring the deterministic physical experiments, we theoretically justify that our method can transfer to the case when the physical process is indeed a Gaussian process, which follows the original idea of Kennedy and O’Hagan’s. Numerical simulations as well as a real-world example illustrate the competitive performance of the proposed method.

## 1 Introduction

Computer experiments are widely adopted by scientists and engineers as a simplified mathematical representation of complex physical processes (Fang et al., 2005). The applications of computer experiments have been popularized to various fields, such as those in hydrology (White and Chaubey, 2005), biology (Cirovic et al., 2006), and weather prediction (Lynch, 2008). The mathematical models of computer experiments need to take *calibration parameter*  $\theta$  as an input, which often represents inherent attributes of physical environment, and is

---

\*Corresponding author: wenjiawang@ust.hk

difficult to measure with tools in reality (Kennedy and O’Hagan, 2001; Plumlee, 2017). The act of estimating the calibration parameters in the sense that matching physical observations to the largest extent is termed as *calibration*, which has been developed as a well-established area of statistics.

However, even with the best-tuned calibration parameters, the computer models may not align perfectly with physical experiments (Kennedy and O’Hagan, 2001). This is mainly because the mathematical forms of computer models are usually based on simplified assumptions (Tuo and Wu, 2015; Plumlee, 2017). Following Tuo and Wu (2015), we name the computer model with inadequacy issue as *imperfect*.

Kennedy and O’Hagan (2001) propose the first study to tackle model inadequacy issue by introducing the discrepancy function with the Gaussian process prior into a Bayesian calibration framework, known as Kennedy-O’Hagan calibration method (abbreviated as KO calibration). The landmark research inspired a lot of statisticians to explore under the Bayesian calibration framework (Higdon et al., 2004; Bayarri et al., 2007; Qian and Wu, 2008; Wang et al., 2009). Despite many successful applications under Bayesian framework, the identification issue remains a fundamentally weak spot, and may sabotage the empirical performance (Gu and Wang, 2018). Another branch of study is the frequentist framework of calibration, which tackles the problem by directly defining an identifiable calibration parameter in a discrepancy-minimal way. Tuo and Wu (2014, 2015) propose  $L_2$  calibration, which resorts to minimizing  $L_2$  distance between physical process and computer model as the identifiable definition of calibration parameter  $\theta_{L_2}^*$ . They prove that the estimate  $\hat{\theta}_{L_2}$  enjoys nice asymptotic properties including  $\sqrt{n}$ -consistency and semi-parametric efficiency under specific regularity conditions. Wong et al. (2017) propose a similar OLS-type calibration method under fixed design, which also enjoys fast rates of convergence. In addition to KO calibration and  $L_2$  calibration, many efforts are made to improve or generalize these two calibration methods (Plumlee, 2017; Gu and Wang, 2018; Plumlee, 2019; Xie and Xu, 2020; Plumlee et al., 2016; Sung et al., 2020; Farah et al., 2014; Gramacy et al., 2015; Joseph and Yan, 2015; Storlie et al., 2015).

Although KO calibration is a classical Bayesian method, its intrinsic nature can be examined by investigating its frequentist properties. Tuo and Wu (2014); Tuo et al. (2020) show that the KO calibration has a simplified frequentist version (they call it *frequentist KO calibration*), where the calibration parameter minimizes the distance between the physical and computer experiments, measured by the the norm in a Reproducing kernel Hilbert space (RKHS). The kernel is found identical to the one used in the kernel interpolator of discrepancy function. If the RKHS can be embedded into a Sobolev space with some smoothness  $m$ , the frequentist KO calibration actually emulates the system with a closer representation for the first and higher order of derivatives, which encourages function shape approximation. Compared to  $L_2$  calibration which ignores the function shape, this is a good property because building calibrated computer experiments that can approximate the shape of physical process well is indeed a practical need. As an illustration, in experiments involving self-driving cars, to ensure alignment with the physical driving track, the simulation system should strive to approximate both velocity (first-order derivative) and acceleration (second-order derivative). In addition to calibration problem, the idea that connects parameter estimation to smoothing techniques also holds crucial significance in fields like solving differential equations, as demonstrated in

Ramsay et al. (2007).

Despite the intriguing frequentist property of KO calibration, Tuo and Wu (2014) argues that the frequentist KO calibration can yield results that are far from minimal  $L_2$  distance. This is due to the fact that, once the kernel interpolator of the discrepancy function is decided by the user (where the smoothness can be large), the chosen over-smooth RKHS forces frequentist KO method to mimic the shape even at a cost of fairly large point-wise magnitude difference, as shown in Figure 1. In this work, we propose a novel statistical procedure of estimating calibration parameters, called Sobolev calibration, which can break the limitation of aforementioned two methods. Practitioners can select the calibration parameter by their own preference on the trade-off between magnitude approximation and shape approximation. Our proposed method can realize a more ideal calibrated experiment, as illustrated in Figure 1 with green line, which mirrors the shape of physical process with a tunable function value shift. We rigorously provide the theoretical guarantee of Sobolev calibration. Theoretical analysis shows that the Sobolev calibration not only enjoys the desirable properties as  $L_2$  calibration, including fast convergence rate, asymptotic normality, and semiparametric efficiency, but also bridges the gap between  $L_2$  calibration and frequentist KO calibration, in the sense that  $L_2$  calibration and frequentist KO calibration are special cases of the proposed Sobolev calibration.

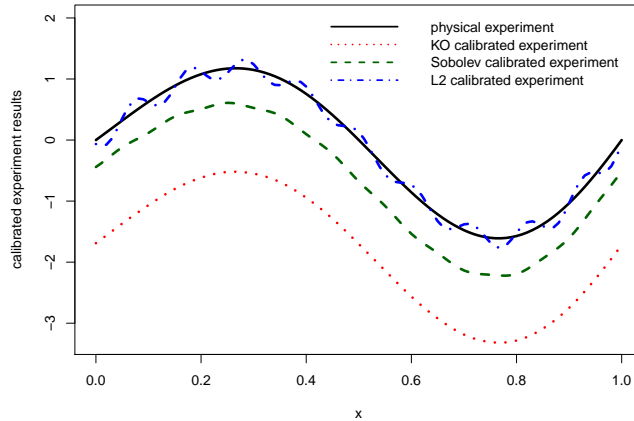


**Figure 1:** Visualization of the calibrated computer models in Example 1 of numerical experiments. The Sobolev calibration, the KO calibration, and the  $L_2$  calibration are presented in dotted lines, while the physical experiment is presented in a solid line.

In the aforementioned theoretical works of frequentist calibration methods, both the physical and computer experiments are assumed to be deterministic functions. In this work, to align with the original idea of KO calibration, we additionally study the scenario when the physical function is a random function following a Gaussian process and demonstrate the theoretical properties. Since the support of a Gaussian process is typically larger than the corresponding RKHS (van der Vaart and van Zanten, 2008), the theoretical development of Gaussian process based calibration is much different with that of the deterministic function based calibration; thus we believe it has its own interest.

The remainder of this paper is organized as follows. In Section 2, we formulate the Sobolev calibration method, and develop an efficient computing method for the optimization problem. In Section 3, we study asymptotic behavior of Sobolev calibration under deterministic case, discuss the uncertainty quantification and build a connection between Sobolev calibration and other two important calibration methods:  $L_2$  calibration and frequentist KO calibration. In Section 4, we explore the Sobolev calibration under the case when the underlying physical process admits Gaussian process, and show the asymptotic results. In Section 5, numerical examples and a real-world example are used to illustrate the performance of our proposed method. Concluding remarks are left in Section 6. Details of the proof, additional experiment results and discussion can be found in the supplement.

## 2 Sobolev Calibration

### 2.1 Background and Problem Settings

Let  $\Omega \subset \mathbb{R}^d$  denote the region of control variables, which is convex and compact. Suppose a physical system  $f_p(\mathbf{x})$  with  $\mathbf{x} \in \Omega$  is of interest. In order to study the response function  $f_p(\cdot)$ , physical experiments are conducted on a set of input points (or control variables)  $\mathbf{X}_n = \{\mathbf{x}_1, \dots, \mathbf{x}_n\} \subset \Omega$ . In physical experiments, the responses are usually corrupted by noise, which may come from the natural uncertainties inherent to the complex systems, such as actuating uncertainty, controller fluctuation, and measurement error. Therefore, we assume that we observe  $y_j^{(p)}$  on  $\mathbf{x}_j$ ,  $j = 1, \dots, n$ , with relationship

$$y_j^{(p)} = f_p(\mathbf{x}_j) + \varepsilon_j, \quad (2.1)$$

where  $\varepsilon_j$  are i.i.d. random variables with mean zero and finite variance. Model (2.1) has been widely considered in calibration problems; see Kennedy and O'Hagan (2001); Tuo and Wu (2015) for example.

In many situations, actual physical experimentation can be costly and difficult, so scientists and engineers use computer models to study a system of interest. Let  $f_s(\mathbf{x}, \boldsymbol{\theta})$  denote a computer model, where  $\mathbf{x} \in \Omega$  and  $\boldsymbol{\theta} \in \Theta$  with  $\Theta \subset \mathbb{R}^q$ . The space  $\Theta$  refers to the parameter space for the *calibration parameter*  $\boldsymbol{\theta}$ , and we assume that  $\Theta$  is a compact region in  $\mathbb{R}^q$ . Since computer models are constructed based on simplified assumptions, they rarely perfectly match the physical responses. One fundamental problem in computer experiments is *calibration*, where the goal is to find a calibration parameter such that the computer model can approximate the physical response well.

Kennedy and O'Hagan (2001) supposes that

$$f_p(\mathbf{x}) = f_s(\mathbf{x}, \boldsymbol{\theta}_0) + \delta_0(\mathbf{x}), \quad (2.2)$$

where  $\boldsymbol{\theta}_0$  is the true value of the calibration parameter. Kennedy and O'Hagan (2001) examines the statistical calibration problem by a Bayesian approach, where  $f_s(\cdot, \cdot)$  and  $\delta_0(\cdot)$  are assumed to be independent realizations of Gaussian processes. Then the calibration parameter is estimated via a Bayesian approach. However, from (2.2) it can be seen that  $\boldsymbol{\theta}_0$

is unidentifiable, because  $(\boldsymbol{\theta}_0, \delta_0(\cdot))$  cannot be uniquely determined. Therefore, it is crucial to define an *identifiable* calibration parameter in order to study the estimation problem. To this end, we rewrite the physical response  $f_p$  as

$$f_p(\mathbf{x}) = f_s(\mathbf{x}, \boldsymbol{\theta}) + \delta_{\boldsymbol{\theta}}(\mathbf{x}), \quad (2.3)$$

where  $\delta_{\boldsymbol{\theta}}$  is the discrepancy function. The identifiable definition of calibration parameter depends on the users' own criteria, and may not agree with each other.

One choice in the existing literature is the  $L_2$  calibration, which minimizes the  $L_2$  difference between  $f_p(\cdot)$  and  $f_s(\cdot, \boldsymbol{\theta})$ , as studied by Tuo and Wu (2014, 2015); Xie and Xu (2020). Consider the following example. Suppose we have two discrepancy functions  $\delta_1 = \sin(10\pi x)$  and  $\delta_2 = \sin(2\pi x)$  over  $\Omega = [0, 1]$ , as shown in Figure 2. Apparently, we have that  $\|\delta_1\|_{L_2(\Omega)} = \|\delta_2\|_{L_2(\Omega)} = \sqrt{1/2}$ , thus  $L_2$  calibration provides no informative judgement between the two functions. However, we can state that for a discrepancy function, less vibration is preferred, which makes  $\delta_2$  as a more desirable discrepancy function.

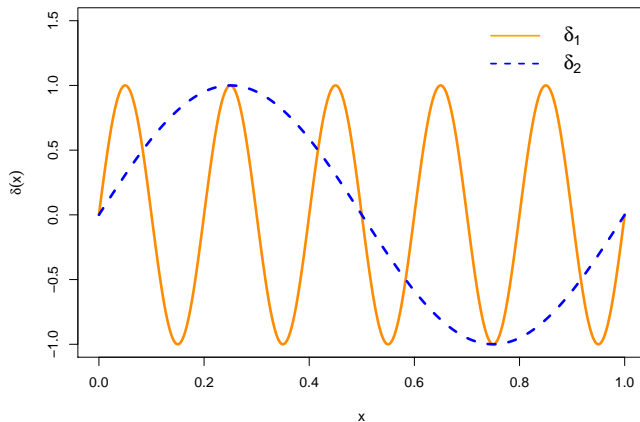


**Figure 2:** Visualization of  $\delta_1 = \sin(10\pi x)$  and  $\delta_2 = \sin(2\pi x)$  over  $\Omega = [0, 1]$ .

Motivated by the previous example, we propose a novel calibration method, *Sobolev calibration*, which generalizes the  $L_2$  calibration and KO calibration, and can be applied to controlling both the  $L_2$  norm and the vibration of the discrepancy function. Specifically, let  $W^m(\Omega)$  be a Sobolev space\* with smoothness  $m$ . Here  $m$  can be a non-integer, and the corresponding Sobolev space is called the *fractional Sobolev space* (Adams and Fournier, 2003). For details, we refer to Section B in the supplement. Let  $\mathcal{H}_m(\Omega)$  be a function space such that  $\mathcal{H}_m(\Omega) = W^m(\Omega)$  with equivalent norms. We provide the identifiable definition of calibration parameter as

$$\boldsymbol{\theta}_S^* = \operatorname{argmin}_{\boldsymbol{\theta} \in \Theta} \|f_p(\cdot) - f_s(\cdot, \boldsymbol{\theta})\|_{\mathcal{H}_m(\Omega)}, \quad (2.4)$$

\*Although a Sobolev space is typically defined on an open set, by extension and restriction theorems (DeVore and Sharpley, 1993; Rychkov, 1999), we can extend a Sobolev space on an open set to its closure.

where  $\|\cdot\|_{\mathcal{H}_m(\Omega)}$  is the norm of the space  $\mathcal{H}_m(\Omega)$ . We will discuss the selection of  $\mathcal{H}_m(\Omega)$  in Section 2.2.2. If  $m = 0$ , then  $W^m(\Omega)$  is equivalent to  $L_2(\Omega)$ , and (2.4) reduces to  $L_2$  calibration. In this work, we are interested in the statistical inference of  $\boldsymbol{\theta}_S^*$ .

**Remark 1.** *It can be shown that even for two discrepancy functions with the same  $L_2$  norm, the difference of their Sobolev norms can be unlimited large, which introduces more fluctuation, as shown in the following proposition.*

**Proposition 2.1.** *For any constants  $c > 0$  and  $m > d/2$ , there exist two discrepancy functions  $\delta_1, \delta_2 \in W^m(\Omega)$  with  $\frac{\|\delta_1\|_{W^m(\Omega)}}{\|\delta_2\|_{W^m(\Omega)}} > c$  while  $\|\delta_1\|_{L_2(\Omega)} = \|\delta_2\|_{L_2(\Omega)}$ .*

*This proposition implies that  $L_2$  calibration can choose functions with large Sobolev norm. Since large Sobolev norm indicates substantial fluctuation which leads to distortion of original shape, this can be considered as a type of over-calibrating that Sobolev calibration can avoid. On the other hand, in Sobolev calibration, since  $m$  can be flexibly chosen, it can be tuned or selected based on practitioners' needs, which avoids another risk that  $L_2$  distance exceeds the satisfying level caused by overlarge  $m$ . In that way, our proposed method would provide additional flexibility by finer level of calibration.*

## 2.2 Estimation of Calibration Parameter $\boldsymbol{\theta}_S^*$

### 2.2.1 Estimating $\boldsymbol{\theta}_S^*$ via a two-step approach

With an appropriate selection of  $\mathcal{H}_m(\Omega)$  that is equivalent to  $W^m(\Omega)$  (the selection of  $\mathcal{H}_m(\Omega)$  is to be introduced in Section 2.2.2), one can estimate  $\boldsymbol{\theta}_S^*$  defined in (2.4) based on the observations  $(\mathbf{x}_j, y_j^{(p)})$  of the physical experiments and the computer models  $f_s(\cdot, \boldsymbol{\theta})$ . Following  $L_2$  calibration, we adopt a two-step approach. That is, we first estimate  $f_p(\cdot)$  via some estimator, and then minimize the discrepancy between the estimated physical process and the surrogate model of computer code. Among theoretical developments in frequentist calibration literature, it is typical to assume that  $f_p(\cdot)$  is a *deterministic function* (Tuo and Wu, 2014, 2015; Plumlee, 2017; Sung et al., 2020; Tuo, 2019; Xie and Xu, 2020). For the ease of presentation, let us focus on the scenario that  $f_p(\cdot)$  is a deterministic function in this section and Section 3. We will consider the scenario where  $f_p(\cdot)$  is a Gaussian process, which is similar to the original idea of KO, in Section 4.

If  $f_p(\cdot)$  is a deterministic function, one widely used approach to recover  $f_p(\cdot)$  is *kernel ridge regression* (Wahba, 1990). Let  $\Phi(\cdot, \cdot)$  be a symmetric and positive definite function and  $\mathcal{N}_\Phi(\Omega)$  be an RKHS generated by  $\Phi$ . For an introduction to RKHSs, we refer to Section B in the supplement. An estimator of  $f_p(\cdot)$  via kernel ridge regression is given by

$$\widehat{f}_p(\cdot) := \operatorname{argmin}_{f \in \mathcal{N}_\Phi(\Omega)} \frac{1}{n} \sum_{j=1}^n \left( y_j^{(p)} - f(\mathbf{x}_j) \right)^2 + \lambda \|f\|_{\mathcal{N}_\Phi(\Omega)}^2, \quad (2.5)$$

where  $\|\cdot\|_{\mathcal{N}_\Phi(\Omega)}$  is the RKHS norm, and  $\lambda$  is the smoothing parameter that can be chosen by certain criterion, for example, generalized cross validation (Wahba, 1990). It follows from the

representer theorem (Schölkopf and Smola, 2002) that the optimal solution to (2.5) is

$$\widehat{f}_p(\cdot) = \mathbf{r}(\cdot)^\top (\mathbf{R} + n\lambda \mathbf{I}_n)^{-1} \mathbf{y}^{(p)}, \quad (2.6)$$

where  $\mathbf{r}(\cdot) = (\Phi(\cdot, \mathbf{x}_1), \dots, \Phi(\cdot, \mathbf{x}_n))^\top$ ,  $\mathbf{R} = (\Phi(\mathbf{x}_j, \mathbf{x}_k))_{j,k} \in \mathbb{R}^{n \times n}$ ,  $\mathbf{y}^{(p)} = (y_1^{(p)}, \dots, y_n^{(p)})^\top$ , and  $\mathbf{I}_n \in \mathbb{R}^{n \times n}$  is an identity matrix. Since the physical experiments are limited,  $n$  is not large and the closed form (2.6) can be computed efficiently, which is one reason why kernel ridge regression is popular in practice.

The Sobolev calibration estimates  $\boldsymbol{\theta}_S^*$  by

$$\widehat{\boldsymbol{\theta}}_S = \operatorname{argmin}_{\boldsymbol{\theta} \in \Theta} \|\widehat{f}_p(\cdot) - \widehat{f}_s(\cdot, \boldsymbol{\theta})\|_{\mathcal{H}_m(\Omega)}, \quad (2.7)$$

where  $\widehat{f}_s(\cdot, \boldsymbol{\theta})$  is a surrogate model (which is usually an approximation of  $f_s(\cdot, \boldsymbol{\theta})$ ) for the computer model  $f_s(\cdot, \boldsymbol{\theta})$ . Typically, computing  $\widehat{f}_s(\cdot, \boldsymbol{\theta})$  is much faster than computing  $f_s(\cdot, \boldsymbol{\theta})$  (such computer experiment  $f_s(\cdot, \boldsymbol{\theta})$  is called *expensive*), otherwise we can directly use  $f_s(\cdot, \boldsymbol{\theta})$  (such computer experiment  $f_s(\cdot, \boldsymbol{\theta})$  is called *cheap*). We also assume that the approximation error of computer experiment is much smaller compared to that of physical experiments, which is reasonable considering the cost of conducting computer experiments is lower than the physical experiments in general. Several methods for constructing surrogate models include Gaussian process modeling (Santner et al., 2003), scattered data approximation (Wendland, 2004), and polynomial chaos approximation (Xiu, 2010).

### 2.2.2 Selection of Function Space $\mathcal{H}_m(\Omega)$

In order to define and estimate  $\boldsymbol{\theta}_S^*$  in (2.4), we need to specify the function space  $\mathcal{H}_m(\Omega)$ . We provide three approaches for selecting  $\mathcal{H}_m(\Omega)$  as follows. Again, we would like to note that since the identifiable definition of calibration parameter depends on the users' own criteria, the choice of the function space is also up to users' specific application.

**Approach 1: Setting  $\mathcal{H}_m(\Omega)$  as a Sobolev space.** If  $m$  is a positive integer, one can compute the Sobolev norm by

$$\|f\|_{\mathcal{H}_m(\Omega)}^2 = \sum_{|\alpha| \leq m} \left( \int_{\Omega} |D^\alpha f(\mathbf{x})|^2 d\mathbf{x} \right),$$

where  $D^\alpha f$  is the weak derivative of  $f$ . This approach is also considered by Plumlee (2017), but asymptotic theory of calibration parameter is lacking. This approach, albeit its easy computation when  $m$  is a positive integer, cannot be easily generalized to the case where  $m$  is not a positive integer.

**Approach 2: Setting  $\mathcal{H}_m(\Omega)$  as an RKHS generated by a Matérn kernel function.** Let  $\Psi_m$  be the (isotropic) Matérn family (Stein, 1999). After a proper reparametrization, the Matérn kernel function with  $m > d/2$  is defined as

$$\Psi_m(\mathbf{x}) = \frac{1}{\Gamma(m - d/2) 2^{m-d/2-1}} \|\mathbf{x}\|_2^{m-d/2} B_{m-d/2}(\|\mathbf{x}\|_2), \quad (2.8)$$

where  $\|\cdot\|_2$  is the Euclidean distance, and  $B_{m-d/2}$  is the modified Bessel function of the second kind. It can be shown that the Sobolev norm  $W^m(\Omega)$  is equivalent to  $\mathcal{N}_{\Psi_m}(\Omega)$ ; see Corollary 10.48 of Wendland (2004). Therefore, if  $m > d/2$ , it is natural to choose  $\mathcal{H}_m(\Omega)$  in (2.4) as  $\mathcal{N}_{\Psi_m}(\Omega)$ .

**Approach 3: Setting  $\mathcal{H}_m(\Omega)$  as a power of an RKHS.** Approach 2 only works when the smoothness  $m$  is larger than  $d/2$ . Therefore, we provide another approach for constructing  $\mathcal{H}_m(\Omega)$  such that  $\mathcal{H}_m(\Omega) = W^m(\Omega)$  and two norms are equivalent, which works for all  $m \geq 0$ . This approach relies on the *powers of RKHSs*.

Let  $\mathcal{K}_{m^*}(\cdot, \cdot)$  be a symmetric kernel function such that the RKHS  $\mathcal{N}_{\mathcal{K}_{m^*}}(\Omega)$  coincides  $W^{m^*}(\Omega)$  with  $m^* > d/2$ , and  $m^*$  is an integer. Such kernel function exists. For example, we can take  $\mathcal{K}_{m^*}(\cdot, \cdot) = \Psi_{m^*}(\cdot - \cdot)$ , where  $\Psi_{m^*}(\cdot - \cdot)$  is as defined in (2.8). Since  $\mathcal{K}_{m^*}(\cdot, \cdot)$  is positive definite, Mercer's theorem implies that it possesses an absolutely and uniformly convergent representation as

$$\mathcal{K}_{m^*}(\mathbf{s}, \mathbf{t}) = \sum_{j=1}^{\infty} \gamma_{\mathcal{K},j} e_j(\mathbf{s}) e_j(\mathbf{t}), \forall \mathbf{s}, \mathbf{t} \in \Omega, \quad (2.9)$$

where  $\gamma_{\mathcal{K},j}$  and  $e_j$  are eigenvalues and eigenfunctions of  $\mathcal{K}_{m^*}(\cdot, \cdot)$ , respectively. The following definition can be found in Steinwart and Scovel (2012); Kanagawa et al. (2018). See Definition 4.11 of Kanagawa et al. (2018) for example.

**Definition 1** (Powers of RKHS). Let  $0 \leq \beta \leq 1$  be a constant, and assume that  $\sum_{j=1}^{\infty} \gamma_{\mathcal{K},j}^{\beta} e_j(\mathbf{s})^2 < \infty$  for all  $\mathbf{s} \in \Omega$ , where  $\gamma_{\mathcal{K},j}$  and  $e_j$  are as in (2.9). Then the  $\beta$ -th power of RKHS  $\mathcal{N}_{\mathcal{K}_{m^*}}(\Omega)$  is defined as

$$\mathcal{N}_{\mathcal{K}_{m^*}}^{\beta}(\Omega) = \left\{ f(\cdot) = \sum_{j=1}^{\infty} a_j \gamma_{\mathcal{K},j}^{\beta/2} e_j(\cdot) : \sum_{j=1}^{\infty} a_j^2 < \infty \right\}, \quad (2.10)$$

with inner product defined as

$$\langle f, g \rangle_{\mathcal{N}_{\mathcal{K}_{m^*}}^{\beta}(\Omega)} = \sum_{j=1}^{\infty} a_j b_j, \text{ for } f(\cdot) = \sum_{j=1}^{\infty} a_j \gamma_{\mathcal{K},j}^{\beta/2} e_j(\cdot), g(\cdot) = \sum_{j=1}^{\infty} b_j \gamma_{\mathcal{K},j}^{\beta/2} e_j(\cdot), f, g \in \mathcal{N}_{\mathcal{K}_{m^*}}^{\beta}(\Omega).$$

The  $\beta$ -th power of kernel function  $\mathcal{K}_{m^*}(\cdot, \cdot)$  is defined by

$$\mathcal{K}_{m^*}^{\beta}(\mathbf{s}, \mathbf{t}) = \sum_{j=1}^{\infty} \gamma_{\mathcal{K},j}^{\beta} e_j(\mathbf{s}) e_j(\mathbf{t}), \forall \mathbf{s}, \mathbf{t} \in \Omega.$$

By selecting  $\beta = m/m^*$  and  $\mathcal{H}_m(\Omega)$  as  $\mathcal{N}_{\mathcal{K}_{m^*}}^{\beta}(\Omega)$ , it can be shown that  $\mathcal{N}_{\mathcal{K}_{m^*}}^{\beta}(\Omega) = W^m(\Omega)$  with equivalent norms. For more details, we refer to Section D in the supplement. In particular, it can be seen that when  $m > d/2$ , the two norms in the objective functions of Approaches 2 and 3 are equivalent. We note that in practice, the kernel functions of Approaches 2 and 3 can have some adjusted parameters, e.g., scale parameter. These parameters can be tuned by practitioners for their own use. We numerically investigate the influence of the scale parameters in Section 5.1.2.



### 2.2.3 Computation

If we choose Approach 1 to select  $\mathcal{H}_m(\Omega)$ , and  $m$  is a positive integer, the Sobolev norm can be directly calculated by  $\|\widehat{f}_p(\cdot) - \widehat{f}_s(\cdot, \boldsymbol{\theta})\|_{\mathcal{H}_m(\Omega)}^2 = \sum_{|\alpha| \leq m} \left( \int_{\Omega} \left| D^\alpha \left( \widehat{f}_p(\mathbf{x}) - \widehat{f}_s(\mathbf{x}, \boldsymbol{\theta}) \right) \right|^2 d\mathbf{x} \right)$ .

If we choose Approach 2 or Approach 3 as stated in Section 2.2.2 to select  $\mathcal{H}_m(\Omega)$ , there is no exact solution to compute  $\|\widehat{f}_p(\cdot) - \widehat{f}_s(\cdot, \boldsymbol{\theta})\|_{\mathcal{H}_m(\Omega)}$ . Therefore, we approximate  $\|\widehat{f}_p(\cdot) - \widehat{f}_s(\cdot, \boldsymbol{\theta})\|_{\mathcal{H}_m(\Omega)}$  by the following approach. Let  $\mathcal{K}_m(\cdot, \cdot)$  be the kernel function of  $\mathcal{H}_m(\Omega)$ . In order to approximate  $\mathcal{H}_m(\Omega)$ , we first draw  $N$  uniformly distributed points on  $\Omega$ , denoted by  $\widetilde{\mathbf{X}} = \{\widetilde{\mathbf{x}}_1, \dots, \widetilde{\mathbf{x}}_N\}$ . Suppose we observe  $g(\widetilde{\mathbf{x}}_1, \boldsymbol{\theta}), \dots, g(\widetilde{\mathbf{x}}_N, \boldsymbol{\theta})$  on  $\widetilde{\mathbf{X}}$ , where  $g(\cdot, \boldsymbol{\theta}) := \widehat{f}_p(\cdot) - \widehat{f}_s(\cdot, \boldsymbol{\theta})$ . Define  $\mathcal{I}_{\mathcal{K}_m, \widetilde{\mathbf{X}}} g(\cdot, \boldsymbol{\theta}) = \widetilde{\mathbf{r}}(\cdot)^T \widetilde{\mathbf{R}}^{-1} \widetilde{\mathbf{g}}_{\boldsymbol{\theta}}$ , where  $\widetilde{\mathbf{r}}(\cdot) = (\mathcal{K}_m(\cdot, \widetilde{\mathbf{x}}_1), \dots, \mathcal{K}_m(\cdot, \widetilde{\mathbf{x}}_N))^T$ ,  $\widetilde{\mathbf{R}} = (\mathcal{K}_m(\widetilde{\mathbf{x}}_j, \widetilde{\mathbf{x}}_k))_{j,k} \in \mathbb{R}^{N \times N}$ , and  $\widetilde{\mathbf{g}}_{\boldsymbol{\theta}} = (g(\widetilde{\mathbf{x}}_1, \boldsymbol{\theta}), \dots, g(\widetilde{\mathbf{x}}_N, \boldsymbol{\theta}))^T$ . Then we have that  $\|\mathcal{I}_{\mathcal{K}_m, \widetilde{\mathbf{X}}} g(\cdot, \boldsymbol{\theta})\|_{\mathcal{H}_m(\Omega)}$  is a good approximation of  $\|g(\cdot, \boldsymbol{\theta})\|_{\mathcal{H}_m(\Omega)}$  (For theoretical justification of this statement, see Section C in the supplement). Therefore,  $\widehat{\boldsymbol{\theta}}_S$  in (2.7) can be approximated by  $\widetilde{\boldsymbol{\theta}}_S = \operatorname{argmin}_{\boldsymbol{\theta} \in \Theta} \|\mathcal{I}_{\mathcal{K}_m, \widetilde{\mathbf{X}}} g(\cdot, \boldsymbol{\theta})\|_{\mathcal{H}_m(\Omega)}^2 = \operatorname{argmin}_{\boldsymbol{\theta} \in \Theta} \widetilde{\mathbf{g}}_{\boldsymbol{\theta}}^T \widetilde{\mathbf{R}}^{-1} \widetilde{\mathbf{g}}_{\boldsymbol{\theta}}$ .

In  $L_2$  calibration, the objective function can be directly approximated via the empirical  $l_2$  norm. The estimated calibration parameter in  $L_2$  calibration, denoted by  $\widehat{\boldsymbol{\theta}}_{L_2}$ , can be approximated by  $\widetilde{\boldsymbol{\theta}}_{L_2} = \operatorname{argmin}_{\boldsymbol{\theta} \in \Theta} \frac{1}{N} \sum_{j=1}^N \left( \widehat{f}_p(\widetilde{\mathbf{x}}_j) - \widehat{f}_s(\widetilde{\mathbf{x}}_j, \boldsymbol{\theta}) \right)^2$ . When  $\widetilde{\mathbf{R}} = c \cdot I_{N \times N}$ , we have  $\widetilde{\boldsymbol{\theta}}_S = \operatorname{argmin}_{\boldsymbol{\theta} \in \Theta} \widetilde{\mathbf{g}}_{\boldsymbol{\theta}}^T \widetilde{\mathbf{g}}_{\boldsymbol{\theta}} = \widetilde{\boldsymbol{\theta}}_{L_2}$ , which indicates that there is a natural connection between the Sobolev calibration and  $L_2$  calibration. The rigorous development of the connection will be given in Section 3.3.

**Remark 2.** One may also solve  $\operatorname{argmin}_{\boldsymbol{\theta} \in \Theta} \mathbf{g}_{\boldsymbol{\theta}}^T \mathbf{R}^{-1} \mathbf{g}_{\boldsymbol{\theta}}$  to approximate  $\widehat{\boldsymbol{\theta}}_S$ , where  $\mathbf{g}_{\boldsymbol{\theta}} = (g(\mathbf{x}_1, \boldsymbol{\theta}), \dots, g(\mathbf{x}_n, \boldsymbol{\theta}))^T$  and  $\mathbf{R} = (\mathcal{K}_m(\mathbf{x}_j, \mathbf{x}_k))_{j,k} \in \mathbb{R}^{n \times n}$ , i.e., use the empirical RKHS norm based on the original data. However, it has been shown in Tuo and Wu (2014) that the empirical  $L_2$  calibration is not semiparametric efficient. Therefore, we do not consider using the empirical RKHS norm to estimate  $\boldsymbol{\theta}_S^*$  in the present work.

## 3 Theoretical Properties of the Sobolev Calibration

In this section, we discuss the asymptotic behavior of  $\widehat{\boldsymbol{\theta}}_S$  in (2.7). In the rest of this work, the following definitions are used. For two positive sequences  $a_n$  and  $b_n$ , we write  $a_n \asymp b_n$  if, for some constants  $C, C' > 0$ ,  $C \leq a_n/b_n \leq C'$ . We use  $C, C', c_j, C_j, j \geq 0$  to denote generic positive constants, of which value can change from line to line. We assume that the observed points  $\mathbf{x}_1, \dots, \mathbf{x}_n$  are uniformly distributed on  $\Omega$ , while we point out that our theory can be easily generalized to the case that  $\mathbf{x}_j$ 's are independently drawn from a distribution with a density that is bounded away from zero and infinity. Such an extension may make mathematical development more involved, and may dilute our main focus in this work. We focus on the case that  $\mathcal{H}_m(\Omega)$  is an RKHS generated by a symmetric kernel function  $\mathcal{K}_m(\cdot, \cdot)$ , which can be ensured if we apply Approach 2 or Approach 3 as stated in Section 2.2.2. Recall that  $\widehat{f}_p(\cdot)$ ,  $\widehat{f}_s(\cdot, \boldsymbol{\theta})$ , and  $\boldsymbol{\theta}_S$  can depend on  $n$ , where the dependency is suppressed for notational simplicity.

### 3.1 Asymptotic Results of the Sobolev Calibration

In this section, we show that the proposed Sobolev calibration enjoys some nice properties as  $L_2$  calibration, including: 1) The estimated  $\widehat{\boldsymbol{\theta}}_S$  is consistent; 2) The convergence rate of  $\widehat{\boldsymbol{\theta}}_S$  is  $\|\widehat{\boldsymbol{\theta}}_S - \boldsymbol{\theta}_S^*\|_2 = O_{\mathbb{P}}(n^{-1/2})$ ; 3)  $\sqrt{n}(\widehat{\boldsymbol{\theta}}_S - \boldsymbol{\theta}_S^*)$  is asymptotic normal; 4) The Sobolev calibration is semiparametric efficient. For the brevity of this paper, we move all the conditions to Section E of the supplement, while we point out that we consider the case where the computer model can even be *rougher* than the physical model at some parameter space of  $\boldsymbol{\theta}$ , which has not been presented in the literature as far as we know.

We start with the consistency of the estimated calibration parameter  $\widehat{\boldsymbol{\theta}}_S$  as stated in the following proposition, whose proof is provided in Section G.2 of the supplement.

**Proposition 3.1** (Consistency of  $\widehat{\boldsymbol{\theta}}_S$ ). *Suppose Conditions (C2), (C4) and (C6) are fulfilled. The estimated calibration parameter  $\widehat{\boldsymbol{\theta}}_S$  is a consistent estimator of  $\boldsymbol{\theta}_S^*$ , i.e.,  $\widehat{\boldsymbol{\theta}}_S \xrightarrow{\mathbb{P}} \boldsymbol{\theta}_S^*$ .*

Now we are ready to present the main theorems in this section, which state the convergence property and semiparametric efficiency of  $\widehat{\boldsymbol{\theta}}_S$ . The proofs of Theorems 3.2 and 3.3 are relegated to Sections G.3 and G.4 of the supplement, respectively.

**Theorem 3.2.** *Under Conditions (C1)-(C6), we have that*

$$\widehat{\boldsymbol{\theta}}_S - \boldsymbol{\theta}_S^* = -2\mathbf{V}^{-1} \left( \frac{1}{n} \sum_{j=1}^n \varepsilon_j A_1(\mathbf{x}_j) \right) + o_{\mathbb{P}}(n^{-1/2}), \quad (3.1)$$

where  $\mathbf{V}$  is as in Condition (C3), and

$$A_1(\mathbf{x}) = \sum_{j=1}^{\infty} \frac{1}{\gamma_j} \phi_j(\mathbf{x}) \int_{\Omega} \frac{\partial f_s(\mathbf{z}, \boldsymbol{\theta}_S^*)}{\partial \boldsymbol{\theta}} \phi_j(\mathbf{z}) d\mathbf{z},$$

where  $\gamma_j$  and  $\phi_j$  are eigenvalues and eigenfunctions of  $\mathcal{K}_m(\mathbf{s}, \mathbf{t})$ , respectively.

Note that Condition (C5) implies that  $A_1(\mathbf{x}) < \infty$  almost everywhere. Theorem 3.2 directly implies the asymptotic normality of  $\sqrt{n}(\widehat{\boldsymbol{\theta}}_S - \boldsymbol{\theta}_S^*)$ , provided that

$$\mathbf{W} := \mathbb{E}(A_1(\mathbf{x})A_1(\mathbf{x})^T) \quad (3.2)$$

exists and is positive definite. By the central limit theorem, we have

$$\sqrt{n}(\widehat{\boldsymbol{\theta}}_S - \boldsymbol{\theta}_S^*) \xrightarrow{d} N(0, 4\sigma^2 \mathbf{V}^{-1} \mathbf{W} \mathbf{V}^{-1}).$$

Theorem 3.2 can be regarded as an extension of Theorem 1 in Tuo and Wu (2014), where it has been shown that  $\widehat{\boldsymbol{\theta}}_{L_2}$  obtained by the  $L_2$  calibration is asymptotically normal.

**Theorem 3.3.** *Under the Conditions of Theorem 3.2, if  $\varepsilon_i$  in (2.1) follows a normal distribution for  $i = 1, \dots, n$ , the Sobolev calibration  $\widehat{\boldsymbol{\theta}}_S$  is semiparametric efficient.*

Calibration problem is a semiparametric model because it covers estimating the physical function given by (2.5) and estimating the  $q$ -dimensional calibration parameter given by (2.7), where the former problem has an infinite dimensional parameter space, but the latter problem is only finite dimensional. For detailed discussion about semiparametric models, we refer to Bickel et al. (1993). The property of semiparametric efficiency implies that the semiparametric model has the same asymptotic variance as the statistical estimation with the same observed data in the finite parameter space. This is a desirable property because the semiparametric model shares the same estimation efficiency with the corresponding parametric model under less assumptions.

We demonstrate that Sobolev calibration reaches the highest calibration parameter estimation efficiency under some regularity conditions, by linking the Sobolev calibration estimator to maximum likelihood estimator in the finite parameter model. Note that normality of random error is additionally required. This assumption is commonly used in modeling physical process (Wu and Hamada, 2011; Tuo and Wu, 2015). However, if the random error is non-Gaussian, the semiparametric efficiency can still be achieved by applying a similar treatment to physical process estimation as Tuo and Wu (2015).

### 3.2 Discussion on Uncertainty Quantification

In practice, the prediction of calibration parameters and the quantification of uncertainty are both crucial to calibration problems. Typically, the confidence intervals for  $\boldsymbol{\theta}_S^*$  and point-wise confidence band for  $f_s(\cdot, \boldsymbol{\theta}_S^*)$  and  $f_p(\cdot)$  are of interest. For frequentist calibration problem, which are considered as a semi-parametric problem, uncertainty is inferred from the probability distribution of the estimate  $\widehat{\boldsymbol{\theta}}$ . Traditionally, bootstrap can be applied to estimate the distribution, as demonstrated in Wong et al. (2017). However, the authors also highlighted that the bootstrap confidence region may introduce additional bias and lead to incorrect asymptotic coverage, making it a sub-optimal approach.

Within the framework of Sobolev calibration, we can utilize the asymptotic normality of  $\widehat{\boldsymbol{\theta}}_S$  obtained in Theorem 3.2 to construct a confidence interval for  $\boldsymbol{\theta}_S^*$ . In addition, since computer experiment is a deterministic function where the only uncertainty comes from the estimation procedure of the calibration parameter, the point-wise confidence band for  $f_s(\cdot, \boldsymbol{\theta}_S^*)$  can be easily inferred at a new point  $\boldsymbol{x}$ . Similarly, once  $\delta_{\boldsymbol{\theta}}(\cdot)$  is estimated based on observations  $\{(\boldsymbol{x}_j, y_j^{(p)} - f_s(\boldsymbol{x}_j, \boldsymbol{\theta}))\}_{j=1}^n$ , the point-wise confidence band for  $f_p(\cdot)$  can also be derived. Since the estimation error of  $\delta_{\boldsymbol{\theta}}(\cdot)$  may introduce additional bias, we recommend using models like Gaussian process to estimate discrepancy function such that the true  $\delta_{\boldsymbol{\theta}}(\cdot)$  can be covered with high probability. For example, if 95% confidence intervals and bands are of interest, the details of computation steps are summarized in Algorithm 1, Section H.1 in the supplement, which can be easily generalized to  $q\%$  confidence interval. Due to semi-parametric efficiency shown in Theorem 3.3, our proposed confidence interval is valid, which is empirically verified by numerical experiments in Section 5.1.1.

### 3.3 Connection with $L_2$ Calibration and KO Calibration

In statistical calibration literature, two widely used methods are  $L_2$  calibration and KO calibration, while only the former has been well studied from a theoretical perspective. In this section, we present how the Sobolev calibration serves as a bridge between these two methods.

In  $L_2$  calibration, the identifiable calibration parameter  $\boldsymbol{\theta}_{L_2}^*$  is defined as the calibration parameter which minimizes the  $L_2$  distance between the computer model  $f_s(\cdot, \boldsymbol{\theta})$  and the physical model  $f_p(\cdot)$ . Theorem 1 of Tuo and Wu (2015) states that, under certain conditions, the estimate of  $\boldsymbol{\theta}_{L_2}^*$  via  $L_2$  calibration, denoted by  $\widehat{\boldsymbol{\theta}}_{L_2}$ , satisfies

$$\widehat{\boldsymbol{\theta}}_{L_2} - \boldsymbol{\theta}_{L_2}^* = -2\mathbf{V}_{L_2}^{-1} \left( \frac{1}{n} \sum_{j=1}^n \varepsilon_j \frac{\partial f_s}{\partial \boldsymbol{\theta}}(\mathbf{x}_j, \boldsymbol{\theta}_{L_2}^*) \right) + o_{\mathbb{P}}(n^{-1/2}), \quad (3.3)$$

where

$$\mathbf{V}_{L_2} := - \int_{\Omega} \frac{\partial^2}{\partial \boldsymbol{\theta} \partial \boldsymbol{\theta}^T} (f_p(\mathbf{z}) - f_s(\mathbf{z}, \boldsymbol{\theta}_{L_2}^*))^2 d\mathbf{z}.$$

In fact, (3.3) can be directly obtained by taking  $m = 0$  in Theorem 3.2, as stated in the following Corollary, whose proof is in Section G.5 of the supplement.

**Corollary 3.4** (Theorem 1 of Tuo and Wu (2015)). *Suppose the conditions in Theorem 3.2 hold when taking  $m = 0$ . Then (3.3) holds.*

Now we consider KO calibration. Although KO calibration is originally established from a Bayesian perspective, Tuo and Wu (2014) studied it from a frequentist perspective under some assumptions including the physical observations are noiseless, and called it frequentist KO calibration. By skipping the prior and using maximum likelihood estimation to estimate the calibration parameter, the frequentist KO calibration is given by

$$\widehat{\boldsymbol{\theta}}_{KO} = \underset{\boldsymbol{\theta} \in \Theta}{\operatorname{argmin}} \| \widehat{f}_p(\cdot) - \widehat{f}_s(\cdot, \boldsymbol{\theta}) \|_{\mathcal{N}_{\Phi}(\Omega)}, \quad (3.4)$$

with the identifiable calibration parameter defined as

$$\boldsymbol{\theta}_{KO}^* = \underset{\boldsymbol{\theta} \in \Theta}{\operatorname{argmin}} \| f_p(\cdot) - f_s(\cdot, \boldsymbol{\theta}) \|_{\mathcal{N}_{\Phi}(\Omega)}. \quad (3.5)$$

Tuo and Wu (2014) studied the asymptotic behavior of  $\widehat{\boldsymbol{\theta}}_{KO}$  and showed that it converges to  $\boldsymbol{\theta}_{KO}^*$  in probability. Tuo et al. (2020) further extend the frequentist KO calibration to a more general case where the physical observations can be disturbed by noise. Although the frequentist KO calibration in Tuo et al. (2020) is slightly different with (3.4), it still converges to (3.5); See Corollary 3.6 of Tuo et al. (2020).

However, it has not been shown that whether KO calibration has similar properties as  $L_2$  calibration, for example, the convergence rate  $O_{\mathbb{P}}(n^{-1/2})$  or the asymptotic normality. To the best of our knowledge, the only theoretical results are in Tuo and Wu (2014) and Tuo et al. (2020), under the assumption that  $\mathcal{N}_{\Phi}(\Omega)$  is equivalent to some Sobolev space  $W^{m_1}(\Omega)$ : Tuo

and Wu (2014) showed the consistency of  $\widehat{\boldsymbol{\theta}}_{KO}$  under noiseless case, while Tuo et al. (2020) provided a convergence rate which can be much slower than  $O_{\mathbb{P}}(n^{-1/2})$ .

As a corollary of Theorem 3.2, if  $\mathcal{N}_{\Phi}(\Omega)$  is equivalent to some Sobolev space  $W^{m_1}(\Omega)$ , the KO calibration parameter enjoys similar desired statistical properties of the  $L_2$  calibration parameter. Corollary 3.5 is a direct result of Theorem 3.2, thus the proof is omitted. In the following context of this paper, we refer to (3.4) as another version of the frequentist KO calibration, or KO calibration for brevity, since it also converges to  $\boldsymbol{\theta}_{KO}^*$  (but with a faster convergence rate).

**Corollary 3.5.** *Suppose the conditions in Theorem 3.2 hold when taking  $m = m_1$ . Then we have*

$$\widehat{\boldsymbol{\theta}}_{KO} - \boldsymbol{\theta}_{KO}^* = -2\mathbf{V}_{KO}^{-1} \left( \frac{1}{n} \sum_{j=1}^n \varepsilon_j A_{KO}(\mathbf{x}_j) \right) + o_{\mathbb{P}}(n^{-1/2}),$$

where

$$A_{KO}(\mathbf{x}) = \sum_{j=1}^{\infty} \frac{1}{\gamma_{\Phi,j}} \varphi_j(\mathbf{x}) \int_{\Omega} \frac{\partial f_s(\mathbf{z}, \boldsymbol{\theta}_{KO}^*)}{\partial \boldsymbol{\theta}} \varphi_j(\mathbf{z}) d\mathbf{z},$$

and

$$\mathbf{V}_{KO} = - \sum_{j=1}^{\infty} \frac{1}{\gamma_{\Phi,j}} \frac{\partial^2}{\partial \boldsymbol{\theta} \partial \boldsymbol{\theta}^T} \left( \int_{\Omega} (f_p(\mathbf{z}) - f_s(\mathbf{z}, \boldsymbol{\theta}_{KO}^*)) \varphi_j(\mathbf{z}) d\mathbf{z} \right)^2,$$

where  $\gamma_{\Phi,j}$  and  $\varphi_j(\cdot)$  are eigenvalues and eigenfunctions of  $\Phi(\cdot, \cdot)$ , respectively.

Corollary 3.5 builds a connection between the Sobolev calibration and KO calibration, and a new justification is provided on why KO calibration is widely used and has good performance. To the best of our knowledge, this is the *first* result of this kind for KO calibration.

From Corollaries 3.4 and 3.5, it can be seen that both  $L_2$  calibration and KO calibration are special cases of Sobolev calibration. Sobolev calibration allows the practitioners to select the intermediate calibration method of  $L_2$  calibration and KO calibration, since  $m$  can be flexibly chosen between 0 and  $m_1 > d/2$ , which avoids both the risks of violent fluctuation caused by over-small  $m$  and value deviation caused by over-large  $m$ . Thus, the Sobolev calibration is more flexible. We believe that the Sobolev calibration is not only of theoretical interest, but also has potential wide applications in practice.

## 4 Extension to Stochastic Physical Experiments

In Section 3, we consider the case that the physical experiment  $f_p(\cdot)$  is a deterministic function. In this section, we extend the scenario to that  $f_p(\cdot)$  admits a Gaussian process, in order to align with the original idea of KO calibration, where Gaussian process is used as the prior distribution of physical process. However, since the underlying true physical experiment

is random, the Gaussian process scenario introduces additional challenges in the theoretical investigation of the Sobolev calibration. For example, the support of a Gaussian process is typically larger than the corresponding reproducing kernel Hilbert space (van der Vaart and van Zanten, 2008). To the best of our knowledge, we are not aware of any theoretical investigation on the original KO calibration idea, where the underlying truth is indeed a Gaussian process. Therefore, by investigating the asymptotic behavior of Sobolev calibration (thus  $L_2$  calibration and KO calibration) under the Gaussian process setting, our results not only fill the theoretical gap, but also provide theoretical justification on the use of Gaussian process model in the calibration problems.

Suppose we observe  $y_j^{(p)}$  on  $\mathbf{x}_j \in \Omega$ ,  $j = 1, \dots, n$ , with relationship as in (2.1), and  $\varepsilon_j$  are i.i.d. random variables with mean zero and finite variance  $\sigma_\varepsilon^2$ . Under the Gaussian process settings, the underlying true physical experiment  $f_p(\cdot)$  is assumed to be a realization of a Gaussian process  $Z(\cdot)$ . From this point of view, we will not differentiate  $f_p(\cdot)$  and  $Z(\cdot)$  in this work. For the ease of mathematical treatment, we assume  $Z(\cdot)$  has mean zero, variance  $\sigma^2$  and correlation function  $\mathcal{K}(\cdot, \cdot)$ , and denote it by  $Z(\cdot) \sim \text{GP}(0, \sigma^2 \mathcal{K}(\cdot, \cdot))$ . We further assume  $\mathcal{K}(\cdot, \cdot)$  is positive definite and integrable on  $\mathbb{R}^d$ , satisfying  $\mathcal{K}(0) = 1$ , and *stationary*, in the sense that the correlation between  $Z(\mathbf{x})$  and  $Z(\mathbf{x}')$  depends only on the difference  $\mathbf{x} - \mathbf{x}'$  between the two input variables  $\mathbf{x}$  and  $\mathbf{x}'$ . Thus, we can rewrite  $\mathcal{K}(\cdot, \cdot)$  as  $\mathcal{K}(\cdot - \cdot)$ .

If  $\varepsilon_j$ 's are Gaussian random variables, then given  $\mathbf{y}^{(p)} = \left(y_1^{(p)}, \dots, y_n^{(p)}\right)^\top$ , the conditional distribution of  $Z(\mathbf{x})$  on a point  $\mathbf{x} \in \Omega$  is a normal distribution with conditional mean and variance given by

$$\mathbb{E}[f_p(\mathbf{x}) \mid \mathbf{y}^{(p)}] = \mathbf{r}_1(\mathbf{x})^\top (\mathbf{R}_1 + \mu \mathbf{I}_n)^{-1} \mathbf{y}^{(p)}, \quad (4.1)$$

$$\text{Var}[f_p(\mathbf{x}) \mid \mathbf{y}^{(p)}] = \sigma^2 \left( \mathcal{K}(\mathbf{x} - \mathbf{x}) - \mathbf{r}_1(\mathbf{x})^\top (\mathbf{R}_1 + \mu \mathbf{I}_n)^{-1} \mathbf{r}_1(\mathbf{x}) \right), \quad (4.2)$$

where  $\mathbf{r}_1(\mathbf{x}) = (\mathcal{K}(\mathbf{x} - \mathbf{x}_1), \dots, \mathcal{K}(\mathbf{x} - \mathbf{x}_n))^\top$ ,  $\mathbf{R}_1 = (\mathcal{K}(\mathbf{x}_j - \mathbf{x}_k))_{j,k}$ ,  $\mathbf{I}_n \in \mathbb{R}^{n \times n}$  is an identity matrix, and  $\mu = \sigma_\varepsilon^2 / \sigma^2$ . The conditional mean (4.1) is a natural predictor of  $Z(\mathbf{x})$ , and the conditional variance (4.2) can be used to construct confidence intervals for statistical uncertainty quantification.

It is well-known that the conditional expectation (4.1) is the best linear predictor for  $f_p(\mathbf{x})$ , in the sense that it has the minimal mean squared prediction error (Gramacy, 2020). Therefore, we define

$$\widehat{f}_p(\mathbf{x}) := \mathbb{E}[f_p(\mathbf{x}) \mid \mathbf{y}^{(p)}] \quad (4.3)$$

as an estimate of  $f_p(\mathbf{x})$  on a point  $\mathbf{x} \in \Omega$ .

Although the true calibration parameter in (2.2)  $\boldsymbol{\theta}_0$  is fixed, recall that because of the identifiability issue as discussed in Section 2.1, our goal is to estimate  $\boldsymbol{\theta}_S^*$  in the Sobolev calibration as in (2.4). However, unlike the deterministic physical experiments, where  $f_p(\cdot)$  is a deterministic function and  $\boldsymbol{\theta}_S^*$  is also deterministic, in this section, we consider  $f_p(\cdot)$  is a random process, and thus,  $\boldsymbol{\theta}_S^*$  is a random variable. The computer model  $f_s(\cdot, \boldsymbol{\theta})$  remains unchanged as in the deterministic case, i.e., the computer model is assumed to be a deterministic function, which is for the ease of mathematical treatment. The case that the computer model is an independent Gaussian process requires additional assumptions on

$f_s(\cdot, \boldsymbol{\theta})$ , and we leave it for the future study. The Sobolev calibration under Gaussian process settings can be further defined in the same form as (2.7), i.e.,

$$\widehat{\boldsymbol{\theta}}_S = \operatorname{argmin}_{\boldsymbol{\theta} \in \Theta} \|\widehat{f}_p(\cdot) - \widehat{f}_s(\cdot, \boldsymbol{\theta})\|_{\mathcal{H}_m(\Omega)}, \quad (4.4)$$

where  $\widehat{f}_p(\cdot)$  is as in (4.3), and  $\widehat{f}_s(\cdot, \boldsymbol{\theta})$  is a surrogate model of the computer model  $f_s(\cdot, \boldsymbol{\theta})$ .

Next, we show that under Gaussian process settings and mild conditions, the proposed Sobolev calibration still enjoys desired properties, including consistency and convergence rate at  $O_{\mathbb{P}}(n^{-1/2})$ . For brevity, we move all the conditions to Section F of the supplement.

We start with the consistency of the estimated calibration parameter  $\widehat{\boldsymbol{\theta}}_S$  as stated in the following proposition, whose proof is provided in Section G.6 of the supplement.

**Proposition 4.1** (Consistency of  $\widehat{\boldsymbol{\theta}}_S$ ). *Suppose Conditions (C2'), (C3') and (C6) are fulfilled. The estimated calibration parameter  $\widehat{\boldsymbol{\theta}}_S$  is a consistent estimator of  $\boldsymbol{\theta}_S^*$ , i.e.,  $\widehat{\boldsymbol{\theta}}_S \xrightarrow{\mathbb{P}} \boldsymbol{\theta}_S^*$ .*

Next, we present the main theorem in this section, which states the convergence property of  $\widehat{\boldsymbol{\theta}}_S$ . The proof of Theorem 4.2 is in Section G.7 of the supplement.

**Theorem 4.2.** *Under Conditions (C1')-(C4'), and (C6), we have that*

$$\widehat{\boldsymbol{\theta}}_S - \boldsymbol{\theta}_S^* = -2\mathbf{V}^{-1} \left( \frac{1}{n} \sum_{j=1}^n \varepsilon_j A_1(\mathbf{x}_j) \right) + O_{\mathbb{P}}(n^{-1/2}). \quad (4.5)$$

where  $\mathbf{V}$  is as in Condition (C3), and  $A_1(\mathbf{x})$  is as in Theorem 3.2.

It is worth noting that in (4.5), we have  $O_{\mathbb{P}}(n^{-1/2})$  instead of  $o_{\mathbb{P}}(n^{-1/2})$  in (3.1), which is because of the randomness of the Gaussian process. Theorem 4.2 directly implies the convergence rate of  $\widehat{\boldsymbol{\theta}}_S$ . Specifically, we have  $\|\widehat{\boldsymbol{\theta}}_S - \boldsymbol{\theta}_S^*\|_2 = O_{\mathbb{P}}(n^{-1/2})$ . Therefore, even if  $f_p(\cdot)$  is a random function following a Gaussian process, we can still guarantee the convergence rate of  $\widehat{\boldsymbol{\theta}}_S$  as  $O_{\mathbb{P}}(n^{-1/2})$ .

## 5 Numerical Experiments

In this section, we conduct numerical experiments to evaluate the estimation performance of our proposed method under finite samples, and compare it with the frequentist KO calibration and  $L_2$  calibration. For the conciseness of this paper, we move all the figures to Section H.4 in the supplement.

### 5.1 Simulation Studies

We consider two examples in this subsection. The underlying physical model is a deterministic function in Example 1, and is a Gaussian process in Example 2. An additional example where the underlying physical model is a deterministic function and has the same form as in Example 2 is put in Section H.3 in the supplement.

**Example 1.** In this example, we show that in some cases, the  $L_2$  calibration can lead to a “wiggly” function, by showing an unstable case where the smoothness of calibrated function is sensitive to calibration parameter.

Suppose the computer experiment is

$$f_s(x, \theta) = f_p(x) - 1/5\sqrt{\theta^2 - \theta + 1} \left( \sin \left( 2\pi x \frac{10}{\exp(\theta^2 + \theta)} \right) + \frac{\cos(2\pi x 10)}{2 \exp \theta^2 + 1} + \theta^2 \right).$$

For the detailed experiment setup, we refer to Section H.3 in the supplement.

The corresponding Sobolev calibration parameter  $\theta_S^*$  is defined as in (2.4), which is  $\theta_S^* \approx 1.3$  by numerical optimization. From Figure H.2 (also see Figure 1), it can be seen that  $L_2$  calibrated experiment should be extraordinarily curved in order to achieve the smallest  $L_2$  distance, which may not be desired in practice, and can sabotage the coverage accuracy of  $f_p(\cdot)$ , as shown in Section 5.1.1. KO calibration, on the other hand, keeps the shape of the physical experiment well, while leads to a larger  $L_2$  discrepancy. Compared with  $L_2$  calibration and KO calibration, Sobolev calibration provides a preferable choice by approximating the function value well while maintaining the shape of physical process.

The corresponding summary statistics of numerical experiment results are shown in Table 1. It can be seen that Sobolev calibration shows a good estimation and has a small statistical estimation error, which empirically verifies the theoretical property of our proposed method.

We further specify a range of  $m$  from small to large, in order to further illustrate the flexibility of Sobolev calibration and how it generalizes the other two methods. The Sobolev calibrated experiments present proximity to  $L_2$  calibration and KO calibration when  $m = 7/8$  and  $m = 9/5$ , respectively, as shown in Figure H.3. Therefore, one can choose their preferred  $m$  to attain the satisfying calibrated experiment under the theoretical guarantee. Specifically, the practitioner can choose  $m$  at a relatively small value to emphasize more on point-wise value approximation, or choose a relatively large  $m$  to pursue better approximation in shape.

**Table 1:** *The mean and standard deviation (SD) of estimated calibration parameters for different methods in Example 1, where  $\theta_S^*$  is 1.3.*

	$\sigma^2 = 0.05$		$\sigma^2 = 0.1$	
	Mean	SD	Mean	SD
Sobolev	1.3321	0.0767	1.3279	0.0921
$L_2$	0.0422	0.0112	0.0484	0.0545
KO	2.1354	0.0191	2.1354	0.0268

**Example 2.** In this example, we choose the underlying physical experiment  $f_p(\cdot)$  to be a Gaussian process. In Section 4, we assume that the mean function of  $f_p(\cdot)$  is zero to simplify the theoretical development, while in this numerical experiment, we set the mean function dependent on the input  $x$  to endow it with practical meaning. This act would not hurt the theoretical merit of Sobolev calibration.



Suppose the underlying physical process is a Gaussian process given by  $f_p(x) \sim \text{GP}(\exp(\pi x/5) \sin 2\pi x, 0.1\Psi_2)$  for  $x \in \Omega = [0, 1]$ . The physical observations are given by  $y_j^{(p)} = f_p(x_j) + \varepsilon_j$ , with  $x_j \sim \text{Uniform}(0, 1)$ ,  $\varepsilon_j \sim N(0, \sigma_\varepsilon^2)$  for  $j = 1, \dots, 200$ . Suppose the computer experiment is

$$f_s(x, \theta) = \exp(\pi x/5) \sin 2\pi x - \sqrt{\theta^2 - \theta + 1} (\sin 2\pi\theta x + \exp(\pi\theta x/2)).$$

$\widehat{f}_p(x)$  in (4.3) is applied to estimate  $f_p(x)$ , and  $\mu$  is chosen through a validation set, where the details are put in Section H.2 in the supplement.

Table 2 summarizes the numerical results of Example 2. Numerical summaries present that when  $f_p(\cdot)$  follows a Gaussian process, the mean and standard deviation of squared estimation error are both small. From Figure H.4, we can see that Sobolev calibration can still maintain good performance even though the underlying physical process is a random Gaussian process.

**Table 2:** *The mean squared errors (MSE) and standard deviation (SD) of estimated calibration parameters with respect to  $\theta_S^*$  for different methods in Example 2.*

	$\sigma^2 = 0.05$		$\sigma^2 = 0.1$	
	MSE	SD	MSE	SD
Sobolev	0.0003	0.0008	0.0010	0.0058
$L_2$	0.0857	0.0921	0.0861	0.0925
KO	0.0013	0.0018	0.0039	0.0248

### 5.1.1 Uncertainty Quantification

In this subsection, we examine the empirical performance of calibration estimates by quantifying the uncertainty associated with calibration parameters  $\widehat{\theta}_{L_2}$ ,  $\widehat{\theta}_S$ , and  $\widehat{\theta}_{KO}$  that experimented in the two examples of simulation studies. We compute the estimated calibration parameters along with 95% confidence intervals, which account for uncertainty in estimation. Furthermore, we compute the 95% confidence bands of computer experiment together with model discrepancy as the predictor of physical process, which account for uncertainty in prediction. Details are provided in Section H.1 in the supplement. Simulation results also include the corresponding interval lengths together with interval scores.

Table 3 summarizes the coverage results of the calibration parameters over 500 trials with  $\sigma^2 = 0.1$ . It shows that the overall coverage rates approach the nominal coverage 95% with relatively narrow intervals, leading to small interval scores. This empirically supports that our construction of confidence interval via asymptotic properties is valid. Table 4 presents the average point-wise coverage results of the computer and physical models, computed at 100 equally spaced points on  $\Omega$ . Notably, all results are satisfactory, with the exception of  $L_2$  calibration coverage rate for the physical process prediction in Example 1. This is due to the fact that  $L_2$  calibration produces a curvy  $f_s(\cdot, \widehat{\theta}_{L_2})$ , resulting in a similarly wiggly  $\delta(\cdot, \widehat{\theta}_{L_2})$ . Consequently, learning a discrepancy function like that based on noisy data becomes

challenging, since it is difficult to differentiate between frequent fluctuations and noise, which results in inaccurate predictions. This empirical phenomenon provides additional evidence for the importance of shape resemblance between the physical function and computer experiment, particularly in the context of physical process prediction.

**Table 3:** Average coverage rates, interval lengths and scores of the calibration parameters  $\theta_{L_2}^*$ ,  $\theta_S^*$ , and  $\theta_{KO}^*$ , respectively.

		Example 1			Example 2			
		coverage	length	score	coverage	length	score	
$L_2$	$m = 0$	0.9740	0.0494	0.3120	$m = 0$	0.9580	0.0294	0.2589
	$m = 7/8$	0.9760	0.6960	0.7435				
Sobolev	$m = 1$	0.9320	0.5896	0.7295	$m = 1$	0.9760	0.1212	0.1652
	$m = 9/8$	0.9980	0.8403	0.8405				
	$m = 9/5$	1	0.3322	0.3322				
KO	$m = 2$	1	0.4776	0.4776	$m = 2$	0.9900	0.4448	0.5735

**Table 4:** Point-wise average coverage rates, interval lengths and scores of  $f_s(\cdot, \theta^*)$  and  $f_p(\cdot)$ .

		Example 1			Example 2		
		$L_2$	Sobolev	KO	$L_2$	Sobolev	KO
		$m = 0$	$m = 1$	$m = 2$	$m = 0$	$m = 1$	$m = 2$
$f_s(\cdot, \theta^*)$	coverage	0.9677	0.9174	1	0.9451	0.9731	0.9885
	length	0.1755	0.6996	1.0687	0.0687	0.3816	1.2384
	score	0.2497	0.9079	1.0687	0.4042	0.4918	1.4927
$f_p(\cdot)$	coverage	0.8255	0.9821	0.9735	0.9506	0.9581	0.9657
	length	0.3535	0.2267	0.1818	0.1802	0.1821	0.1906
	score	0.7231	0.2363	0.1959	0.2317	0.2082	0.2108

### 5.1.2 Adjustment to Scale Parameters

Throughout the theoretical development of Sobolev calibration, we only require that the function space  $\mathcal{H}_m(\Omega)$  is chosen as equivalent to the Sobolev space  $W^m(\Omega)$ , without restrictions on the specification of kernel function parameters. In this subsection, we numerically investigate how adjusting the kernel function's parameters affects the calibration parameter estimation in this subsection. Using the setup from Example 1 with  $m = 1$  and  $\sigma^2 = 0.1$ , we consider four different length-scale parameter values  $\gamma = \{0.01, 0.1, 1, 10\}$ , for the Matérn kernel function  $\Psi(x, x') = \exp(-\gamma |x - x'|)$ . The simulation results are summarized in Table 5, where the mean and standard deviation of  $\hat{\theta}_S$  are computed over 500 trials. Numerical results suggest that under a wide range of length-scale parameters, Sobolev calibration performs reasonably well with the Sobolev norms of discrepancy  $\|\delta(\cdot, \hat{\theta}_S)\|_{W^m(\Omega)}$  lying between 0.9 to 2.5, which are much smaller than the Sobolev norm of  $L_2$  calibration (6.7834). Figure H.5 describes the calibrated computer experiments under various length-scale parameters. In this setting, since the aim is to avoid over-calibrating the smooth underlying physical function,

we would recommend choosing  $\gamma = 0.1$ , with the smallest Sobolev norm that serves as the measurement objective for length-scale parameters.

**Table 5:** The mean and standard deviation (shown in parentheses) of  $\widehat{\theta}_S$ , RKHS norm and Sobolev norm of discrepancy function for different length-scale parameters in Example 1.

$\gamma$	$\theta_S^*$	$\widehat{\theta}_S$	$\ \delta(\cdot, \widehat{\theta}_S)\ _{\mathcal{H}_m(\Omega)}$	$\ \delta(\cdot, \widehat{\theta}_S)\ _{W^m(\Omega)}$
0.01	2.0400	1.0728(0.0005)	11.3731	1.6456
0.1	1.7800	1.5172(0.2575)	1.5871	<b>0.9943</b>
1	1.3000	1.3279(0.0921)	0.9077	1.1015
10	0.8800	0.8109(0.0914)	0.7393	2.4583

## 5.2 Ion Channel Example

In this subsection, we introduce a real-world example, which is widely used for calibration experiment; see Plumlee et al. (2016); Plumlee (2017); Xie and Xu (2020) for example. The dataset is collected by Ednie and Bennett (2011) for whole cell voltage clamp experiments on the sodium ion channels of cardiac cell membranes. For more details of the experiment, we refer to Plumlee et al. (2016).

In this example, we consider log scale of time as input  $x$ , and obtain 19 normalized current records as output. The computer model is the classical Markov model  $f_s(x, \boldsymbol{\theta}) = \mathbf{e}_1^T \exp[\exp(x)A(\boldsymbol{\theta})]\mathbf{e}_4$ , where the first exp is matrix exponential function,  $\mathbf{e}_i$  is the column vector with one at the  $i$ th element and zero otherwise, and  $A(\boldsymbol{\theta})$  with  $\boldsymbol{\theta} = [\theta_1, \theta_2, \theta_3]^T$  is defined as a  $4 \times 4$  matrix, where  $A(\boldsymbol{\theta})_{[1,1]} = -\theta_2 - \theta_3$ ,  $A(\boldsymbol{\theta})_{[1,2]} = \theta_1$ ,  $A(\boldsymbol{\theta})_{[2,1]} = \theta_2$ ,  $A(\boldsymbol{\theta})_{[2,2]} = -\theta_1 - \theta_2$ ,  $A(\boldsymbol{\theta})_{[2,3]} = \theta_1$ ,  $A(\boldsymbol{\theta})_{[3,2]} = \theta_2$ ,  $A(\boldsymbol{\theta})_{[3,3]} = -\theta_1 - \theta_2$ ,  $A(\boldsymbol{\theta})_{[3,4]} = \theta_1$ ,  $A(\boldsymbol{\theta})_{[4,3]} = \theta_2$ ,  $A(\boldsymbol{\theta})_{[4,4]} = -\theta_1$ , and other elements are zero.

We still consider  $\mathcal{H}_m(\Omega)$  and  $\mathcal{H}_{m_1}(\Omega)$  are RKHSs generated by Matérn kernel functions  $\Psi_1(x)$  and  $\Psi_2(x)$  respectively. Figure H.6 in the supplement shows calibrated computer models by three methods and the discrepancy between observations and computer models. It can be seen that  $L_2$  calibration achieves a more accurate approximation at each observation but sacrifices control of oscillations considering the entire function. Sobolev calibration obtain smoother function by specifying  $m = 1$  to additionally focus on the first-order derivative. KO calibration loses more approximation accuracy. Therefore, Sobolev calibration provides more flexibility for users in practice as illustrated in this real-world example.

## 6 Conclusions and Discussion

In this work, we propose a novel calibration framework, called Sobolev calibration, which allows the practitioners to adjust the identifiable calibration parameter based on practical needs. The performance of calibration can be enhanced by rebalancing the approximation in function value and function shape. We show that the estimation of the calibration parameter is consistent, asymptotically normal and semiparametric efficient by rigorous theoretical analysis. Moreover, we investigate the case where the underlying physical experiment is a

realization of Gaussian process, which aligns with the original idea of KO calibration. Even if the underlying physical experiment is a random process, we prove that the estimation error still has a convergence rate  $O_{\mathbb{P}}(n^{-1/2})$ .

Our work can be extended in several ways. First, our method is based on random design, where the control variables  $\boldsymbol{x}$  are sampled from uniform distribution. Since fixed designs are popular in computer experiments (Wu and Hamada, 2011), the framework under fixed design is worth investigating, which requires future work. Second, the Sobolev calibration is a frequentist approach. Note that the recent works (Tuo, 2019; Xie and Xu, 2020) succeed in extending the  $L_2$  calibration to a Bayesian framework, it is worth to explore an extension to develop a Bayesian Sobolev calibration framework in the future.

## References

- Adams, R. A. and Fournier, J. J. (2003). *Sobolev Spaces*, volume 140. Academic Press.
- Bayarri, M. J., Berger, J. O., Paulo, R., Sacks, J., Cafeo, J. A., Cavendish, J., Lin, C.-H., and Tu, J. (2007). A framework for validation of computer models. *Technometrics*, 49(2):138–154.
- Bickel, P. J., Klaassen, C. A., Bickel, P. J., Ritov, Y., Klaassen, J., Wellner, J. A., and Ritov, Y. (1993). *Efficient and Adaptive Estimation for Semiparametric Models*, volume 4. Johns Hopkins University Press Baltimore.
- Cirovic, S., Bhola, R. M., Hose, D. R., Howard, I. C., Lawford, P., Marr, J. E., and Parsons, M. A. (2006). Computer modelling study of the mechanism of optic nerve injury in blunt trauma. *British Journal of Ophthalmology*, 90(6):778–783.
- DeVore, R. A. and Sharpley, R. C. (1993). Besov spaces on domains in  $R^d$ . *Transactions of the American Mathematical Society*, 335(2):843–864.
- Ednie, A. R. and Bennett, E. S. (2011). Modulation of voltage-gated ion channels by sialylation. *Comprehensive Physiology*, 2(2):1269–1301.
- Fang, K.-T., Li, R., and Sudjianto, A. (2005). *Design and Modeling for Computer Experiments*. CRC Press.
- Farah, M., Birrell, P., Conti, S., and Angelis, D. D. (2014). Bayesian emulation and calibration of a dynamic epidemic model for A/H1N1 influenza. *Journal of the American Statistical Association*, 109(508):1398–1411.
- Gramacy, R. B. (2020). *Surrogates: Gaussian Process Modeling, Design, and Optimization for the Applied Sciences*. Chapman and Hall/CRC.
- Gramacy, R. B., Bingham, D., Holloway, J. P., Grosskopf, M. J., Kuranz, C. C., Rutter, E., Trantham, M., and Drake, R. P. (2015). Calibrating a large computer experiment simulating radiative shock hydrodynamics. *The Annals of Applied Statistics*, 9(3):1141–1168.

- Gu, M. and Wang, L. (2018). Scaled gaussian stochastic process for computer model calibration and prediction. *SIAM/ASA Journal on Uncertainty Quantification*, 6(4):1555–1583.
- Higdon, D., Kennedy, M., Cavendish, J. C., Cafoe, J. A., and Ryne, R. D. (2004). Combining field data and computer simulations for calibration and prediction. *SIAM Journal on Scientific Computing*, 26(2):448–466.
- Joseph, V. R. and Yan, H. (2015). Engineering-driven statistical adjustment and calibration. *Technometrics*, 57(2):257–267.
- Kanagawa, M., Hennig, P., Sejdinovic, D., and Sriperumbudur, B. K. (2018). Gaussian processes and kernel methods: A review on connections and equivalences. *arXiv preprint arXiv:1807.02582*.
- Kennedy, M. C. and O’Hagan, A. (2001). Bayesian calibration of computer models. *Journal of the Royal Statistical Society. Series B (Statistical Methodology)*, 63(3):425–464.
- Lynch, P. (2008). The origins of computer weather prediction and climate modeling. *Journal of Computational Physics*, 227(7):3431–3444.
- Plumlee, M. (2017). Bayesian calibration of inexact computer models. *Journal of the American Statistical Association*, 112(519):1274–1285.
- Plumlee, M. (2019). Computer model calibration with confidence and consistency. *Journal of the Royal Statistical Society: Series B (Statistical Methodology)*, 81(3):519–545.
- Plumlee, M., Joseph, V. R., and Yang, H. (2016). Calibrating functional parameters in the ion channel models of cardiac cells. *Journal of the American Statistical Association*, 111(514):500–509.
- Qian, P. Z. and Wu, C. J. (2008). Bayesian hierarchical modeling for integrating low-accuracy and high-accuracy experiments. *Technometrics*, 50(2):192–204.
- Ramsay, J. O., Hooker, G., Campbell, D., and Cao, J. (2007). Parameter estimation for differential equations: a generalized smoothing approach. *Journal of the Royal Statistical Society Series B: Statistical Methodology*, 69(5):741–796.
- Rychkov, V. S. (1999). On restrictions and extensions of the Besov and Triebel–Lizorkin spaces with respect to Lipschitz domains. *Journal of the London Mathematical Society*, 60(1):237–257.
- Santner, T. J., Williams, B. J., and Notz, W. I. (2003). *The Design and Analysis of Computer Experiments*. Springer Science & Business Media.
- Schölkopf, B. and Smola, A. J. (2002). *Learning with Kernels: Support Vector Machines, Regularization, Optimization, and Beyond*. MIT Press.
- Stein, M. L. (1999). *Interpolation of Spatial Data: Some Theory for Kriging*. Springer Science & Business Media.

- Steinwart, I. and Scovel, C. (2012). Mercer’s theorem on general domains: On the interaction between measures, kernels, and RKHSs. *Constructive Approximation*, 35(3):363–417.
- Storlie, C. B., Lane, W. A., Ryan, E. M., Gattiker, J. R., and Higdon, D. M. (2015). Calibration of computational models with categorical parameters and correlated outputs via Bayesian smoothing spline ANOVA. *Journal of the American Statistical Association*, 110(509):68–82.
- Sung, C.-L., Hung, Y., Rittase, W., Zhu, C., and Wu, C. (2020). Calibration for computer experiments with binary responses and application to cell adhesion study. *Journal of the American Statistical Association*, 115(532):1664–1674.
- Tuo, R. (2019). Adjustments to computer models via projected kernel calibration. *SIAM/ASA Journal on Uncertainty Quantification*, 7(2):553–578.
- Tuo, R., Wang, Y., and Jeff Wu, C. (2020). On the improved rates of convergence for Matérn-type kernel ridge regression with application to calibration of computer models. *SIAM/ASA Journal on Uncertainty Quantification*, pages 1522–1547.
- Tuo, R. and Wu, C. (2014). A theoretical framework for calibration in computer models: Parametrization, estimation and convergence properties. *Technical Report*.
- Tuo, R. and Wu, C. (2015). Efficient calibration for imperfect computer. *The Annals of Statistics*, 43(6):2331–2352.
- van der Vaart, A. W. and van Zanten, J. H. (2008). Reproducing kernel Hilbert spaces of Gaussian priors. In *Pushing the Limits of Contemporary Statistics: Contributions in Honor of Jayanta K. Ghosh*, pages 200–222. Institute of Mathematical Statistics.
- Wahba, G. (1990). Spline models for observational data. *Society for Industrial and Applied Mathematics*.
- Wang, S., Chen, W., and Tsui, K.-L. (2009). Bayesian validation of computer models. *Technometrics*, 51(4):439–451.
- Wendland, H. (2004). *Scattered Data Approximation*, volume 17. Cambridge University Press.
- White, K. L. and Chaubey, I. (2005). Sensitivity analysis, calibration, and validations for a multisite and multivariable swat model 1. *JAWRA Journal of the American Water Resources Association*, 41(5):1077–1089.
- Wong, R. K., Storlie, C. B., and Lee, T. C. (2017). A frequentist approach to computer model calibration. *Journal of the Royal Statistical Society. Series B (Statistical Methodology)*, pages 635–648.
- Wu, C. J. and Hamada, M. S. (2011). *Experiments: Planning, Analysis, and Optimization*, volume 552. John Wiley & Sons.
- Xie, F. and Xu, Y. (2020). Bayesian projected calibration of computer models. *Journal of the American Statistical Association*, pages 1–18.
- Xiu, D. (2010). *Numerical Methods for Stochastic Computations*. Princeton University Press.

# Supplementary Material for “Sobolev Calibration of Imperfect Computer Models”

In this supplement, we provide the support material to supplement the main article, including general notations used in technical proofs, introduction to reproducing kernel Hilbert spaces (RKHSs) and Sobolev spaces, powers of RKHSs, conditions listed for propositions and theorems, details of technical proofs, experimental details and figures from numerical examples.

## A Notation

We use  $\langle \cdot, \cdot \rangle_n$  to denote the empirical inner product, which is defined by

$$\langle f, g \rangle_n = \frac{1}{n} \sum_{k=1}^n f(x_k)g(x_k)$$

for two functions  $f$  and  $g$ , and let  $\|g\|_n^2 = \langle g, g \rangle_n$  be the empirical norm of function  $g$ . In particular, let

$$\langle \epsilon, f \rangle_n = \frac{1}{n} \sum_{k=1}^n \epsilon_k f(x_k)$$

for a function  $f$ , where  $\epsilon = (\epsilon_1, \dots, \epsilon_n)^T$ . Let  $a \vee b = \max(a, b)$  for two real numbers  $a, b$ . We use  $H(\cdot, \mathcal{F}, \|\cdot\|)$  and  $H_B(\cdot, \mathcal{F}, \|\cdot\|)$  to denote the entropy number and the bracket entropy number of class  $\mathcal{F}$  with the (empirical) norm  $\|\cdot\|$ , respectively. Let  $\mathcal{B}_{\mathcal{F}}(r) = \{f \in \mathcal{F} : \|f\|_{\mathcal{F}} \leq r\}$  denote the ball with radius  $r$  in  $\mathcal{F}$ , where  $r > 0$ . We say “ $\mathcal{F}_1$  and  $\mathcal{F}_2$  are equivalent” for two Hilbert spaces  $\mathcal{F}_1$  and  $\mathcal{F}_2$  if  $\mathcal{F}_1 = \mathcal{F}_2$  with equivalent norms. Through the proof, we assume  $\text{Vol}(\Omega) = 1$  for the ease of notational simplicity. We use  $C, C', c_j, C_j, j \geq 0$  to denote generic positive constants, of which value can change from line to line.

## B Introduction to Reproducing Kernel Hilbert Spaces and Sobolev Spaces

Suppose  $K : \Omega \times \Omega \rightarrow \mathbb{R}$  is a symmetric positive definite kernel, where  $\Omega \subset \mathbb{R}^d$ . Define the linear space

$$F_K(\Omega) = \left\{ \sum_{i=1}^n \beta_i K(\cdot, \mathbf{x}_i) : \beta_i \in \mathbb{R}, \mathbf{x}_i \in \Omega, n \in \mathbb{N} \right\}, \quad (\text{B.1})$$

and equip this space with the bilinear form

$$\left\langle \sum_{i=1}^n \beta_i K(\cdot, \mathbf{x}_i), \sum_{j=1}^m \gamma_j K(\cdot, \mathbf{x}'_j) \right\rangle_K := \sum_{i=1}^n \sum_{j=1}^m \beta_i \gamma_j K(\mathbf{x}_i, \mathbf{x}'_j). \quad (\text{B.2})$$

Then the *reproducing kernel Hilbert space* (RKHS)  $\mathcal{N}_K(\Omega)$  generated by the kernel function  $K$  is defined as the closure of  $F_K(\Omega)$  under the inner product  $\langle \cdot, \cdot \rangle_K$ , and the norm of  $\mathcal{N}_K(\Omega)$  is  $\|f\|_{\mathcal{N}_K(\Omega)} = \sqrt{\langle f, f \rangle_{\mathcal{N}_K(\Omega)}}$ , where  $\langle \cdot, \cdot \rangle_{\mathcal{N}_K(\Omega)}$  is induced by  $\langle \cdot, \cdot \rangle_K$ . We refer the readers to Wendland (2004) for more details. In particular, we have the following theorem, which gives another characterization of the RKHS when  $K$  is defined by a stationary kernel function  $\Phi$ , via the Fourier transform of  $\Phi$ . For an integrable function  $f \in L_1(\mathbb{R}^d)$ , its Fourier transform is defined as

$$\mathcal{F}(f)(\boldsymbol{\omega}) = (2\pi)^{-d/2} \int_{\mathbb{R}^d} f(\mathbf{x}) e^{-i\mathbf{x}^T \boldsymbol{\omega}} d\mathbf{x}.$$

**Theorem B.1** (Theorem 10.12 of Wendland (2004)). *Let  $\Phi$  be a positive definite kernel function which is continuous and integrable in  $\mathbb{R}^d$ . Define*

$$\mathcal{G} := \{f \in L_2(\mathbb{R}^d) \cap C(\mathbb{R}^d) : \mathcal{F}(f)/\sqrt{\mathcal{F}(\Phi)} \in L_2(\mathbb{R}^d)\},$$

with the inner product

$$\langle f, g \rangle_{\mathcal{N}_\Phi(\mathbb{R}^d)} = (2\pi)^{-d} \int_{\mathbb{R}^d} \frac{\mathcal{F}(f)(\boldsymbol{\omega}) \overline{\mathcal{F}(g)(\boldsymbol{\omega})}}{\mathcal{F}(\Phi)(\boldsymbol{\omega})} d\boldsymbol{\omega}.$$

Then  $\mathcal{G} = \mathcal{N}_\Phi(\mathbb{R}^d)$ , and both inner products coincide.

The Sobolev norm for functions on the whole space is

$$\|f\|_{W^m(\mathbb{R}^d)} = \left( \int_{\mathbb{R}^d} |\mathcal{F}(f)(\boldsymbol{\omega})|^2 (1 + \|\boldsymbol{\omega}\|_2^2)^m d\boldsymbol{\omega} \right)^{1/2}. \quad (\text{B.3})$$

Then the Sobolev space  $W^m(\mathbb{R}^d)$  consists of functions with finite norm defined in (B.3). This function space is also called a Bessel potential space, which is a complex interpolation space of  $L_2(\mathbb{R}^d)$  and  $W^k(\mathbb{R}^d)$  with  $k > m$  an integer (Almeida and Samko, 2006; Gurka et al., 2007). The Sobolev space on  $\Omega$  can be defined via restriction.

Since the Fourier transform of  $\Psi_m$  defined in (2.8) satisfies (Tuo and Wu, 2014)

$$c_1(1 + \|\boldsymbol{\omega}\|_2^2)^{-m} \leq \mathcal{F}(\Psi_m)(\boldsymbol{\omega}) \leq c_2(1 + \|\boldsymbol{\omega}\|_2^2)^{-m},$$

from Theorem B.1 and (B.3) it can be seen that the RKHS  $\mathcal{N}_{\Psi_m}(\mathbb{R}^d)$  generated by  $\Psi_m$  is equivalent to  $W^m(\mathbb{R}^d)$ . By some restriction technique (see Adams and Fournier (2003) and Wendland (2004)), it can be further shown that  $\mathcal{N}_{\Psi_m}(\Omega) = W^m(\Omega)$  with equivalent norms.

## C Justification of Approximation in Section 2.2.3

Define the integral operator  $\mathcal{T} : L_2(\Omega) \rightarrow L_2(\Omega)$  by

$$\mathcal{T}f(\mathbf{x}) = \int_{\Omega} \mathcal{K}_m(\mathbf{x}, \mathbf{x}') f(\mathbf{x}') d\mathbf{x}', f \in L_2(\Omega), \mathbf{x} \in \Omega.$$



If  $g \in \mathcal{T}(L_2(\Omega))$ , the proof of Theorem 11.23 of Wendland (2004) implies that

$$\left| \|g(\cdot, \boldsymbol{\theta})\|_{\mathcal{H}_m(\Omega)} - \|\mathcal{I}_{\mathcal{K}_m, \tilde{\mathbf{X}}}g(\cdot, \boldsymbol{\theta})\|_{\mathcal{H}_m(\Omega)} \right| \leq \|g(\cdot, \boldsymbol{\theta}) - \mathcal{I}_{\mathcal{K}_m, \tilde{\mathbf{X}}}g(\cdot, \boldsymbol{\theta})\|_{\mathcal{H}_m(\Omega)} \leq C \|P_{\mathcal{K}_m, \tilde{\mathbf{X}}}\|_{L_2(\Omega)}, \quad (\text{C.1})$$

where the first inequality is because of the triangle inequality. The function  $P_{\mathcal{K}_m, \tilde{\mathbf{X}}}(\mathbf{x})$  is defined and can be bounded by

$$\begin{aligned} P_{\mathcal{K}_m, \tilde{\mathbf{X}}}(\mathbf{x})^2 &= \min_{\mathbf{u}=(u_1, \dots, u_N)^T \in \mathbb{R}^N} \mathcal{K}_m(\mathbf{x}, \mathbf{x}) - 2 \sum_{j=1}^N u_j \mathcal{K}_m(\mathbf{x}, \mathbf{x}_j) + \sum_{j,k=1}^N u_j u_k \mathcal{K}_m(\mathbf{x}_j, \mathbf{x}_k) \\ &\leq \mathcal{K}_m(\mathbf{x}, \mathbf{x}) - \mathcal{K}_m(\mathbf{x}, \tilde{\mathbf{x}}_l), \end{aligned}$$

where  $l$  is chosen such that  $\tilde{\mathbf{x}}_l = \operatorname{argmin}_{\tilde{\mathbf{x}}_j \in \tilde{\mathbf{X}}_N} \|\mathbf{x} - \tilde{\mathbf{x}}_j\|_2$ . As  $N$  goes to infinity, we have that  $\min_{\tilde{\mathbf{x}}_j \in \tilde{\mathbf{X}}_N} \|\mathbf{x} - \tilde{\mathbf{x}}_j\|_2$  converges to zero for all  $\mathbf{x} \in \Omega$ , because  $\tilde{\mathbf{x}}_1, \dots, \tilde{\mathbf{x}}_N$  are uniformly distributed, and eventually spread well in  $\Omega$ . Therefore, as long as  $\mathcal{K}_m(\cdot, \cdot)$  is continuous,  $P_{\mathcal{K}_m, \tilde{\mathbf{X}}}(\mathbf{x})$  converges to zero as  $N$  goes to infinity. We note that under certain conditions of kernel functions (differentiability, stationarity, etc.), sharper convergence rate of  $P_{\mathcal{K}_m, \tilde{\mathbf{X}}}(\mathbf{x})$  can be obtained; see Chapter 11 of Wendland (2004).

Since  $P_{\mathcal{K}_m, \tilde{\mathbf{X}}}(\mathbf{x})$  converges to zero for all  $\mathbf{x} \in \Omega$ , together with (C.1), it can be seen that  $\|\mathcal{I}_{\mathcal{K}_m, \tilde{\mathbf{X}}}g(\cdot, \boldsymbol{\theta})\|_{\mathcal{H}_m(\Omega)}$  is a good approximation of  $\|g(\cdot, \boldsymbol{\theta})\|_{\mathcal{H}_m(\Omega)}$ . One advantage of this approximation is that the RKHS norm of  $\mathcal{I}_{\mathcal{K}_m, \tilde{\mathbf{X}}}g(\cdot, \boldsymbol{\theta})$  can be directly computed by  $\|\mathcal{I}_{\mathcal{K}_m, \tilde{\mathbf{X}}}g(\cdot, \boldsymbol{\theta})\|_{\mathcal{H}_m(\Omega)}^2 = \tilde{\mathbf{g}}_{\boldsymbol{\theta}}^T \tilde{\mathbf{R}}^{-1} \tilde{\mathbf{g}}_{\boldsymbol{\theta}}$ . Therefore,  $\hat{\boldsymbol{\theta}}_S$  in (2.7) can be approximated by  $\tilde{\boldsymbol{\theta}}_S = \operatorname{argmin}_{\boldsymbol{\theta} \in \Theta} \tilde{\mathbf{g}}_{\boldsymbol{\theta}}^T \tilde{\mathbf{R}}^{-1} \tilde{\mathbf{g}}_{\boldsymbol{\theta}}$ .

## D Powers of Reproducing kernel Hilbert spaces

Recall that  $\mathcal{K}_{m^*}(\cdot, \cdot)$  is a symmetric kernel function such that the RKHS  $\mathcal{N}_{\mathcal{K}_{m^*}}(\Omega)$  coincides  $W^{m^*}(\Omega)$  with  $m^* > d/2$ , and  $m^*$  is an integer. Also recall that by Mercer's theorem, it possesses an absolutely and uniformly convergent representation as

$$\mathcal{K}_{m^*}(\mathbf{s}, \mathbf{t}) = \sum_{j=1}^{\infty} \gamma_{\mathcal{K}, j} e_j(\mathbf{s}) e_j(\mathbf{t}), \quad \forall \mathbf{s}, \mathbf{t} \in \Omega, \quad (\text{D.1})$$

where  $\gamma_{\mathcal{K}, j}$  and  $e_j$  are eigenvalues and eigenfunctions of  $\mathcal{K}_{m^*}(\cdot, \cdot)$ , respectively. Let  $\mathcal{N}_{\mathcal{K}_{m^*}}^{\beta}(\Omega)$  be the  $\beta$ -th power of RKHS  $\mathcal{N}_{\mathcal{K}_{m^*}}(\Omega)$ , and  $\mathcal{K}_{m^*}^{\beta}(\cdot, \cdot)$  be the  $\beta$ -th power of kernel function, defined as in Definition 1.

Proposition 4.2 of Steinwart and Scovel (2012) shows that  $\mathcal{N}_{\mathcal{K}_{m^*}}^{\beta}(\Omega)$  is indeed an RKHS generated by the kernel function  $\mathcal{K}_{m^*}^{\beta}(\cdot, \cdot)$ . Furthermore, we can compactly embed this space into  $L_2(\Omega)$ . With a slight abuse of notation, we still use  $\mathcal{N}_{\mathcal{K}_{m^*}}^{\beta}(\Omega)$  to denote the embedded space, where the eigenfunctions can be different on a set with Lebesgue measure zero. As pointed by Steinwart and Scovel (2012), even if  $\sum_{j=1}^{\infty} \gamma_{\mathcal{K}, j}^{\beta} e_j(\mathbf{s})^2 < \infty$  for all  $\mathbf{s} \in \Omega$  does not hold, we can always define the space  $\mathcal{N}_{\mathcal{K}_{m^*}}^{\beta}(\Omega)$  by the way as in (2.10).

An important property of  $\mathcal{N}_{\mathcal{K}_{m^*}}^\beta(\Omega)$  is that the space  $\mathcal{N}_{\mathcal{K}_{m^*}}^\beta(\Omega)$  is equivalent to a real interpolation space of  $L_2(\Omega)$  and  $W^{m^*}(\Omega)$ , denoted by  $[L_2(\Omega), W^{m^*}(\Omega)]_{\beta,2}$  (Steinwart and Scovel, 2012). The space defined by the real interpolation method is called Besov space, and denoted by  $B_{2,2}^r = [L_2(\Omega), W^{m^*}(\Omega)]_{r/m^*,2}$  for  $m^* > r > 0$ . In general, the real interpolation space (used for constructing Besov space) and the complex interpolation space (used for constructing Bessel potential space with norm (B.3)) are different, but fortunately in our case, the Sobolev space with norm (B.3) coincides  $B_{2,2}^m$  with equivalent norms (Edmunds and Triebel, 2008). Putting all things together, we can see that  $\mathcal{N}_{\mathcal{K}_{m^*}}^\beta(\Omega) = W^m(\Omega)$  with equivalent norms, where  $\beta = m/m^*$ .

## E Conditions in Section 3

In this section, we list the conditions used in Section 3 with discussion. Since  $\mathcal{K}_m(\cdot, \cdot)$  is a symmetric and positive definite kernel function, Mercer's theorem implies that

$$\mathcal{K}_m(\mathbf{s}, \mathbf{t}) = \sum_{j=1}^{\infty} \gamma_j \phi_j(\mathbf{s}) \phi_j(\mathbf{t}), \forall \mathbf{s}, \mathbf{t} \in \Omega, \quad (\text{E.1})$$

where  $\gamma_j$  and  $\phi_j$  are eigenvalues and eigenfunctions of  $\mathcal{K}_m(\cdot, \cdot)$ , respectively, and the convergence is absolute and uniform (provided that  $\mathcal{K}_m(\mathbf{s}, \mathbf{t})$  exists). We write  $\boldsymbol{\theta} = (\theta_1, \dots, \theta_q)^\top$ .

(C1) The random variables  $\mathbf{x}_j$  and  $\varepsilon_j$  in (2.1) are independent;  $\mathbf{x}_j$ 's are i.i.d. uniformly distributed on  $\Omega$ ;  $\varepsilon_j$ 's are i.i.d. random variables which are sub-Gaussian (van de Geer, 2000), i.e., satisfying

$$C^2(\mathbb{E} \exp(|\varepsilon_j|^2/C^2) - 1) \leq C', \quad j = 1, \dots, n.$$

(C2)  $\boldsymbol{\theta}^*$  is the unique solution to (2.4), and is an interior point of  $\Theta$ .

(C3) The matrix

$$\mathbf{V} := - \sum_{j=1}^{\infty} \frac{1}{\gamma_j} \frac{\partial^2}{\partial \boldsymbol{\theta} \partial \boldsymbol{\theta}^\top} \left( \int_{\Omega} (f_p(\mathbf{z}) - f_s(\mathbf{z}, \boldsymbol{\theta}^*)) \phi_j(\mathbf{z}) d\mathbf{z} \right)^2$$

is invertible, where  $\gamma_j$  and  $\phi_j(\cdot)$  are as in (E.1).

(C4) There exists  $m_1 > d/2$  such that  $m_1 \geq m$  (if  $m \leq d/2$ , then clearly  $m_1 \geq m$  holds) and the RKHS  $\mathcal{N}_{\Phi}(\Omega)$  in (2.5) is equivalent to  $W^{m_1}(\Omega)$ . Furthermore,  $\|f_p(\cdot)\|_{W^{m_1}(\Omega)} < \infty$ ,  $\lambda = o_{\mathbb{P}}(n^{-1/2-\epsilon_0})$  for some constant  $\epsilon_0 > 0$ ,  $\lambda^{-1} = O_{\mathbb{P}}(n^{\frac{2m_1}{2m_1+d}})$ , and  $\left\| f_p(\cdot) - \widehat{f}_p(\cdot) \right\|_{W^m(\Omega)} = o_{\mathbb{P}}(1)$ .

(C5) There exists  $\alpha_0 > 2m + m_1 - \kappa$  with  $0 \leq \kappa < \min(\frac{2m_1^2 - m_1 d}{2m_1 + d}, \frac{m_1}{1 + 4\epsilon_0})$  such that for all  $j, k = 1, \dots, q$  and  $t = 1, 2, \dots$ ,

$$\sup_{\boldsymbol{\theta} \in \Theta} \|f_s(\cdot, \boldsymbol{\theta})\|_{W^{\alpha_0}(\Omega)} + \left\| \frac{\partial f_s(\cdot, \boldsymbol{\theta})}{\partial \theta_j} \right\|_{W^{\alpha_0}(\Omega)} + \left\| \frac{\partial^2}{\partial \theta_j \partial \theta_k} f_s(\cdot, \boldsymbol{\theta}) \right\|_{W^{\alpha_0}(\Omega)} < \infty,$$

$$\frac{\partial^2}{\partial \theta_j \partial \theta_k} f_s(\cdot, \cdot) \in \mathcal{C}^1(\Omega \times \Theta), \phi_t(\cdot) \in W^{\max(\alpha_0, m_1)}(\Omega),$$

where  $m_1$  and  $\epsilon_0$  are as in Condition (C4).

(C6)  $\sup_{\boldsymbol{\theta} \in \Theta} \|f_s(\cdot, \boldsymbol{\theta}) - \widehat{f}_s(\cdot, \boldsymbol{\theta})\|_{W^{2m}(\Omega)} + \left\| \frac{\partial \widehat{f}_s(\cdot, \boldsymbol{\theta})}{\partial \theta_j} - \frac{\partial f_s(\cdot, \boldsymbol{\theta})}{\partial \theta_j} \right\|_{W^{2m}(\Omega)} = o_{\mathbb{P}}(n^{-1/2})$ , for all  $j = 1, \dots, q$ .

Conditions (C1)-(C3) are regularity conditions on the model. Similar conditions are also assumed in Tuo and Wu (2014); Xie and Xu (2020). Because we use Sobolev norm instead of the  $L_2$  norm used in Tuo and Wu (2014), there is an extra  $\gamma_j^{-1}$  in the expression of the matrix  $\mathbf{V}$  in Condition (C3). The matrix  $\mathbf{V}$  reduces to the invertible matrix in Theorem 1 of Tuo and Wu (2014) if  $m = 0$ .

Condition (C4) requires that the RKHS used in kernel ridge regression (2.5) has a higher smoothness than  $m$ . By the Gagliardo–Nirenberg interpolation inequality for functions in Sobolev spaces (Leoni, 2017; Brezis and Mironescu, 2019), the condition  $\|f_p(\cdot) - \widehat{f}_p(\cdot)\|_{W^m(\Omega)} = o_{\mathbb{P}}(1)$  can be easily fulfilled as long as  $m_1 > m$  and  $\|f_p(\cdot) - \widehat{f}_p(\cdot)\|_{L_2(\Omega)} = o_{\mathbb{P}}(1)$ , while the later has been widely established in literature; see van de Geer (2000); Fischer and Steinwart (2020) for example. Even if  $m_1 = m$ , as long as  $f_p(\cdot)$  has a smoothness higher than  $m$ , the condition  $\|f_p(\cdot) - \widehat{f}_p(\cdot)\|_{W^m(\Omega)} = o_{\mathbb{P}}(1)$  can be ensured (Lin et al., 2017).

Condition (C5) imposes regularity conditions on the computer model, while Condition (C6) imposes conditions on the surrogate model  $\widehat{f}_s(\cdot, \cdot)$ . In particular, the requirement  $\phi_t(\cdot) \in W^{\max(\alpha_0, m_1)}(\Omega)$  can be fulfilled if  $\mathcal{H}_m(\Omega)$  is an  $(m/\max(\alpha_0, m_1))$ -th power of an RKHS that is equivalent to  $W^{\max(\alpha_0, m_1)}(\Omega)$ . Moreover, Conditions (C5) and (C6) state that the computer model needs to be smoother than the Sobolev norm used in the Sobolev calibration, and the surrogate model needs to approximate the computer model well, in the sense that the Sobolev norm of the error is small. These conditions are reasonable considering the controllable cost of running codes. Also, these conditions reduce to the assumptions used in the  $L_2$  calibration if  $m = 0$ . Note that the assumption that the computer model lies in a function space with higher smoothness has also been used in Theorem 3.4 of Tuo et al. (2020), which states a convergence rate of the estimated calibration parameter via KO calibration. By the Sobolev embedding theorem (Adams and Fournier, 2003), Conditions (C5) and (C6) imply that for all  $1 \leq t < \infty$ ,  $j, k = 1, \dots, q$ ,  $\phi_t(\cdot) \in W^{\alpha'}(\Omega)$  and

$$\sup_{\boldsymbol{\theta} \in \Theta} \|f_s(\cdot, \boldsymbol{\theta})\|_{W^{\alpha'}(\Omega)} + \left\| \frac{\partial f_s(\cdot, \boldsymbol{\theta})}{\partial \theta_j} \right\|_{W^{\alpha'}(\Omega)} + \left\| \frac{\partial^2}{\partial \theta_j \partial \theta_k} f_s(\cdot, \boldsymbol{\theta}) \right\|_{W^{\alpha'}(\Omega)} < \infty,$$

for all  $0 \leq \alpha' \leq \alpha_0$ , and

$$\sup_{\boldsymbol{\theta} \in \Theta} \|f_s(\cdot, \boldsymbol{\theta}) - \widehat{f}_s(\cdot, \boldsymbol{\theta})\|_{W^{2m'}(\Omega)} + \left\| \frac{\partial \widehat{f}_s(\cdot, \boldsymbol{\theta})}{\partial \theta_j} - \frac{\partial f_s(\cdot, \boldsymbol{\theta})}{\partial \theta_j} \right\|_{W^{2m'}(\Omega)} = o_{\mathbb{P}}(n^{-1/2}),$$

for all  $j = 1, \dots, q$ ,  $0 \leq m' \leq m$ .

Condition (C5) is weaker than the conditions in Tuo and Wu (2014); Xie and Xu (2020), even if at the case  $m = 0$ . To see this, we set  $m = 0$ . In Tuo and Wu (2014); Xie and Xu (2020), it is required that  $\alpha_0 = m_1$ , while Condition (C5) implies that  $\alpha_0 > m_1 - \kappa$  is sufficient. Since  $\kappa$  can be larger than zero, it is possible that  $\alpha_0 < m_1$ . In other words, we consider the case where the computer model can even be *rougher* than the physical model at some parameter space of  $\boldsymbol{\theta}$ , which has not been presented in the literature as far as we know.

## F Conditions in Section 4

In this section, we list the conditions used in Section 4 with discussion. Without loss of generality, we assume that the variance of the Gaussian process satisfies  $\sigma^2 = 1$ , thus the correlation function equals the covariance function.

(C1') The random variables  $\boldsymbol{x}_j$  and  $\varepsilon_j$  in (2.1) are independent;  $\boldsymbol{x}_j$ 's are i.i.d. uniformly distributed on  $\Omega$ ;  $\varepsilon_j$ 's are i.i.d. normally distributed random variables.

(C2') Conditions (C2)-(C3) hold with probability one for  $f_p(\cdot)$ .

(C3') There exists  $m_2 > \max(d, m + d/2)$  such that

$$c_1(1 + \|\boldsymbol{\omega}\|_2^2)^{-m_2} \leq \mathcal{F}(\mathcal{K})(\boldsymbol{\omega}) \leq c_2(1 + \|\boldsymbol{\omega}\|_2^2)^{-m_2}, \forall \boldsymbol{\omega} \in \mathbb{R}^d,$$

where  $c_1$  and  $c_2$  are positive constants, and  $\mathcal{F}(\mathcal{K})(\boldsymbol{\omega})$  is the Fourier transform of  $\mathcal{K}$ .

(C4') Condition (C5) holds for  $\alpha_0 = 2m + m_2$  and in particular we have  $\phi_t(\cdot) \in W^{\alpha_0}(\Omega)$ .

Condition (C1') is a regularity condition on the model. The assumption that  $\varepsilon_j$ 's are normal is only for the ease of proof, and can be relaxed to the sub-Gaussian noise, with some additional mathematical treatment as in Wang and Jing (2021). Condition (C2') is a technical assumption for the Gaussian process  $f_p(\cdot)$  and the computer model  $f_s(\cdot, \boldsymbol{\theta})$ . Condition (C3') implies that the sample paths of  $f_p(\cdot)$  lie in  $W^{\tilde{m}}(\Omega)$  with probability one for some  $\tilde{m} > d/2$  (Steinwart, 2019). Condition (C4') is stronger than Condition (C5), which is because the Gaussian process has introduced more randomness than the deterministic function case, and it requires higher smoothness on the computer model.

## G Technical Proofs of Propositions and Theorems

In this section, we provide technical proofs of propositions and theorems in the main text.

## G.1 Proof of Proposition 2.1

Let  $\mathcal{N}_{\Psi_m}(\Omega)$  be the RKHS generated by  $\Psi_m$  defined in (2.8). Thus, as stated in Section B in the supplement, we have  $\mathcal{N}_{\Psi_m}(\Omega) = W^m(\Omega)$  with equivalent norms. By Mercer's Theorem, we have

$$\Psi_m(\mathbf{s}, \mathbf{t}) = \sum_{j=1}^{\infty} \gamma_j \phi_j(\mathbf{s}) \phi_j(\mathbf{t}), \forall \mathbf{s}, \mathbf{t} \in \Omega,$$

where  $\phi_j$  and  $\gamma_j$  are the eigenfunctions and eigenvalues of  $\Psi_m(\cdot, \cdot)$ , respectively, and the convergence is absolute and uniform. Furthermore, we have that  $\gamma_j \rightarrow 0$  as  $j \rightarrow \infty$  and  $\|\phi_j\|_{L_2(\Omega)} = 1$ . Theorem 10.29 of Wendland (2004) implies that  $\|\phi_k\|_{\mathcal{N}_{\Psi_m}(\Omega)}^2 = \sum_{j=1}^{\infty} \frac{\langle \phi_k(\cdot), \phi_j(\cdot) \rangle_{L_2(\Omega)}^2}{\gamma_j} = \frac{1}{\gamma_k}$ . Also, the equivalence of  $\|\cdot\|_{\mathcal{N}_{\Psi_m}(\Omega)}$  and  $\|\cdot\|_{W^m(\Omega)}$  implies that  $c_1 \|\phi_k\|_{\mathcal{N}_{\Psi_m}(\Omega)} \leq \|\phi_k\|_{W^m(\Omega)} \leq c_2 \|\phi_k\|_{\mathcal{N}_{\Psi_m}(\Omega)}$ . Thus, we can find  $k$  such that  $\gamma_k < \frac{c_1 \gamma_1}{c_2}$ . Let  $\delta_2 = \phi_1$  and  $\delta_1 = \phi_k$ . It can be easily verified that  $\|\delta_1\|_{L_2(\Omega)} = \|\delta_2\|_{L_2(\Omega)} = 1$  and  $\frac{\|\delta_1\|_{W^m(\Omega)}}{\|\delta_2\|_{W^m(\Omega)}} \geq \frac{c_1 \|\delta_1\|_{\mathcal{N}_{\Psi_m}(\Omega)}}{c_2 \|\delta_2\|_{\mathcal{N}_{\Psi_m}(\Omega)}} = \frac{c_1 \gamma_1}{c_2 \gamma_k} > c$ . This finishes the proof.  $\blacksquare$

## G.2 Proof of Proposition 3.1

From the definition of  $\widehat{\boldsymbol{\theta}}_S$  and  $\boldsymbol{\theta}_S^*$  in (2.7) and (2.4), it suffices to prove that  $\|\widehat{f}_p(\cdot) - \widehat{f}_s(\cdot, \boldsymbol{\theta})\|_{\mathcal{H}_m(\Omega)}$  converges to  $\|f_p(\cdot) - f_s(\cdot, \boldsymbol{\theta})\|_{\mathcal{H}_m(\Omega)}$  uniformly with respect to  $\boldsymbol{\theta}$  in probability. This is ensured by

$$\begin{aligned} & \left| \left\| \widehat{f}_p(\cdot) - \widehat{f}_s(\cdot, \boldsymbol{\theta}) \right\|_{\mathcal{H}_m(\Omega)} - \|f_p(\cdot) - f_s(\cdot, \boldsymbol{\theta})\|_{\mathcal{H}_m(\Omega)} \right| \\ & \leq \left\| \widehat{f}_p(\cdot) - \widehat{f}_s(\cdot, \boldsymbol{\theta}) - (f_p(\cdot) - f_s(\cdot, \boldsymbol{\theta})) \right\|_{\mathcal{H}_m(\Omega)} \\ & \leq \left\| \widehat{f}_p(\cdot) - f_p(\cdot) \right\|_{\mathcal{H}_m(\Omega)} + \left\| \widehat{f}_s(\cdot, \boldsymbol{\theta}) - f_s(\cdot, \boldsymbol{\theta}) \right\|_{\mathcal{H}_m(\Omega)} \\ & \leq C_1 \left( \left\| \widehat{f}_p(\cdot) - f_p(\cdot) \right\|_{W^m(\Omega)} + \left\| \widehat{f}_s(\cdot, \boldsymbol{\theta}) - f_s(\cdot, \boldsymbol{\theta}) \right\|_{W^m(\Omega)} \right) \\ & = o_{\mathbb{P}}(1), \end{aligned}$$

where the first and second inequalities are from the triangle inequality, the third inequality is because of the equivalence of  $\|\cdot\|_{W^m(\Omega)}$  and  $\|\cdot\|_{\mathcal{H}_m(\Omega)}$ , and the last equality is guaranteed by Conditions (C4) and (C6). This finishes the proof.

## G.3 Proof of Theorem 3.2

We first present several lemmas used in this proof. Lemma G.1 is Theorem 3.1 of van de Geer (2014). Lemma G.2 is Lemma 8.4 of van de Geer (2000). Lemma G.3 is Lemma H.2 of Wang and Jing (2021). Lemma G.4 is a direct result of Theorem 10.2 and Theorem 5.16 of van de Geer (2000).

**Lemma G.1.** Let  $\mathcal{F}$  and  $\mathcal{G}$  be two function classes. Let  $R_1 := \sup_{f \in \mathcal{F}} \|f\|_{L_2(\Omega)}$ ,  $K_1 := \sup_{f \in \mathcal{F}} \|f\|_{L_\infty(\Omega)}$ ,  $R_2 := \sup_{g \in \mathcal{G}} \|g\|_{L_2(\Omega)}$ ,  $K_2 := \sup_{g \in \mathcal{G}} \|g\|_{L_\infty(\Omega)}$ . Suppose  $R_1 K_2 \leq R_2 K_1$ . Consider values  $t > 4$  and  $n$  such that

$$\begin{aligned} \left( \frac{2R_1 J_\infty(K_1, \mathcal{F}) + R_1 K_1 \sqrt{t}}{\sqrt{n}} + \frac{4J_\infty(K_1, \mathcal{F})^2 + K_1^2 t}{n} \right) &\leq \frac{R_1^2}{C_1}, \\ \left( \frac{2R_2 J_\infty(K_2, \mathcal{G}) + R_2 K_2 \sqrt{t}}{\sqrt{n}} + \frac{4J_\infty(K_2, \mathcal{G})^2 + K_2^2 t}{n} \right) &\leq \frac{R_2^2}{C_1}, \end{aligned} \quad (\text{G.1})$$

where

$$J_\infty(z, \mathcal{F}) := C_2 \inf_{\delta > 0} \left[ z \int_{\delta/4}^1 \sqrt{\mathcal{H}_\infty(uz/2, \mathcal{F})} du + \sqrt{n} \delta z \right],$$

with  $C_2$  as another constant. Denote the empirical measure of  $f$  by  $P_n f$  and its theoretical measure by  $Pf$ . Then with probability at least  $1 - 12 \exp(-t)$ ,

$$\frac{1}{8C_1} \sup_{f \in \mathcal{F}, g \in \mathcal{G}} \left| (P_n - P)fg \right| \leq \frac{R_1 J_\infty(K_2, \mathcal{G}) + R_2 J_\infty(R_1 K_2 / R_2, \mathcal{F}) + R_1 K_2 \sqrt{t}}{\sqrt{n}} + \frac{K_1 K_2 t}{n}.$$

**Lemma G.2.** Let  $\mathcal{K}(\cdot, \cdot)$  be a kernel function such that

$$\mathcal{H}(\delta, \mathcal{B}_{\mathcal{N}_{\mathcal{K}}(\Omega)}(1), \|\cdot\|_{L_\infty(\Omega)}) \leq C_1 \left( \frac{1}{\delta} \right)^{\frac{d}{m}}.$$

Then for all  $t > C$ , with probability at least  $1 - C_1 \exp(-C_2 t^2)$ ,

$$\sup_{g \in \mathcal{N}_{\mathcal{K}}(\Omega)} \frac{|\langle \epsilon, g \rangle_n|}{\|g\|_n^{1-\frac{d}{2m}} \|g\|_{\mathcal{N}_{\mathcal{K}}(\Omega)}^{\frac{d}{2m}}} \leq t n^{-\frac{1}{2}}.$$

**Lemma G.3.** Let  $m_1 \geq m_0 > d/2$ ,  $\mathcal{K}(\cdot, \cdot)$  be a positive definite kernel function on  $\Omega$  such that  $\mathcal{N}_{\mathcal{K}}(\Omega)$  is equivalent to  $W^{m_1}(\Omega)$ , and  $f \in W^{m_0}(\Omega)$ . Let  $f^*$  be the solution to the optimization problem

$$\min_{\tilde{f} \in \mathcal{N}_{\mathcal{K}}(\Omega)} \|f - \tilde{f}\|_{L_2(\Omega)}^2 + \lambda_0 \|\tilde{f}\|_{\mathcal{N}_{\mathcal{K}}(\Omega)}^2.$$

Then we have

$$\|f - f^*\|_{L_2(\Omega)}^2 + \lambda_0 \|f^*\|_{\mathcal{N}_{\mathcal{K}}(\Omega)}^2 \leq C \lambda_0^{\frac{m_0}{m_1}} \|f\|_{W^{m_0}(\Omega)}^2.$$

**Lemma G.4.** Suppose  $f \in W^m(\Omega)$ , the reproducing kernel Hilbert space  $\mathcal{N}_{\Phi_1}(\Omega)$  generated by  $\Phi_1(\cdot, \cdot)$  is equivalent to  $W^m(\Omega)$ , and  $\lambda^{-1} = O_{\mathbb{P}}(n^{\frac{2m}{2m+d}})$ . Furthermore, assume Condition (C1) holds. Let  $(\mathbf{x}_j, y_j)$ ,  $j = 1, \dots, n$  be observations satisfying

$$y_j = f(\mathbf{x}_j) + \varepsilon_j.$$

Then the estimator given by

$$\hat{f}(\cdot) := \operatorname{argmin}_{g \in \mathcal{N}_{\Phi_1}(\Omega)} \frac{1}{n} \sum_{j=1}^n (y_j - g(\mathbf{x}_j))^2 + \lambda \|g\|_{\mathcal{N}_{\Phi_1}(\Omega)}^2,$$

satisfies

$$\|\hat{f} - f\|_{L_2(\Omega)} = O_{\mathbb{P}}(\lambda^{\frac{1}{2}} \vee n^{-\frac{1}{2}} \lambda^{-\frac{d}{4m}}), \quad \|\hat{f}\|_{\mathcal{N}_{\Phi_1}(\Omega)} = O_{\mathbb{P}}(1 \vee n^{-\frac{1}{2}} \lambda^{-\frac{2m+d}{4m}}).$$

Before the proof of Theorem 3.2, let us introduce some additional notation and results. Let  $\alpha = \max(\alpha_0, m_1)$ , where  $\alpha_0$  is as in Condition (C5). Choose an RKHS that is equivalent to  $W^\alpha(\Omega)$ . Denote this RKHS as  $\mathcal{N}_\alpha(\Omega)$ , and the corresponding kernel function as  $\Psi_\alpha(\cdot, \cdot)$ . Then Mercer's Theorem implies that it possesses an absolutely and uniformly convergent representations as

$$\Psi_\alpha(\mathbf{s}, \mathbf{t}) = \sum_{j=1}^{\infty} \gamma_{\Psi,j} \psi_j(\mathbf{s}) \psi_j(\mathbf{t}), \forall \mathbf{s}, \mathbf{t} \in \Omega,$$

where  $\gamma_{\Psi,j}$  and  $\psi_j$  are eigenvalues and eigenfunctions of  $\Psi_\alpha(\cdot, \cdot)$ , respectively. Therefore, for  $0 \leq \beta \leq 1$ , we can construct  $\beta$ -th powers of  $\mathcal{N}_\alpha(\Omega)$  as

$$\mathcal{N}_\alpha^\beta(\Omega) = \left\{ f(\cdot) = \sum_{j=1}^{\infty} a_j \gamma_{\Psi,j}^{\beta/2} \psi_j(\cdot) : \sum_{j=1}^{\infty} a_j^2 < \infty \right\},$$

with inner product defined as

$$\langle f, g \rangle_{\mathcal{N}_\alpha^\beta(\Omega)} = \sum_{j=1}^{\infty} a_j b_j, \text{ for } f(\cdot) = \sum_{j=1}^{\infty} a_j \gamma_{\Psi,j}^{\beta/2} \psi_j(\cdot), g(\cdot) = \sum_{j=1}^{\infty} b_j \gamma_{\Psi,j}^{\beta/2} \psi_j(\cdot), f, g \in \mathcal{N}_\alpha^\beta(\Omega). \quad (\text{G.2})$$

In particular, Steinwart and Scovel (2012) showed that  $\{\gamma_{\Psi,j}^{\beta/2} \psi_j(\cdot)\}$  is an orthonormal basis of  $\mathcal{N}_\alpha^\beta(\Omega)$ , and Proposition 4.2 of Steinwart and Scovel (2012) (and the arguments thereafter) implies that  $\mathcal{N}_\alpha^\beta(\Omega)$  is independent of the choice of  $\psi_j(\cdot) \in W^\alpha(\Omega)$ , i.e., the orthonormal basis of  $L_2(\Omega)$  (but needs to be in  $W^\alpha(\Omega)$ ). By Condition (C5),  $\phi_j(\cdot) \in W^\alpha(\Omega)$ , thus  $\mathcal{N}_\alpha^\beta(\Omega)$  can be also expressed as

$$\mathcal{N}_\alpha^\beta(\Omega) = \left\{ f(\cdot) = \sum_{j=1}^{\infty} a_j \gamma_{\Psi,j}^{\beta/2} \phi_j(\cdot) : \sum_{j=1}^{\infty} a_j^2 < \infty \right\},$$

with inner product defined as in (G.2), by replacing  $\psi_j(\cdot)$  with  $\phi_j(\cdot)$ . Furthermore,  $\mathcal{N}_\alpha^\beta(\Omega)$  is equivalent to the interpolation space of  $W^{\alpha\beta}(\Omega) = [L_2(\Omega), W^\alpha(\Omega)]_{\beta,2}$ . The space  $\mathcal{N}_\alpha^\beta(\Omega)$  will play an important role in the proofs of Theorems 3.2 and 4.2, as we will see later.

*Proof of Theorem 3.2.* By Theorem 10.29 of Wendland (2004), for any  $\boldsymbol{\theta}$ , we have

$$\begin{aligned} \|f_p(\cdot) - f_s(\cdot, \boldsymbol{\theta})\|_{\mathcal{H}_m(\Omega)}^2 &= \sum_{j=1}^{\infty} \frac{\langle f_p(\cdot) - f_s(\cdot, \boldsymbol{\theta}), \phi_j(\cdot) \rangle_{L_2(\Omega)}^2}{\gamma_j}, \\ \|\widehat{f}_p(\cdot) - \widehat{f}_s(\cdot, \boldsymbol{\theta})\|_{\mathcal{H}_m(\Omega)}^2 &= \sum_{j=1}^{\infty} \frac{\langle \widehat{f}_p(\cdot) - \widehat{f}_s(\cdot, \boldsymbol{\theta}), \phi_j(\cdot) \rangle_{L_2(\Omega)}^2}{\gamma_j}. \end{aligned}$$

Since  $\boldsymbol{\theta}_S^*$  minimizes (2.4) and  $\widehat{\boldsymbol{\theta}}_S$  minimizes (2.7), by Conditions (C2) and (C5) we have that

for  $t = 1, \dots, q$ ,

$$\begin{aligned}
0 &= \frac{\partial}{\partial \theta_t} \|f_p(\cdot) - f_s(\cdot, \boldsymbol{\theta})\|_{\mathcal{H}_m(\Omega)}^2 \Big|_{\boldsymbol{\theta}=\boldsymbol{\theta}_S^*} \\
&= - \sum_{j=1}^{\infty} \frac{2}{\gamma_j} \int_{\Omega} (f_p(\mathbf{z}) - f_s(\mathbf{z}, \boldsymbol{\theta}_S^*)) \phi_j(\mathbf{z}) d\mathbf{z} \int_{\Omega} \frac{\partial f_s(\mathbf{z}, \boldsymbol{\theta}_S^*)}{\partial \theta_t} \phi_j(\mathbf{z}) d\mathbf{z} \\
&= - 2 \left\langle f_p(\cdot) - f_s(\cdot, \boldsymbol{\theta}_S^*), \frac{\partial f_s(\cdot, \boldsymbol{\theta}_S^*)}{\partial \theta_t} \right\rangle_{\mathcal{H}_m(\Omega)}, \tag{G.3}
\end{aligned}$$

and

$$\begin{aligned}
0 &= \frac{\partial}{\partial \theta_t} \left\| \widehat{f}_p(\cdot) - \widehat{f}_s(\cdot, \boldsymbol{\theta}) \right\|_{\mathcal{H}_m(\Omega)}^2 \Big|_{\boldsymbol{\theta}=\widehat{\boldsymbol{\theta}}_S} \\
&= - \sum_{j=1}^{\infty} \frac{2}{\gamma_j} \int_{\Omega} (\widehat{f}_p(\mathbf{z}) - \widehat{f}_s(\mathbf{z}, \widehat{\boldsymbol{\theta}}_S)) \phi_j(\mathbf{z}) d\mathbf{z} \int_{\Omega} \frac{\partial \widehat{f}_s(\mathbf{z}, \widehat{\boldsymbol{\theta}}_S)}{\partial \theta_t} \phi_j(\mathbf{z}) d\mathbf{z} \\
&= - \sum_{j=1}^{\infty} \frac{2}{\gamma_j} \int_{\Omega} (\widehat{f}_p(\mathbf{z}) - f_s(\mathbf{z}, \widehat{\boldsymbol{\theta}}_S)) \phi_j(\mathbf{z}) d\mathbf{z} \int_{\Omega} \frac{\partial f_s(\mathbf{z}, \widehat{\boldsymbol{\theta}}_S)}{\partial \theta_t} \phi_j(\mathbf{z}) d\mathbf{z} + I_1 + I_2, \tag{G.4}
\end{aligned}$$

where

$$\begin{aligned}
I_1 &= - \sum_{j=1}^{\infty} \frac{2}{\gamma_j} \int_{\Omega} (f_s(\mathbf{z}, \widehat{\boldsymbol{\theta}}_S) - \widehat{f}_s(\mathbf{z}, \widehat{\boldsymbol{\theta}}_S)) \phi_j(\mathbf{z}) d\mathbf{z} \int_{\Omega} \frac{\partial \widehat{f}_s(\mathbf{z}, \widehat{\boldsymbol{\theta}}_S)}{\partial \theta_t} \phi_j(\mathbf{z}) d\mathbf{z}, \\
I_2 &= - \sum_{j=1}^{\infty} \frac{2}{\gamma_j} \int_{\Omega} (\widehat{f}_p(\mathbf{z}) - f_s(\mathbf{z}, \widehat{\boldsymbol{\theta}}_S)) \phi_j(\mathbf{z}) d\mathbf{z} \int_{\Omega} \left( \frac{\partial \widehat{f}_s(\mathbf{z}, \widehat{\boldsymbol{\theta}}_S)}{\partial \theta_t} - \frac{\partial f_s(\mathbf{z}, \widehat{\boldsymbol{\theta}}_S)}{\partial \theta_t} \right) \phi_j(\mathbf{z}) d\mathbf{z}.
\end{aligned}$$

Consider the  $\beta$ -th power of  $\mathcal{N}_{\alpha}(\Omega)$  with  $\alpha\beta = m$ . Then  $\mathcal{N}_{\alpha}^{m/\alpha}(\Omega)$  is equivalent to  $W^m(\Omega)$ , thus is also equivalent to  $\mathcal{H}_m(\Omega)$ . By the equivalence of  $\mathcal{N}_{\alpha}^{m/\alpha}(\Omega)$  and  $\mathcal{H}_m(\Omega)$ , the eigenvalues of two spaces satisfy  $C_1\gamma_j \leq \gamma_{\Psi,j}^{m/\alpha} \leq C_2\gamma_j$ .

The first term  $I_1$  can be bounded by

$$\begin{aligned}
|I_1| &\leq 2 \left( \sum_{j=1}^{\infty} \left( \int_{\Omega} (f_s(\mathbf{z}, \widehat{\boldsymbol{\theta}}_S) - \widehat{f}_s(\mathbf{z}, \widehat{\boldsymbol{\theta}}_S)) \phi_j(\mathbf{z}) d\mathbf{z} \right)^2 \right)^{1/2} \\
&\quad \times \left( \sum_{j=1}^{\infty} \frac{1}{\gamma_j^2} \left( \int_{\Omega} \frac{\partial \widehat{f}_s(\mathbf{z}, \widehat{\boldsymbol{\theta}}_S)}{\partial \theta_t} \phi_j(\mathbf{z}) d\mathbf{z} \right)^2 \right)^{1/2} \\
&\leq 2C_3 \|f_s(\cdot, \widehat{\boldsymbol{\theta}}_S) - \widehat{f}_s(\cdot, \widehat{\boldsymbol{\theta}}_S)\|_{L_2(\Omega)} \left( \sum_{j=1}^{\infty} \frac{1}{\gamma_{\Psi,j}^{2m/\alpha}} \left( \int_{\Omega} \frac{\partial \widehat{f}_s(\mathbf{z}, \widehat{\boldsymbol{\theta}}_S)}{\partial \theta_t} \phi_j(\mathbf{z}) d\mathbf{z} \right)^2 \right)^{1/2} \\
&= o_{\mathbb{P}}(n^{-1/2}) \left\| \frac{\partial \widehat{f}_s(\cdot, \widehat{\boldsymbol{\theta}}_S)}{\partial \theta_t} \right\|_{\mathcal{N}_{\alpha}^{2m/\alpha}(\Omega)}, \tag{G.5}
\end{aligned}$$



where the first inequality is because of the Cauchy-Schwarz inequality, the second inequality is because  $\phi_j(\cdot)$  is an orthogonal basis of  $L_2(\Omega)$  and our construction of  $\mathcal{N}_\alpha^{2m/\alpha}(\Omega)$ , and the last equality is by Condition (C6).

Because of the equivalence of  $\mathcal{N}_\alpha^{2m/\alpha}(\Omega)$  and  $W^{2m}(\Omega)$ , together with Conditions (C5) and (C6), we have

$$\begin{aligned} \left\| \frac{\partial \widehat{f}_s(\cdot, \widehat{\boldsymbol{\theta}}_S)}{\partial \theta_t} \right\|_{\mathcal{N}_\alpha^{2m/\alpha}(\Omega)} &\leq C_4 \left\| \frac{\partial \widehat{f}_s(\cdot, \widehat{\boldsymbol{\theta}}_S)}{\partial \theta_t} \right\|_{W^{2m}(\Omega)} \\ &\leq C_4 \left( \left\| \frac{\partial f_s(\cdot, \widehat{\boldsymbol{\theta}}_S)}{\partial \theta_t} \right\|_{W^{2m}(\Omega)} + \left\| \frac{\partial \widehat{f}_s(\cdot, \widehat{\boldsymbol{\theta}}_S)}{\partial \theta_t} - \frac{\partial f_s(\cdot, \widehat{\boldsymbol{\theta}}_S)}{\partial \theta_t} \right\|_{W^{2m}(\Omega)} \right) \\ &\leq C_5, \end{aligned} \tag{G.6}$$

where the second inequality is because of the triangle inequality, and the third inequality is because of Conditions (C5) and (C6). Plugging (G.6) in (G.5) leads to

$$I_1 = o_{\mathbb{P}}(n^{-1/2}). \tag{G.7}$$

Similarly, the second term  $I_2$  can be bounded by

$$\begin{aligned} |I_2| &\leq 2 \left( \sum_{j=1}^{\infty} \frac{1}{\gamma_j^2} \left( \int_{\Omega} \left( \frac{\partial \widehat{f}_s(\mathbf{z}, \widehat{\boldsymbol{\theta}}_S)}{\partial \theta_t} - \frac{\partial f_s(\mathbf{z}, \widehat{\boldsymbol{\theta}}_S)}{\partial \theta_t} \right) \phi_j(\mathbf{z}) d\mathbf{z} \right)^2 \right)^{1/2} \\ &\quad \times \left( \sum_{j=1}^{\infty} \left( \int_{\Omega} (\widehat{f}_p(\mathbf{z}) - f_s(\mathbf{z}, \widehat{\boldsymbol{\theta}}_S)) \phi_j(\mathbf{z}) d\mathbf{z} \right)^2 \right)^{1/2} \\ &\leq 2C_6 \left\| \frac{\partial \widehat{f}_s(\cdot, \widehat{\boldsymbol{\theta}}_S)}{\partial \theta_t} - \frac{\partial f_s(\cdot, \widehat{\boldsymbol{\theta}}_S)}{\partial \theta_t} \right\|_{\mathcal{N}_\alpha^{2m/\alpha}(\Omega)} \left\| \widehat{f}_p(\cdot) - f_s(\cdot, \widehat{\boldsymbol{\theta}}_S) \right\|_{L_2(\Omega)} \\ &\leq 2C_7 \left\| \frac{\partial \widehat{f}_s(\cdot, \widehat{\boldsymbol{\theta}}_S)}{\partial \theta_t} - \frac{\partial f_s(\cdot, \widehat{\boldsymbol{\theta}}_S)}{\partial \theta_t} \right\|_{W^{2m}(\Omega)} \left( \left\| \widehat{f}_p(\cdot) \right\|_{L_2(\Omega)} + \left\| f_s(\cdot, \widehat{\boldsymbol{\theta}}_S) \right\|_{L_2(\Omega)} \right) \\ &= o_{\mathbb{P}}(n^{-1/2}) \left( \left\| \widehat{f}_p(\cdot) \right\|_{L_2(\Omega)} + \left\| f_s(\cdot, \widehat{\boldsymbol{\theta}}_S) \right\|_{L_2(\Omega)} \right), \end{aligned} \tag{G.8}$$

where the first inequality is because of the Cauchy-Schwarz inequality, the second inequality is because  $\phi_j(\cdot)$  is an orthogonal basis of  $L_2(\Omega)$  and because of our construction of  $\mathcal{N}_\alpha^{2m/\alpha}(\Omega)$ , the third inequality is by the triangle inequality and the equivalence of  $\mathcal{N}_\alpha^{2m/\alpha}(\Omega)$  and  $W^{2m}(\Omega)$ , and the last equality is by Condition (C6).

Condition (C4) implies that

$$\left\| \widehat{f}_p(\cdot) \right\|_{L_2(\Omega)} \leq \left\| f_p(\cdot) \right\|_{L_2(\Omega)} + \left\| \widehat{f}_p(\cdot) - f_p(\cdot) \right\|_{L_2(\Omega)} \leq C_8 + o_{\mathbb{P}}(1),$$

which, together with (G.8) and Condition (C5), implies that

$$I_2 = o_{\mathbb{P}}(n^{-1/2}). \tag{G.9}$$

Combining (G.7) and (G.9) leads to

$$I_1 + I_2 = o_{\mathbb{P}}(n^{-1/2}). \quad (\text{G.10})$$

Plugging (G.10) in (G.4) leads to

$$\begin{aligned} o_{\mathbb{P}}(n^{-1/2}) &= \sum_{j=1}^{\infty} \frac{2}{\gamma_j} \int_{\Omega} (\widehat{f}_p(\mathbf{z}) - f_s(\mathbf{z}, \widehat{\boldsymbol{\theta}}_S)) \phi_j(\mathbf{z}) d\mathbf{z} \int_{\Omega} \frac{\partial f_s(\mathbf{z}, \widehat{\boldsymbol{\theta}}_S)}{\partial \theta_t} \phi_j(\mathbf{z}) d\mathbf{z} \\ &= \sum_{j=1}^{\infty} \frac{2}{\gamma_j} \int_{\Omega} (f_p(\mathbf{z}) - f_s(\mathbf{z}, \widehat{\boldsymbol{\theta}}_S)) \phi_j(\mathbf{z}) d\mathbf{z} \int_{\Omega} \frac{\partial f_s(\mathbf{z}, \widehat{\boldsymbol{\theta}}_S)}{\partial \theta_t} \phi_j(\mathbf{z}) d\mathbf{z} \\ &\quad + \sum_{j=1}^{\infty} \frac{2}{\gamma_j} \int_{\Omega} (\widehat{f}_p(\mathbf{z}) - f_p(\mathbf{z})) \phi_j(\mathbf{z}) d\mathbf{z} \int_{\Omega} \frac{\partial f_s(\mathbf{z}, \widehat{\boldsymbol{\theta}}_S)}{\partial \theta_t} \phi_j(\mathbf{z}) d\mathbf{z} \\ &= J_1 + J_2, \end{aligned} \quad (\text{G.11})$$

where the change of summation order can be checked by verifying the terms in  $J_1$  and  $J_2$  are absolutely summable. If  $J_1$  and  $J_2$  are absolutely summable, then Riemann rearrangement theorem justifies the change of summation order. In fact, by Conditions (C4), (C5), and (C6), we can see that  $J_1$  and  $J_2$  are absolutely summable. Take  $J_1$  as an example. To verify the absolute convergence, we need to bound

$$\sum_{j=1}^{\infty} \frac{2}{\gamma_j} \left| \int_{\Omega} (f_p(\mathbf{z}) - f_s(\mathbf{z}, \widehat{\boldsymbol{\theta}}_S)) \phi_j(\mathbf{z}) d\mathbf{z} \int_{\Omega} \frac{\partial f_s(\mathbf{z}, \widehat{\boldsymbol{\theta}}_S)}{\partial \theta_t} \phi_j(\mathbf{z}) d\mathbf{z} \right|,$$

which can be done by

$$\begin{aligned} &\sum_{j=1}^{\infty} \frac{2}{\gamma_j} \left| \int_{\Omega} (f_p(\mathbf{z}) - f_s(\mathbf{z}, \widehat{\boldsymbol{\theta}}_S)) \phi_j(\mathbf{z}) d\mathbf{z} \int_{\Omega} \frac{\partial f_s(\mathbf{z}, \widehat{\boldsymbol{\theta}}_S)}{\partial \theta_t} \phi_j(\mathbf{z}) d\mathbf{z} \right| \\ &\leq 2 \left( \sum_{j=1}^{\infty} \left( \int_{\Omega} (f_p(\mathbf{z}) - f_s(\mathbf{z}, \widehat{\boldsymbol{\theta}}_S)) \phi_j(\mathbf{z}) d\mathbf{z} \right)^2 \right)^{1/2} \left( \sum_{j=1}^{\infty} \frac{1}{\gamma_j^2} \left( \int_{\Omega} \frac{\partial f_s(\mathbf{z}, \widehat{\boldsymbol{\theta}}_S)}{\partial \theta_t} \phi_j(\mathbf{z}) d\mathbf{z} \right)^2 \right)^{1/2} \\ &\leq 2C_9 \|f_p(\cdot) - f_s(\cdot, \widehat{\boldsymbol{\theta}}_S)\|_{L_2(\Omega)} \left\| \frac{\partial f_s(\mathbf{z}, \widehat{\boldsymbol{\theta}}_S)}{\partial \theta_t} \right\|_{W^{2m}(\Omega)} \\ &< \infty, \end{aligned}$$

where the first inequality is by the Cauchy-Schwarz inequality, the second inequality can be obtained similarly as in bounding  $I_1$  in (G.5), and the last inequality is by Conditions (C4) and (C5). In the rest of the Supplement, we do not provide justification of the change of summation order for the brevity of the proofs. One can check the change of summation order by a similar approach as above by verifying the absolute convergence.

Consider  $J_1$ . Define

$$v_t(\boldsymbol{\theta}) = 2 \left\langle f_p(\cdot) - f_s(\cdot, \boldsymbol{\theta}), \frac{\partial f_s(\cdot, \boldsymbol{\theta})}{\partial \theta_t} \right\rangle_{\mathcal{H}_m(\Omega)}.$$

Then we have  $J_1 = v_t(\widehat{\boldsymbol{\theta}}_S)$ , and by (G.3),  $v_t(\boldsymbol{\theta}_S^*) = 0$ . By applying Taylor expansion to  $v_t(\boldsymbol{\theta})$  at point  $\boldsymbol{\theta}_S^*$ , we obtain

$$J_1 = v_t(\boldsymbol{\theta}_S^*) + \frac{\partial v_t(\widetilde{\boldsymbol{\theta}})}{\partial \boldsymbol{\theta}^\top}(\widehat{\boldsymbol{\theta}}_S - \boldsymbol{\theta}_S^*) = \frac{\partial v_t(\widetilde{\boldsymbol{\theta}})}{\partial \boldsymbol{\theta}^\top}(\widehat{\boldsymbol{\theta}}_S - \boldsymbol{\theta}_S^*),$$

which, together with (G.11), leads to

$$\frac{\partial v_t(\widetilde{\boldsymbol{\theta}})}{\partial \boldsymbol{\theta}^\top}(\widehat{\boldsymbol{\theta}}_S - \boldsymbol{\theta}_S^*) + J_2 = o_{\mathbb{P}}(n^{-1/2}), \quad (\text{G.12})$$

where  $\widetilde{\boldsymbol{\theta}}$  lies between  $\boldsymbol{\theta}_S^*$  and  $\widehat{\boldsymbol{\theta}}_S$ .

By the consistency of  $\widehat{\boldsymbol{\theta}}_S$  as in Proposition 3.1, we have  $\widetilde{\boldsymbol{\theta}} \xrightarrow{p} \boldsymbol{\theta}^*$ . This implies that

$$\begin{aligned} \frac{\partial v(\widetilde{\boldsymbol{\theta}})}{\partial \boldsymbol{\theta}^\top} &= - \sum_{j=1}^{\infty} \frac{1}{\gamma_j} \frac{\partial^2}{\partial \boldsymbol{\theta} \partial \boldsymbol{\theta}^\top} \left( \int_{\Omega} (f_p(\mathbf{z}) - f_s(\mathbf{z}, \widetilde{\boldsymbol{\theta}})) \phi_j(\mathbf{z}) d\mathbf{z} \right)^2 \\ &\xrightarrow{\mathbb{P}} - \sum_{j=1}^{\infty} \frac{1}{\gamma_j} \frac{\partial^2}{\partial \boldsymbol{\theta} \partial \boldsymbol{\theta}^\top} \left( \int_{\Omega} (f_p(\mathbf{z}) - f_s(\mathbf{z}, \boldsymbol{\theta}_S^*)) \phi_j(\mathbf{z}) d\mathbf{z} \right)^2 \\ &= \mathbf{V}, \end{aligned} \quad (\text{G.13})$$

where  $v(\boldsymbol{\theta}) = 2 \left\langle f_p(\cdot) - f_s(\cdot, \boldsymbol{\theta}), \frac{\partial f_s(\cdot, \boldsymbol{\theta})}{\partial \boldsymbol{\theta}} \right\rangle_{\mathcal{H}_m(\Omega)} = (v_1(\boldsymbol{\theta}), \dots, v_q(\boldsymbol{\theta}))^\top$  and  $\mathbf{V}$  is as in Condition (C3).

Consider  $J_2$ . Define

$$A_{1t}(\cdot, \boldsymbol{\theta}) = \sum_{j=1}^{\infty} \frac{1}{\gamma_j} \int_{\Omega} \frac{\partial f_s(\mathbf{z}, \boldsymbol{\theta})}{\partial \theta_t} \phi_j(\mathbf{z}) d\mathbf{z} \cdot \phi_j(\cdot).$$

Theorem 10.29 of Wendland (2004) implies that

$$\sup_{\boldsymbol{\theta} \in \Theta} \|A_{1t}(\cdot, \boldsymbol{\theta})\|_{\mathcal{N}_\alpha^{\beta_1}(\Omega)}^2 = \sup_{\boldsymbol{\theta} \in \Theta} \sum_{j=1}^{\infty} \frac{1}{\gamma_j^2 \gamma_{\Psi, j}^{\beta_1}} \left( \int_{\Omega} \frac{\partial f_s(\mathbf{z}, \boldsymbol{\theta})}{\partial \theta_t} \phi_j(\mathbf{z}) d\mathbf{z} \right)^2 \leq C_{10}, \quad (\text{G.14})$$

where  $\beta_1 = \frac{1}{\alpha} \left( \frac{2m_1 d}{2m_1 + d} + \epsilon_1 \right)$  with  $\epsilon_1 = \frac{2m_1^2 - m_1 d}{2m_1 + d} - \kappa > 0$ , and the last inequality is by Condition (C5) and the equivalence of  $\mathcal{N}_\alpha^{m/\alpha}(\Omega)$  and  $\mathcal{H}_m(\Omega)$ . Thus,  $A_{1t}(\cdot, \boldsymbol{\theta}) \in W^{\alpha\beta_1}(\Omega)$  because of the equivalence of  $\mathcal{N}_\alpha^{\beta_1}(\Omega)$  and  $W^{\alpha\beta_1}(\Omega)$ . We also have

$$m_1 - \kappa = \alpha\beta_1 > \frac{2m_1 d}{2m_1 + d} > \frac{d}{2}, \text{ and } 2m + \alpha\beta_1 < \alpha.$$

Let

$$\mathcal{L}_n(f) = \frac{1}{n} \sum_{j=1}^n (y_j - f(\mathbf{x}_j))^2 + \lambda_n \|f\|_{\mathcal{N}_\Phi(\Omega)}^2.$$

Since  $\widehat{f}_p(\cdot)$  minimizes  $\mathcal{L}_n$  over  $\mathcal{N}_\Phi(\Omega)$ , we have

$$\begin{aligned}
0 &= \frac{\partial}{\partial \eta} \mathcal{L}_n \left( \widehat{f}_p(\cdot) + \eta \widehat{A}_{1t}(\cdot, \widehat{\boldsymbol{\theta}}_S) \right) \Big|_{\eta=0} \\
&= \frac{2}{n} \sum_{k=1}^n \left( \widehat{f}_p(\mathbf{x}_k) - y_k \right) \widehat{A}_{1t}(\mathbf{x}_k, \widehat{\boldsymbol{\theta}}_S) + 2\lambda \left\langle \widehat{f}_p(\cdot), \widehat{A}_{1t}(\cdot, \widehat{\boldsymbol{\theta}}_S) \right\rangle_{\mathcal{N}_\Phi(\Omega)} \\
&= \frac{2}{n} \sum_{k=1}^n \left( \widehat{f}_p(\mathbf{x}_k) - f_p(\mathbf{x}_k) \right) A_{1t}(\mathbf{x}_k, \widehat{\boldsymbol{\theta}}_S) \\
&\quad + \frac{2}{n} \sum_{k=1}^n \left( \widehat{f}_p(\mathbf{x}_k) - f_p(\mathbf{x}_k) \right) \left( \widehat{A}_{1t}(\mathbf{x}_k, \widehat{\boldsymbol{\theta}}_S) - A_{1t}(\mathbf{x}_k, \widehat{\boldsymbol{\theta}}_S) \right) \\
&\quad - \frac{2}{n} \sum_{k=1}^n \varepsilon_k A_{1t}(\mathbf{x}_k, \widehat{\boldsymbol{\theta}}_S) - \frac{2}{n} \sum_{k=1}^n \varepsilon_k \left( \widehat{A}_{1t}(\mathbf{x}_k, \widehat{\boldsymbol{\theta}}_S) - A_{1t}(\mathbf{x}_k, \widehat{\boldsymbol{\theta}}_S) \right) \\
&\quad + 2\lambda \left\langle \widehat{f}_p(\cdot), \widehat{A}_{1t}(\cdot, \widehat{\boldsymbol{\theta}}_S) \right\rangle_{\mathcal{N}_\Phi(\Omega)} \\
&:= Q_1 + Q_2 - Q_3 - Q_4 + Q_5, \tag{G.15}
\end{aligned}$$

where  $\widehat{A}_{1t}(\cdot, \widehat{\boldsymbol{\theta}}_S) \in \mathcal{N}_\Phi(\Omega)$  is a function to be chosen later.

Since  $\alpha\beta_1 < m_1$ ,  $A_{1t}(\cdot, \boldsymbol{\theta})$  may not be in  $W^{m_1}(\Omega)$ . Therefore, the function  $\widehat{A}_{1t}(\cdot, \boldsymbol{\theta})$  should be a good approximation of  $A_{1t}(\cdot, \boldsymbol{\theta})$  and is in the RKHS  $\mathcal{N}_\Phi(\Omega)$ . We select  $\widehat{A}_{1t}(\cdot, \boldsymbol{\theta})$  as the solution to the optimization problem

$$\min_{\widetilde{f}(\cdot) \in \mathcal{N}_\Phi(\Omega)} \|A_{1t}(\cdot, \boldsymbol{\theta}) - \widetilde{f}(\cdot)\|_{L_2(\Omega)}^2 + \lambda_0 \|\widetilde{f}(\cdot)\|_{\mathcal{N}_\Phi(\Omega)}^2,$$

where  $\lambda_0 = C_{11}n^{-\delta}$  with  $\delta = \frac{1}{2} \left( \frac{2m_1\epsilon_0}{m_1 - \alpha\beta_1} + \frac{m_1}{2\alpha\beta_1} \right) > 0$ . Since  $m_1 > \alpha\beta_1$ , we have

$$\begin{aligned}
\frac{2m_1\epsilon_0}{m_1 - \alpha\beta_1} &\geq \frac{m_1}{2\alpha\beta_1} \Leftrightarrow (1 + 4\epsilon_0)\alpha\beta_1 \geq m_1 \\
\Leftrightarrow (1 + 4\epsilon_0)(m_1 - \kappa) &\geq m_1 \Leftrightarrow \kappa \leq \frac{m_1}{1 + 4\epsilon_0},
\end{aligned}$$

which holds because of Condition (C5). Thus,  $\delta \in \left[ \frac{m_1}{2\alpha\beta_1}, \frac{2m_1\epsilon_0}{m_1 - \alpha\beta_1} \right]$ .

Lemma G.3 and (G.14) imply that

$$\sup_{\boldsymbol{\theta} \in \Theta} \|A_{1t}(\cdot, \boldsymbol{\theta}) - \widehat{A}_{1t}(\cdot, \boldsymbol{\theta})\|_{L_2(\Omega)}^2 \leq C_{12}\lambda_0^{\frac{\alpha\beta_1}{m_1}}, \sup_{\boldsymbol{\theta} \in \Theta} \|\widehat{A}_{1t}(\cdot, \boldsymbol{\theta})\|_{\mathcal{N}_\Phi(\Omega)}^2 \leq C_{13}\lambda_0^{\frac{\alpha\beta_1 - m_1}{m_1}}. \tag{G.16}$$

In the following, we consider each term in (G.15).

(i) Consider  $Q_1$ . Define  $h_{1,\boldsymbol{\theta}}(\cdot) := (\widehat{f}_p(\cdot) - f_p(\cdot))A_{1t}(\cdot, \boldsymbol{\theta})$ . Let  $\mathcal{G}_1 = \{g(\cdot) : g(\cdot) = A_{1t}(\cdot, \boldsymbol{\theta}), \boldsymbol{\theta} \in \Theta\}$ , and  $\mathcal{F}_1 = \{f(\cdot) \in \mathcal{N}_\Phi(\Omega) : f(\cdot) = \widehat{f}_p(\cdot) - f_p(\cdot)\}$ . We will use Lemma G.1 to bound the difference of the empirical inner product and the  $L_2$  inner product between functions  $\widehat{f}_p(\cdot) - f_p(\cdot)$  and  $A_{1t}(\cdot, \boldsymbol{\theta})$ . In order to do so, we first consider  $\mathcal{G}_1$ . Since  $A_{1t}(\cdot, \boldsymbol{\theta}) \in W^{\alpha\beta_1}(\Omega)$

and  $\alpha\beta_1 > d/2$ , (G.14) implies that  $\mathcal{G}_1 \subset \mathcal{B}_{W^{\alpha\beta_1}(\Omega)}(C_{10})$ , where we also use the equivalence of  $W^{\alpha\beta_1}(\Omega)$  and  $\mathcal{N}_\alpha^{\beta_1}(\Omega)$ . Thus, the entropy number of  $\mathcal{G}_1$  can be bounded by (Edmunds and Triebel, 2008)

$$H(\delta, \mathcal{G}_1, \|\cdot\|_{L_\infty(\Omega)}) \leq C_{14} \left(\frac{1}{\delta}\right)^{\frac{d}{\alpha\beta_1}}. \quad (\text{G.17})$$

Furthermore, the Gagliardo–Nirenberg interpolation inequality for functions in Sobolev spaces (abbreviated as the interpolation inequality in the rest of the Supplement) (Brezis and Mironescu, 2019) implies that

$$\|g\|_{L_\infty(\Omega)} \leq C_{15} \|g\|_{L_2(\Omega)}^{1-\frac{d}{2\alpha\beta_1}} \|g\|_{W^{\alpha\beta_1}(\Omega)}^{\frac{d}{2\alpha\beta_1}} \leq C_{16} \|g\|_{W^{\alpha\beta_1}(\Omega)}^{\frac{d}{2\alpha\beta_1}} \leq C_{17}, \forall g \in \mathcal{G}_1, \quad (\text{G.18})$$

where the second inequality is because of the Sobolev embedding theorem, and the last inequality is because  $\mathcal{G}_1 \subset \mathcal{B}_{W^{\alpha\beta_1}(\Omega)}(C_{10})$ . Therefore, (G.18) implies that  $R_2 = \sup_{g \in \mathcal{G}_1} \|g(\cdot)\|_{L_2(\Omega)}$  and  $K_2 = \sup_{g \in \mathcal{G}_1} \|g(\cdot)\|_{L_\infty(\Omega)}$  satisfy  $R_2 \leq K_2 \leq C_{17}$ , where we recall  $\text{Vol}(\Omega) = 1$  through the proof. Thus, we can choose  $R_2 = K_2 = C_{17}$  in the following calculations without changing the result. In order to apply Lemma G.1, we need to compute  $J_\infty(K_2, \mathcal{G}_1)$ .

Direct computation shows that

$$\begin{aligned} J_\infty(K_2, \mathcal{G}_1) &= C_{18} \inf_{\delta > 0} \left[ K_2 \int_{\delta/4}^1 \sqrt{\mathcal{H}_\infty(uK_2/2, \mathcal{F})} du + \sqrt{n}\delta K_2 \right] \\ &\leq C_{18} \inf_{\delta > 0} \left[ C_{19} K_2 \int_{\delta/4}^1 (uK_2)^{-\frac{d}{2\alpha\beta_1}} du + \sqrt{n}\delta K_2 \right] \\ &\leq C_{20} K_2^{1-\frac{d}{2\alpha\beta_1}} \leq C_{21}, \end{aligned} \quad (\text{G.19})$$

where the first inequality is by (G.17), the second inequality is because  $2\alpha\beta_1 > d$  and  $\int_0^1 u^{-\frac{d}{2\alpha\beta_1}} du$  is finite, and the last inequality is because we have chosen  $K_2 = C_{17}$ .

Next, we turn to  $\mathcal{F}_1$ . Let  $R_1 = \sup_{f \in \mathcal{F}_1} \|f(\cdot)\|_{L_2(\Omega)}$  and  $K_1 = \sup_{f \in \mathcal{F}_1} \|f(\cdot)\|_{L_\infty(\Omega)}$ . Clearly  $R_1 K_2 \leq K_1 R_2$  because we have chosen  $R_2 = K_2 = C_{17}$ . Lemma G.4 implies that  $\|\widehat{f}_p(\cdot)\|_{\mathcal{N}_\Phi(\Omega)} = O_{\mathbb{P}}(1 \vee n^{-1/2} \lambda^{-\frac{2m_1+d}{4m_1}})$ , thus  $\|\widehat{f}_p(\cdot)\|_{W^{m_1}(\Omega)} = O_{\mathbb{P}}(1 \vee n^{-1/2} \lambda^{-\frac{2m_1+d}{4m_1}})$  by the equivalence of  $\|\cdot\|_{\mathcal{N}_\Phi(\Omega)}$  and  $\|\cdot\|_{W^{m_1}(\Omega)}$ . Furthermore,  $R_1 = O_{\mathbb{P}}(\lambda \vee n^{-1/2} \lambda^{-\frac{d}{4m_1}})$  by Lemma G.4. By a similar computation as in (G.19), we obtain

$$J_\infty(R_1, \mathcal{F}_\infty) \leq C_{20} R_1^{1-\frac{d}{2m_1}}, J_\infty(K_1, \mathcal{F}_\infty) \leq C_{20} K_1^{1-\frac{d}{2m_1}},$$

where we note that Condition (C4) implies  $\mathcal{F}_1 \subset \mathcal{N}_\Phi(\Omega)$ . By the interpolation inequality,

$$\|\widehat{f}_p(\cdot) - f_p(\cdot)\|_{L_\infty(\Omega)} \leq C_{21} \|\widehat{f}_p(\cdot) - f_p(\cdot)\|_{L_2(\Omega)}^{1-\frac{d}{2m_1}} \|\widehat{f}_p(\cdot) - f_p(\cdot)\|_{\mathcal{N}_\Phi(\Omega)}^{\frac{d}{2m_1}},$$

which implies  $K_1 \leq C_{21} R_1^{1-\frac{d}{2m_1}} (\|\widehat{f}_p(\cdot)\|_{\mathcal{N}_\Phi(\Omega)}^{\frac{d}{2m_1}} + \|f_p(\cdot)\|_{\mathcal{N}_\Phi(\Omega)}^{\frac{d}{2m_1}}) = o_{\mathbb{P}}(1)$ , where we also use Condition (C4). Thus, it can be checked that (G.1) is satisfied for sufficient large  $n$ . Then we can apply Lemma G.1 to  $(\widehat{f}_p(\cdot) - f_p(\cdot))A_{1t}(\cdot, \boldsymbol{\theta})$  and obtain that

$$\sup_{\boldsymbol{\theta} \in \Theta} \left| (P_n - P)h_{1,\boldsymbol{\theta}}(\cdot) \right| = o_{\mathbb{P}}(n^{-1/2}),$$

where  $P_n f := \sum_{i=1}^n f(X_i)/n$  and  $Pf := \sum_{i=1}^n \mathbb{E}f(X_i)/n$ . Therefore, we have

$$\begin{aligned} \left| Q_1 - 2 \int_{\Omega} \left( \widehat{f}_p(\mathbf{z}) - f_p(\mathbf{z}) \right) A_{1t}(\mathbf{z}, \widehat{\boldsymbol{\theta}}_S) d\mathbf{z} \right| &\leq 2 \sup_{\boldsymbol{\theta} \in \Theta} \left| \frac{1}{n} \sum_{j=1}^n h_{1,\boldsymbol{\theta}}(\mathbf{x}_j) - \int_{\Omega} h_{1,\boldsymbol{\theta}}(\mathbf{z}) d\mathbf{z} \right| \\ &= o_{\mathbb{P}}(n^{-1/2}), \end{aligned}$$

which implies

$$Q_1 = 2 \int_{\Omega} \left( \widehat{f}_p(\mathbf{z}) - f_p(\mathbf{z}) \right) A_{1t}(\mathbf{z}, \widehat{\boldsymbol{\theta}}_S) d\mathbf{z} + o_{\mathbb{P}}(n^{-1/2}). \quad (\text{G.20})$$

(ii) Consider  $Q_2$ . It follows from a similar approach as in (i) that

$$\begin{aligned} Q_2 &= 2 \int_{\Omega} \left( \widehat{f}_p(\mathbf{z}) - f_p(\mathbf{z}) \right) \left( A_{1t}(\mathbf{z}, \widehat{\boldsymbol{\theta}}_S) - \widehat{A}_{1t}(\mathbf{z}, \widehat{\boldsymbol{\theta}}_S) \right) d\mathbf{z} + o_{\mathbb{P}}(n^{-1/2}) \\ &\leq 2 \|\widehat{f}_p(\cdot) - f_p(\cdot)\|_{L_2(\Omega)} \|A_{1t}(\cdot, \widehat{\boldsymbol{\theta}}_S) - \widehat{A}_{1t}(\cdot, \widehat{\boldsymbol{\theta}}_S)\|_{L_2(\Omega)} + o_{\mathbb{P}}(n^{-1/2}) \\ &= o_{\mathbb{P}}(n^{-1/4}) O_{\mathbb{P}}(\lambda_0^{\frac{\alpha\beta_1}{2m_1}}) + o_{\mathbb{P}}(n^{-1/2}) \\ &= o_{\mathbb{P}}(n^{-1/4}) O_{\mathbb{P}}(n^{-\frac{m_1}{2\alpha\beta_1} \frac{\alpha\beta_1}{2m_1}}) + o_{\mathbb{P}}(n^{-1/2}) \\ &= o_{\mathbb{P}}(n^{-1/4}) O_{\mathbb{P}}(n^{-1/4}) + o_{\mathbb{P}}(n^{-1/2}) = o_{\mathbb{P}}(n^{-1/2}), \end{aligned} \quad (\text{G.21})$$

where the first inequality is by the Cauchy-Schwarz inequality, and the second equality is by Lemma G.4 and (G.16).

(iii) Consider  $Q_4$ . Define function class  $\mathcal{G}_2 = \left\{ g(\cdot) \mid g(\cdot) = A_{1t}(\cdot, \boldsymbol{\theta}) - \widehat{A}_{1t}(\cdot, \boldsymbol{\theta}), \boldsymbol{\theta} \in \Theta \right\}$ . Since  $\alpha\beta_1 < m_1$ ,  $\mathcal{G} \subset \mathcal{N}_{\alpha}^{\beta_1}(\Omega) = W^{\alpha\beta_1}(\Omega)$ . Lemma G.2 implies

$$\begin{aligned} &\langle \boldsymbol{\varepsilon}, A_{1t}(\cdot, \boldsymbol{\theta}) - \widehat{A}_{1t}(\cdot, \boldsymbol{\theta}) \rangle_n \\ &= O_{\mathbb{P}}(n^{-1/2}) \|A_{1t}(\cdot, \boldsymbol{\theta}) - \widehat{A}_{1t}(\cdot, \boldsymbol{\theta})\|_{L_2(\Omega)}^{1-\frac{d}{2\alpha\beta_1}} \|A_{1t}(\cdot, \boldsymbol{\theta}) - \widehat{A}_{1t}(\cdot, \boldsymbol{\theta})\|_{W^{\alpha\beta_1}(\Omega)}^{\frac{d}{2\alpha\beta_1}}, \forall \boldsymbol{\theta} \in \Theta. \end{aligned} \quad (\text{G.22})$$

By the triangle inequality,

$$\sup_{\boldsymbol{\theta} \in \Theta} \|\widehat{A}_{1t}(\cdot, \boldsymbol{\theta})\|_{L_2(\Omega)} \leq \sup_{\boldsymbol{\theta} \in \Theta} \|A_{1t}(\cdot, \boldsymbol{\theta})\|_{L_2(\Omega)} + \sup_{\boldsymbol{\theta} \in \Theta} \|A_{1t}(\cdot, \boldsymbol{\theta}) - \widehat{A}_{1t}(\cdot, \boldsymbol{\theta})\|_{L_2(\Omega)} \leq C_{22}, \quad (\text{G.23})$$

where the last inequality is by (G.14) and (G.16). The interpolation inequality and (G.16) imply that

$$\|\widehat{A}_{1t}(\cdot, \boldsymbol{\theta})\|_{W^{\alpha\beta_1}(\Omega)} \leq C_{23} \|\widehat{A}_{1t}(\cdot, \boldsymbol{\theta})\|_{L_2(\Omega)}^{1-\frac{\alpha\beta_1}{m_1}} \|\widehat{A}_{1t}(\cdot, \boldsymbol{\theta})\|_{W^{m_1}(\Omega)}^{\frac{\alpha\beta_1}{m_1}} \leq C_{24} \lambda_0^{\frac{(\alpha\beta_1-m_1)\alpha\beta_1}{2m_1^2}}, \quad (\text{G.24})$$

where the last inequality is by (G.16) and (G.23). Plugging (G.23) and (G.24) into (G.22) leads to

$$\begin{aligned} &\langle \boldsymbol{\varepsilon}, A_{1t}(\cdot, \boldsymbol{\theta}) - \widehat{A}_{1t}(\cdot, \boldsymbol{\theta}) \rangle_n \\ &= O_{\mathbb{P}}(n^{-1/2}) \lambda_0^{\left(1-\frac{d}{2\alpha\beta_1}\right) \frac{\alpha\beta_1}{2m_1}} \left( \|A_{1t}(\cdot, \boldsymbol{\theta})\|_{W^{\alpha\beta_1}(\Omega)} + \|\widehat{A}_{1t}(\cdot, \boldsymbol{\theta})\|_{W^{\alpha\beta_1}(\Omega)} \right)^{\frac{d}{2\alpha\beta_1}} \\ &= O_{\mathbb{P}}(n^{-1/2}) \lambda_0^{\left(1-\frac{d}{2\alpha\beta_1}\right) \frac{\alpha\beta_1}{2m_1}} \lambda_0^{\frac{d}{2\alpha\beta_1} \left( \frac{(\alpha\beta_1-m_1)\alpha\beta_1}{2m_1^2} \right)} \\ &= o_{\mathbb{P}}(n^{-1/2}), \quad \forall \boldsymbol{\theta} \in \Theta, \end{aligned} \quad (\text{G.25})$$

where the first equality is by (G.22), the second equality is by (G.16) and interpolation inequality, and the last equality is because  $\lambda_0 = o(1)$  and

$$\left(1 - \frac{d}{2\alpha\beta_1}\right) \frac{\alpha\beta_1}{2m_1} + \frac{d}{2\alpha\beta_1} \left(\frac{(\alpha\beta_1 - m_1)\alpha\beta_1}{2m_1^2}\right) = \frac{\alpha\beta_1(2m_1 + d) - 2m_1d}{4m_1^2} > 0,$$

where we use  $\alpha\beta_1 > \frac{2m_1d}{2m_1+d}$ . Therefore, (G.25) implies that

$$|Q_4| \leq 2 \sup_{\boldsymbol{\theta} \in \Theta} |\langle \boldsymbol{\varepsilon}, A_{1t}(\cdot, \boldsymbol{\theta}) - \widehat{A}_{1t}(\cdot, \boldsymbol{\theta}) \rangle_n| = o_{\mathbb{P}}(n^{-1/2}). \quad (\text{G.26})$$

(iv) Consider  $Q_5$ . By the Cauchy-Schwarz inequality,

$$|Q_5| \leq 2\lambda \left\| \widehat{f}_p(\cdot) \right\|_{\mathcal{N}_{\Phi}(\Omega)} \left\| \widehat{A}_{1t}(\cdot, \widehat{\boldsymbol{\theta}}_S) \right\|_{\mathcal{N}_{\Phi}(\Omega)}.$$

By (G.16) and Condition (C4), we have

$$\begin{aligned} |Q_5| &= o_{\mathbb{P}}(n^{-\frac{1}{2}-\epsilon_0}) O_{\mathbb{P}}(\lambda_0^{\frac{\alpha\beta_1-m_1}{2m_1}}) \\ &= o_{\mathbb{P}}(n^{-\frac{1}{2}-\epsilon_0}) O_{\mathbb{P}}(n^{\delta \frac{m_1-\alpha\beta_1}{2m_1}}) \\ &= o_{\mathbb{P}}(n^{-\frac{1}{2}-\epsilon_0}) O_{\mathbb{P}}(n^{\frac{2m_1\epsilon_0}{m_1-\alpha\beta_1} \frac{m_1-\alpha\beta_1}{2m_1}}) = o_{\mathbb{P}}(n^{-1/2}). \end{aligned} \quad (\text{G.27})$$

By (G.20), (G.21), (G.26), and (G.27), we can rearrange  $J_2$  as

$$\begin{aligned} J_2 &= 2 \int_{\Omega} \left( \widehat{f}_p(\mathbf{z}) - f_p(\mathbf{z}) \right) A_{1t}(\mathbf{z}, \widehat{\boldsymbol{\theta}}_S) d\mathbf{z} = \frac{2}{n} \sum_{k=1}^n \varepsilon_k A_{1t}(\mathbf{x}_k, \widehat{\boldsymbol{\theta}}_S) + o_{\mathbb{P}}(n^{-1/2}) \\ &= \frac{2}{n} \sum_{k=1}^n \varepsilon_k A_{1t}(\mathbf{x}_k, \boldsymbol{\theta}_S^*) + \frac{2}{n} \sum_{k=1}^n \varepsilon_k \left( A_{1t}(\mathbf{x}_k, \widehat{\boldsymbol{\theta}}_S) - A_{1t}(\mathbf{x}_k, \boldsymbol{\theta}_S^*) \right) + o_{\mathbb{P}}(n^{-1/2}). \end{aligned} \quad (\text{G.28})$$

Define function class  $\mathcal{G}_3 = \left\{ g(\cdot) \left| g(\cdot) = A_{1t}(\cdot, \boldsymbol{\theta}) - A_{1t}(\cdot, \boldsymbol{\theta}_S^*), \boldsymbol{\theta} \in \Theta \right. \right\}$ . Thus  $\mathcal{G}_3 \subset W^{\alpha\beta_1}(\Omega)$ .

Lemma G.2 implies

$$\begin{aligned} &\langle \boldsymbol{\varepsilon}, A_{1t}(\cdot, \boldsymbol{\theta}) - A_{1t}(\cdot, \boldsymbol{\theta}_S^*) \rangle_n \\ &= o_{\mathbb{P}}(n^{-1/2}) \|A_{1t}(\cdot, \boldsymbol{\theta}) - A_{1t}(\cdot, \boldsymbol{\theta}_S^*)\|_{L_2(\Omega)}^{1-\frac{d}{2\alpha\beta_1}} \|A_{1t}(\cdot, \boldsymbol{\theta}) - A_{1t}(\cdot, \boldsymbol{\theta}_S^*)\|_{W^{\alpha\beta_1}(\Omega)}^{\frac{d}{2\alpha\beta_1}} \\ &= o_{\mathbb{P}}(n^{-1/2}) \|A_{1t}(\cdot, \boldsymbol{\theta}) - A_{1t}(\cdot, \boldsymbol{\theta}_S^*)\|_{L_2(\Omega)}^{1-\frac{d}{2\alpha\beta_1}} \left( \|A_{1t}(\cdot, \boldsymbol{\theta})\|_{W^{\alpha\beta_1}(\Omega)} + \|A_{1t}(\cdot, \boldsymbol{\theta}_S^*)\|_{W^{\alpha\beta_1}(\Omega)} \right)^{\frac{d}{2\alpha\beta_1}} \\ &= o_{\mathbb{P}}(n^{-1/2}) \|A_{1t}(\cdot, \boldsymbol{\theta}) - A_{1t}(\cdot, \boldsymbol{\theta}_S^*)\|_{L_2(\Omega)}^{1-\frac{d}{2\alpha\beta_1}}, \forall \boldsymbol{\theta} \in \Theta, \end{aligned}$$

where the second equality is because of the triangle inequality, and the last equality is by (G.14). Therefore,

$$\begin{aligned} \left| \frac{2}{n} \sum_{k=1}^n \varepsilon_k \left( A_{1t}(\mathbf{x}_k, \widehat{\boldsymbol{\theta}}_S) - A_{1t}(\mathbf{x}_k, \boldsymbol{\theta}_S^*) \right) \right| &= o_{\mathbb{P}}(n^{-1/2}) \|A_{1t}(\cdot, \widehat{\boldsymbol{\theta}}_S) - A_{1t}(\cdot, \boldsymbol{\theta}_S^*)\|_{L_2(\Omega)}^{1-\frac{d}{2\alpha\beta_1}} \\ &= o_{\mathbb{P}}(n^{-1/2}), \end{aligned} \quad (\text{G.29})$$

where the last inequality is because of the consistency of  $\widehat{\boldsymbol{\theta}}_S$ .

By (G.12),(G.13),(G.28) and (G.29), we obtain that

$$(\mathbf{V} + \mathbf{E})(\widehat{\boldsymbol{\theta}}_S - \boldsymbol{\theta}_S^*) + \frac{2}{n} \sum_{k=1}^n \varepsilon_k A_1(\mathbf{x}_k) = o_{\mathbb{P}}(n^{-1/2}).$$

where each element in  $\mathbf{E}$  is  $o_{\mathbb{P}}(1)$  and

$$A_1(\cdot) = \sum_{j=1}^{\infty} \frac{1}{\gamma_j} \int_{\Omega} \frac{\partial f_s(\mathbf{z}, \boldsymbol{\theta}_S^*)}{\partial \boldsymbol{\theta}} \phi_j(\mathbf{z}) d\mathbf{z} \cdot \phi_j(\cdot) = (A_{11}(\cdot, \boldsymbol{\theta}_S^*), \dots, A_{1q}(\cdot, \boldsymbol{\theta}_S^*))^T.$$

Since  $\mathbf{E}$  converges to zero in probability, we have

$$\widehat{\boldsymbol{\theta}}_S - \boldsymbol{\theta}_S^* = -2\mathbf{V}^{-1} \left( \frac{1}{n} \sum_{k=1}^n \varepsilon_k A_1(\mathbf{x}_k, \boldsymbol{\theta}_S^*) \right) + o_{\mathbb{P}}(n^{-1/2}),$$

which finishes the proof. ■

## G.4 Proof of Theorem 3.3

The proof of Theorem 3.3 is along the line of the proof of Theorem 2 in Tuo and Wu (2015), while we modify the original proof such that it fits the Sobolev calibration context.

*Proof of Theorem 3.3.* For the calibration problem given by (2.1) and (2.4), consider the  $q$ -dimensional parametric model indexed by  $\boldsymbol{\gamma}$ :

$$f_{p\boldsymbol{\gamma}}(\cdot) = f_p(\cdot) + \boldsymbol{\gamma}^T A_1(\cdot), \quad (\text{G.30})$$

where  $A_1(\cdot)$  is defined in Theorem 3.2 and  $\boldsymbol{\gamma} \in \mathbb{R}^q$ . Combining (2.1) and (G.30) yields

$$y_j^{(p)} = f_p(\cdot) + \boldsymbol{\gamma}^T A_1(\cdot) + \varepsilon_j \quad (\text{G.31})$$

for  $j = 1, \dots, n$ . Note that (G.31) is a linear regression model with  $\boldsymbol{\gamma}$  as parameter of interest, and the true value of  $\boldsymbol{\gamma}$  is 0 regarding (2.1).

Since  $\varepsilon_i$  follows a normal distribution, the maximum likelihood estimator for  $\boldsymbol{\gamma}$  is equivalent to ordinary least square estimator, with regular asymptotic expression:

$$\widehat{\boldsymbol{\gamma}}_n = \frac{1}{n} \mathbf{W}^{-1} \sum_{i=1}^n \varepsilon_i A_1(\mathbf{x}_i) + o_p(n^{-1/2}) \quad (\text{G.32})$$

where  $\mathbf{W}$  is defined in (3.2).

A natural estimator for  $\boldsymbol{\theta}_S^*$  is

$$\widehat{\boldsymbol{\theta}}_{S_n} = \underset{\boldsymbol{\theta} \in \Theta}{\operatorname{argmin}} \|f_{p\widehat{\boldsymbol{\gamma}}_n}(\cdot) - f_s(\cdot, \boldsymbol{\theta})\|_{\mathcal{H}_m(\Omega)},$$



where we assume that  $f_s(\cdot, \boldsymbol{\theta})$  is cheap for simplicity.

Define

$$\boldsymbol{\theta}(\mathbf{t}) = \underset{\boldsymbol{\theta} \in \Theta}{\operatorname{argmin}} \|f_{pt}(\cdot) - f_s(\cdot, \boldsymbol{\theta})\|_{\mathcal{H}_m(\Omega)} \quad (\text{G.33})$$

as a function of  $\mathbf{t}$ . Let

$$\begin{aligned} \Upsilon(\boldsymbol{\theta}, \mathbf{t}) &= -2 \left\langle f_{pt}(\cdot) - f_s(\cdot, \boldsymbol{\theta}), \frac{\partial f_s(\cdot, \boldsymbol{\theta})}{\partial \boldsymbol{\theta}} \right\rangle_{\mathcal{H}_m(\Omega)} \\ &= -2 \left\langle f_p(\cdot) - \mathbf{t}^T A_1(\cdot) - f_s(\cdot, \boldsymbol{\theta}), \frac{\partial f_s(\cdot, \boldsymbol{\theta})}{\partial \boldsymbol{\theta}} \right\rangle_{\mathcal{H}_m(\Omega)}. \end{aligned}$$

Then (G.33) implies  $\Upsilon(\boldsymbol{\theta}, \mathbf{t}) = 0$  for all  $\mathbf{t}$  near 0. From the implicit function theorem, we have

$$\left. \frac{\partial \boldsymbol{\theta}(\mathbf{t})}{\partial \mathbf{t}^T} \right|_{\mathbf{t}=0} = - \left( \frac{\partial \Upsilon}{\partial \boldsymbol{\theta}^T}(\boldsymbol{\theta}_S^*, 0) \right)^{-1} \frac{\partial \Upsilon}{\partial \mathbf{t}^T}(\boldsymbol{\theta}_S^*, 0). \quad (\text{G.34})$$

First we calculate

$$- \left( \frac{\partial \Upsilon}{\partial \boldsymbol{\theta}^T}(\boldsymbol{\theta}_S^*, 0) \right)^{-1} = - \left( \sum_{j=1}^{\infty} \frac{1}{\gamma_j} \frac{\partial^2}{\partial \boldsymbol{\theta} \partial \boldsymbol{\theta}^T} \left( \int_{\Omega} (f_p(\mathbf{z}) - f_s(\mathbf{z}, \boldsymbol{\theta}_S^*)) \phi_j(\mathbf{z}) d\mathbf{z} \right)^2 \right)^{-1} = -\mathbf{V}^{-1}. \quad (\text{G.35})$$

Then we calculate

$$\begin{aligned} & \frac{\partial \Upsilon}{\partial \mathbf{t}^T}(\boldsymbol{\theta}_S^*, 0) \\ &= \frac{\partial}{\partial \mathbf{t}^T} \left( -2 \sum_{j=1}^{\infty} \frac{1}{\gamma_j} \langle f_p(\cdot) - \mathbf{t}^T A_1(\cdot) - f_s(\cdot, \boldsymbol{\theta}), \phi_j(\cdot) \rangle_{L_2(\Omega)} \left\langle \frac{\partial f_s(\cdot, \boldsymbol{\theta})}{\partial \boldsymbol{\theta}}, \phi_j(\cdot) \right\rangle_{L_2(\Omega)} \right) \Big|_{\boldsymbol{\theta}=\boldsymbol{\theta}_S^*, \mathbf{t}=0} \\ &= 2 \sum_{j=1}^{\infty} \frac{1}{\gamma_j} \langle A_1(\cdot), \phi_j(\cdot) \rangle_{L_2(\Omega)} \left( \left\langle \frac{\partial f_s(\cdot, \boldsymbol{\theta})}{\partial \boldsymbol{\theta}}, \phi_j(\cdot) \right\rangle_{L_2(\Omega)} \right)^T \Big|_{\boldsymbol{\theta}=\boldsymbol{\theta}_S^*, \mathbf{t}=0} \\ &= 2 \sum_{j=1}^{\infty} \frac{1}{\gamma_j} \\ & \times \left\langle \sum_{i=1}^{\infty} \frac{1}{\gamma_i} \phi_i(\cdot) \int_{\Omega} \frac{\partial f_s(\mathbf{z}, \boldsymbol{\theta})}{\partial \boldsymbol{\theta}} \phi_i(\mathbf{z}) d\mathbf{z}, \phi_j(\cdot) \right\rangle_{L_2(\Omega)} \left( \left\langle \frac{\partial f_s(\cdot, \boldsymbol{\theta})}{\partial \boldsymbol{\theta}}, \phi_j(\cdot) \right\rangle_{L_2(\Omega)} \right)^T \Big|_{\boldsymbol{\theta}=\boldsymbol{\theta}_S^*, \mathbf{t}=0} \\ &= 2 \sum_{j=1}^{\infty} \left( \frac{1}{\gamma_j} \int_{\Omega} \frac{\partial f_s(\mathbf{z}, \boldsymbol{\theta})}{\partial \boldsymbol{\theta}} \phi_j(\mathbf{z}) d\mathbf{z} \right) \left( \frac{1}{\gamma_j} \int_{\Omega} \frac{\partial f_s(\mathbf{z}, \boldsymbol{\theta})}{\partial \boldsymbol{\theta}} \phi_j(\mathbf{z}) d\mathbf{z} \right)^T \Big|_{\boldsymbol{\theta}=\boldsymbol{\theta}_S^*, \mathbf{t}=0} \\ &= 2\mathbb{E}(A_1(\mathbf{x})A_1(\mathbf{x})^T) \\ &= 2\mathbf{W}. \end{aligned} \quad (\text{G.36})$$

By combining (G.34), (G.35), (G.36), we have

$$\left. \frac{\partial \boldsymbol{\theta}(t)}{\partial t^T} \right|_{t=0} = -2\mathbf{V}^{-1}\mathbf{W}. \quad (\text{G.37})$$

By the delta method, we obtain

$$\widehat{\boldsymbol{\theta}}_{S_n} - \boldsymbol{\theta}_S^* = \boldsymbol{\theta}(\widehat{\gamma}_n) - \boldsymbol{\theta}(0) = \left. \frac{\partial \boldsymbol{\theta}(t)}{\partial t^T} \right|_{t=0} \widehat{\gamma}_n + o_p(n^{-1/2}),$$

which, together with (G.37) and (G.32), yields

$$\widehat{\boldsymbol{\theta}}_{S_n} - \boldsymbol{\theta}_S^* = -2\mathbf{V}^{-1} \left( \frac{1}{n} \sum_{i=1}^n \varepsilon_i A_1(\mathbf{x}_i) \right) + o_p(n^{-1/2}). \quad (\text{G.38})$$

Apparently, (G.38) and (3.1) have the same form, which implies that the asymptotic expression of the Sobolev calibration is same as the maximum likelihood estimator for the  $q$ -dimensional parametric model. This finishes the proof.  $\blacksquare$

## G.5 Proof of Corollary 3.4

By taking  $m = 0$  in (2.4), the Sobolev calibration is equivalent to  $L_2$  calibration. Furthermore, when  $m = 0$ , since  $\phi_j(\cdot)$ 's are an orthonormal basis in  $L_2(\Omega)$ , we can express  $\mathbf{V}$  and  $A_1(\mathbf{x})$  in Theorem 3.2 as

$$\begin{aligned} \mathbf{V} &= - \sum_{j=1}^{\infty} \frac{\partial^2}{\partial \boldsymbol{\theta} \partial \boldsymbol{\theta}^T} \left( \int_{\Omega} (f_p(\mathbf{z}) - f_s(\mathbf{z}, \boldsymbol{\theta}^*)) \phi_j(\mathbf{z}) d\mathbf{z} \right)^2 \\ &= \frac{\partial^2}{\partial \boldsymbol{\theta} \partial \boldsymbol{\theta}^T} \left( - \sum_{j=1}^{\infty} \left( \int_{\Omega} (f_p(\mathbf{z}) - f_s(\mathbf{z}, \boldsymbol{\theta}^*)) \phi_j(\mathbf{z}) d\mathbf{z} \right)^2 \right) \\ &= - \frac{\partial^2}{\partial \boldsymbol{\theta} \partial \boldsymbol{\theta}^T} \int_{\Omega} (f_p(\mathbf{z}) - f_s(\mathbf{z}, \boldsymbol{\theta}^*))^2 d\mathbf{z} = \mathbf{V}_{L_2}, \end{aligned} \quad (\text{G.39})$$

and

$$A_1(\mathbf{x}) = \sum_{j=1}^{\infty} \phi_j(\mathbf{x}) \int_{\Omega} \frac{\partial f_s(\mathbf{z}, \boldsymbol{\theta}_S^*)}{\partial \boldsymbol{\theta}} \phi_j(\mathbf{z}) d\mathbf{z} = \frac{\partial f_s(\mathbf{x}, \boldsymbol{\theta}_S^*)}{\partial \boldsymbol{\theta}}. \quad (\text{G.40})$$

Thus, we can see that Corollary 3.4 is a direct result of Theorem 3.2, (G.39) and (G.40).

## G.6 Proof of Proposition 4.1

Let  $m_3 = (m_2 - d/2 + \max(m, d/2))/2$ , thus we have  $m_3 > \max(d/2, m)$ . By Condition (C3'), the sample path of  $f_p(\cdot)$  lies in  $W^{m_3}(\Omega)$  with probability one (Steinwart, 2019). Hence,

$$\|f_p(\cdot)\|_{W^{m_3}(\Omega)} < \infty$$

with probability one. Therefore,  $\widehat{f}_p(\cdot)$  has the same form as the kernel ridge regression estimator using an oversmoothed kernel function for  $f_p(\cdot) \in W^{m_3}(\Omega)$ , with  $\lambda \asymp 1/n$ . Corollary 4.1 of Fischer and Steinwart (2020) implies that  $\left\| \widehat{f}_p(\cdot) - f_p(\cdot) \right\|_{L_2(\Omega)} = o_{\mathbb{P}}(1)$  and

$$\begin{aligned} \left\| \widehat{f}_p(\cdot) - f_p(\cdot) \right\|_{W^{m_3}(\Omega)} &= O_{\mathbb{P}}(1). \text{ Thus,} \\ &\left\| \widehat{f}_p(\cdot) - f_p(\cdot) \right\|_{\mathcal{H}^m(\Omega)} \leq C_1 \left\| \widehat{f}_p(\cdot) - f_p(\cdot) \right\|_{W^m(\Omega)} \\ &\leq C_2 \left\| \widehat{f}_p(\cdot) - f_p(\cdot) \right\|_{L_2(\Omega)}^{\frac{m_3-m}{m_3}} \left\| \widehat{f}_p(\cdot) - f_p(\cdot) \right\|_{W^{m_3}(\Omega)}^{\frac{m}{m_3}} \\ &= o_{\mathbb{P}}(1). \end{aligned} \tag{G.41}$$

From the definition of  $\widehat{\boldsymbol{\theta}}_S$  and  $\boldsymbol{\theta}_S^*$  in (2.7) and (2.4), it suffices to prove that  $\left\| \widehat{f}_p(\cdot) - \widehat{f}_s(\cdot, \boldsymbol{\theta}) \right\|_{\mathcal{H}_m(\Omega)}$  converges to  $\left\| f_p(\cdot) - f_s(\cdot, \boldsymbol{\theta}) \right\|_{\mathcal{H}_m(\Omega)}$  uniformly with respect to  $\boldsymbol{\theta}$  in probability. This is ensured by

$$\begin{aligned} &\left| \left\| \widehat{f}_p(\cdot) - \widehat{f}_s(\cdot, \boldsymbol{\theta}) \right\|_{\mathcal{H}_m(\Omega)} - \left\| f_p(\cdot) - f_s(\cdot, \boldsymbol{\theta}) \right\|_{\mathcal{H}_m(\Omega)} \right| \\ &\leq \left\| \widehat{f}_p(\cdot) - \widehat{f}_s(\cdot, \boldsymbol{\theta}) - (f_p(\cdot) - f_s(\cdot, \boldsymbol{\theta})) \right\|_{\mathcal{H}_m(\Omega)} \\ &\leq \left\| \widehat{f}_p(\cdot) - f_p(\cdot) \right\|_{\mathcal{H}_m(\Omega)} + \left\| \widehat{f}_s(\cdot, \boldsymbol{\theta}) - f_s(\cdot, \boldsymbol{\theta}) \right\|_{\mathcal{H}_m(\Omega)} \\ &\leq \left\| \widehat{f}_p(\cdot) - f_p(\cdot) \right\|_{\mathcal{H}_m(\Omega)} + C_3 \left\| \widehat{f}_s(\cdot, \boldsymbol{\theta}) - f_s(\cdot, \boldsymbol{\theta}) \right\|_{W^m(\Omega)} \\ &= o_{\mathbb{P}}(1), \end{aligned}$$

where the first and second inequalities are from the triangle inequality, the third inequality is because of the equivalence of  $\|\cdot\|_{W^m(\Omega)}$  and  $\|\cdot\|_{\mathcal{H}_m(\Omega)}$ , and the last equality is guaranteed by (G.41) and Condition (C6).

## G.7 Proof of Theorem 4.2

We first present several lemmas used in this proof. Lemma G.5 is an intermediate step in the proof of Lemma F.8 of Wang (2021). Lemma G.6 is a direct consequence of Theorems 1.3.3 and 2.1.1 of Adler and Taylor (2009).

**Lemma G.5.** *Suppose Conditions (C1') and (C3') hold. We have*

$$\sup_{\mathbf{x} \in \Omega} \left\| \mathcal{K}(\cdot, \mathbf{x}) - r_1(\cdot)^{\top} (\mathbf{R}_1 + \widehat{\mu}_n I_n)^{-1} r_1(\mathbf{x}) \right\|_{L_{\infty}(\Omega)} = O_{\mathbb{P}} \left( n^{-\left(1 - \frac{d}{2m_2}\right)} \right)$$

where  $r_1(\mathbf{x}) = (\mathcal{K}(\mathbf{x} - \mathbf{x}_1), \dots, \mathcal{K}(\mathbf{x} - \mathbf{x}_n))^{\top}$ ,  $\mathbf{R}_1 = (\mathcal{K}(\mathbf{x}_j - \mathbf{x}_k))_{jk}$ , and  $\widehat{\mu}_n \asymp C$  which is a constant.

**Lemma G.6.** *Let  $Z_t$  be a centered separable Gaussian process on a  $\mathfrak{d}$ -compact  $T$ , where  $\mathfrak{d}$  is the metric defined by*

$$\mathfrak{d}(t_1, t_2) = \sqrt{\mathbb{E}(Z_{t_1} - Z_{t_2})^2}.$$

Then there exists a universal constant  $K$  such that for all  $u > 0$ ,

$$\mathbb{P} \left( \sup_{t \in T} |Z_t| > K \int_0^{D/2} \sqrt{\log N(\epsilon, T, \mathfrak{d})} d\epsilon + u \right) \leq 2e^{-u^2/2\sigma_T^2},$$

where  $\sigma_T^2 = \sup_{t \in T} \mathbb{E} Z_t^2$ ,  $N(\epsilon, T, \mathfrak{d})$  is the  $\epsilon$ -covering number of the metric space  $(T, \mathfrak{d})$ , and  $D$  is the diameter of  $T$ .

*Proof of Theorem 4.2.* For the brevity of the proof, we will use the same notation as in the proof of Theorem 3.2, while keeping in mind that  $f_p(\cdot)$  is a Gaussian process. The first half of the proof is merely repeating the proof of Theorem 3.2, and the main difference comes from the second half of the proof, where we calculate  $J_2$  defined in (G.11). For the first half of the proof, the only difference is that the term  $I_2$  in (G.4) is bounded by

$$|I_2| = o_{\mathbb{P}}(n^{-1/2}) \left( \left\| \widehat{f}_p(\cdot) \right\|_{L_2(\Omega)} + \left\| f_s(\cdot, \widehat{\boldsymbol{\theta}}_S) \right\|_{L_2(\Omega)} \right). \quad (\text{G.42})$$

Since the sample path of  $f_p(\cdot)$  lies in  $\mathcal{H}_{m_3}(\Omega)$  with probability one by Condition (C3') (Steinwart, 2019), where  $m_3 = (m_2 - d/2 + \max(m, d/2))/2$ , together with Corollary 4.1 of Fischer and Steinwart (2020), we have that

$$\left\| \widehat{f}_p(\cdot) \right\|_{L_2(\Omega)} \leq \left\| \widehat{f}_p(\cdot) - f_p(\cdot) \right\|_{L_2(\Omega)} + \left\| f_p(\cdot) \right\|_{L_2(\Omega)} = O_{\mathbb{P}}(1),$$

which, together with (G.42) and Condition (C4'), implies that

$$I_2 = o_{\mathbb{P}}(n^{-1/2}).$$

Recall that

$$v_t(\boldsymbol{\theta}) = 2 \left\langle f_p(\cdot) - f_s(\cdot, \boldsymbol{\theta}), \frac{\partial f_s(\cdot, \boldsymbol{\theta})}{\partial \boldsymbol{\theta}_t} \right\rangle_{\mathcal{H}_m(\Omega)},$$

and

$$J_2 = \sum_{j=1}^{\infty} \frac{2}{\gamma_j} \int_{\Omega} (\widehat{f}_p(\mathbf{z}) - f_p(\mathbf{z})) \phi_j(\mathbf{z}) d\mathbf{z} \int_{\Omega} \frac{\partial f_s(\mathbf{z}, \widehat{\boldsymbol{\theta}}_S)}{\partial \boldsymbol{\theta}_t} \phi_j(\mathbf{z}) d\mathbf{z}.$$

Following the approach of obtaining (G.12) as in the proof of Theorem 3.2, we have

$$\frac{\partial v_t(\widetilde{\boldsymbol{\theta}})}{\partial \boldsymbol{\theta}^T} (\widehat{\boldsymbol{\theta}}_S - \boldsymbol{\theta}_S^*) + J_2 = o_{\mathbb{P}}(n^{-1/2}), \quad (\text{G.43})$$

where  $\widetilde{\boldsymbol{\theta}}$  lies between  $\boldsymbol{\theta}_S^*$  and  $\widehat{\boldsymbol{\theta}}_S$  and

$$\frac{\partial v(\widetilde{\boldsymbol{\theta}})}{\partial \boldsymbol{\theta}^T} \xrightarrow{p} \mathbf{V}, \quad (\text{G.44})$$

with  $v(\boldsymbol{\theta}) = 2 \left\langle f_p(\cdot) - f_s(\cdot, \boldsymbol{\theta}), \frac{\partial f_s(\cdot, \boldsymbol{\theta})}{\partial \boldsymbol{\theta}} \right\rangle_{\mathcal{H}_m(\Omega)} = (v_1(\boldsymbol{\theta}), \dots, v_q(\boldsymbol{\theta}))^T$  and  $\mathbf{V}$  as in Condition (C2').

Next, we consider  $J_2$ . Since  $f_p(\cdot)$  is a Gaussian process, the calculation of  $J_2$  is much different with that in the proof of Theorem 3.2. We still define

$$\mathcal{L}_n(f) = \frac{1}{n} \sum_{j=1}^n \left( y_j^{(p)} - f(\mathbf{x}_j) \right)^2 + \frac{\mu}{n} \|f\|_{\mathcal{N}_{\mathcal{K}}(\Omega)}^2,$$

and obtain

$$\begin{aligned} 0 &= \left. \frac{\partial}{\partial \eta} \mathcal{L}_n \left( \widehat{f}_p(\cdot) + \eta A_{1t}(\cdot, \widehat{\boldsymbol{\theta}}_S) \right) \right|_{\eta=0} \\ &= \frac{2}{n} \sum_{k=1}^n \left( \widehat{f}_p(\mathbf{x}_k) - f_p(\mathbf{x}_k) \right) A_{1t}(\mathbf{x}_k, \widehat{\boldsymbol{\theta}}_S) - \frac{2}{n} \sum_{k=1}^n \varepsilon_k A_{1t}(\mathbf{x}_k, \widehat{\boldsymbol{\theta}}_S) \\ &\quad + \frac{2\mu}{n} \left\langle \widehat{f}_p(\cdot), A_{1t}(\cdot, \widehat{\boldsymbol{\theta}}_S) \right\rangle_{\mathcal{N}_{\mathcal{K}}(\Omega)} \\ &:= Q_1 - Q_2 + Q_3, \end{aligned} \tag{G.45}$$

where we recall that  $A_{1t}(\cdot, \widehat{\boldsymbol{\theta}}_S)$  is defined by

$$A_{1t}(\cdot, \boldsymbol{\theta}) = \sum_{j=1}^{\infty} \frac{1}{\gamma_j} \int_{\Omega} \frac{\partial f_s(\mathbf{z}, \boldsymbol{\theta})}{\partial \theta_t} \phi_j(\mathbf{z}) d\mathbf{z} \cdot \phi_j(\cdot).$$

Then  $A_{1t}(\cdot, \widehat{\boldsymbol{\theta}}_S) \in \mathcal{N}_{\mathcal{K}}(\Omega)$  is given by

$$\begin{aligned} \sup_{\boldsymbol{\theta} \in \Theta} \|A_{1t}(\cdot, \boldsymbol{\theta})\|_{\mathcal{N}_{\mathcal{K}}(\Omega)}^2 &= \sup_{\boldsymbol{\theta} \in \Theta} \sum_{j=1}^{\infty} \frac{1}{\gamma_j^2 \gamma_{\Psi_j}^{m_2/\alpha}} \left( \int_{\Omega} \frac{\partial f_s(\mathbf{z}, \boldsymbol{\theta})}{\partial \theta_t} \phi_j(\mathbf{z}) d\mathbf{z} \right)^2 \\ &\leq C_1 \sup_{\boldsymbol{\theta} \in \Theta} \left\| \frac{\partial f_s(\mathbf{z}, \boldsymbol{\theta})}{\partial \theta_t} \right\|_{W^{2m+m_2}}^2 < \infty, \end{aligned} \tag{G.46}$$

where the last inequality is guaranteed by Condition (C4'). Under the Gaussian process settings,  $f_p(\cdot)$  is no longer in  $\mathcal{N}_{\mathcal{K}}(\Omega)$ . Therefore, we cannot follow the proof in Theorem 3.2. In the following, we consider each term in (G.45).

(1) Consider  $Q_1$ . Let

$$g(\boldsymbol{\theta}) = \frac{1}{n} \sum_{k=1}^n \left( \widehat{f}_p(\mathbf{x}_k) - f_p(\mathbf{x}_k) \right) A_{1t}(\mathbf{x}_k, \boldsymbol{\theta}) - \int_{\Omega} \left( \widehat{f}_p(\mathbf{z}) - f_p(\mathbf{z}) \right) A_{1t}(\mathbf{z}, \boldsymbol{\theta}) d\mathbf{z},$$

which is a centered Gaussian process, since it is a linear transformation of a centered Gaussian process. Thus,

$$\begin{aligned} &g(\boldsymbol{\theta}_1) - g(\boldsymbol{\theta}_2) \\ &= \frac{1}{n} \sum_{k=1}^n \left( \widehat{f}_p(\mathbf{x}_k) - f_p(\mathbf{x}_k) \right) (A_{1t}(\mathbf{x}_k, \boldsymbol{\theta}_1) - A_{1t}(\mathbf{x}_k, \boldsymbol{\theta}_2)) \\ &\quad - \int_{\Omega} \left( \widehat{f}_p(\mathbf{z}) - f_p(\mathbf{z}) \right) (A_{1t}(\mathbf{z}, \boldsymbol{\theta}_1) - A_{1t}(\mathbf{z}, \boldsymbol{\theta}_2)) d\mathbf{z}. \end{aligned}$$

Denote

$$\begin{aligned}
& l(x, y) \\
&= (\mathcal{K}(x, y) - \mathbf{r}_1(x)^\top (\mathbf{R}_1 + \mu \mathbf{I}_n)^{-1} \mathbf{r}_1(y)) (A_{1t}(x, \boldsymbol{\theta}_1) - A_{1t}(x, \boldsymbol{\theta}_2)) (A_{1t}(y, \boldsymbol{\theta}_1) - A_{1t}(y, \boldsymbol{\theta}_2))
\end{aligned} \tag{G.47}$$

By (G.47), the metric  $\mathfrak{d}$  of  $g(\cdot)$  can be computed by

$$\begin{aligned}
\mathfrak{d}(\boldsymbol{\theta}_1, \boldsymbol{\theta}_2)^2 &= \mathbb{E}(g(\boldsymbol{\theta}_1) - g(\boldsymbol{\theta}_2))^2 \\
&= \frac{1}{n^2} \sum_{j=1}^n \sum_{k=1}^n l(\mathbf{x}_k, \mathbf{x}_j) - \frac{2}{n} \sum_{j=1}^n \int_{\Omega} l(\mathbf{z}, \mathbf{x}_j) d\mathbf{z} + \int_{\Omega} \int_{\Omega} l(\mathbf{z}_1, \mathbf{z}_2) d\mathbf{z}_1 d\mathbf{z}_2.
\end{aligned} \tag{G.48}$$

In order to apply Lemma G.6, we need to compute  $\sigma_{\boldsymbol{\theta}}^2 = \sup_{\boldsymbol{\theta} \in \Theta} \mathbb{E}g(\boldsymbol{\theta})^2$ , the diameter  $D$ , and  $\log N(\epsilon, T, \mathfrak{d})$ .

Direct computation shows that

$$\begin{aligned}
\mathbb{E}g(\boldsymbol{\theta})^2 &= \frac{1}{n^2} \sum_{j=1}^n \sum_{k=1}^n (\mathcal{K}(\mathbf{x}_k, \mathbf{x}_j) - \mathbf{r}_1(\mathbf{x}_k)^\top (\mathbf{R}_1 + \mu \mathbf{I}_n)^{-1} \mathbf{r}_1(\mathbf{x}_j)) A_{1t}(\mathbf{x}_k, \boldsymbol{\theta}) A_{1t}(\mathbf{x}_j, \boldsymbol{\theta}) \\
&\quad - \frac{2}{n} \sum_{j=1}^n \int_{\Omega} (\mathcal{K}(\mathbf{z}, \mathbf{x}_j) - \mathbf{r}_1(\mathbf{z})^\top (\mathbf{R}_1 + \mu \mathbf{I}_n)^{-1} \mathbf{r}_1(\mathbf{x}_j)) A_{1t}(\mathbf{z}, \boldsymbol{\theta}) A_{1t}(\mathbf{x}_j, \boldsymbol{\theta}) d\mathbf{z} \\
&\quad + \int_{\Omega} \int_{\Omega} (\mathcal{K}(\mathbf{z}_1, \mathbf{z}_2) - \mathbf{r}_1(\mathbf{z}_1)^\top (\mathbf{R}_1 + \mu \mathbf{I}_n)^{-1} \mathbf{r}_1(\mathbf{z}_2)) A_{1t}(\mathbf{z}_1, \boldsymbol{\theta}) A_{1t}(\mathbf{z}_2, \boldsymbol{\theta}) d\mathbf{z}_1 d\mathbf{z}_2 \\
&= \frac{1}{n} \sum_{j=1}^n A_{1t}(\mathbf{x}_j, \boldsymbol{\theta}) \left( \frac{1}{n} \sum_{k=1}^n (\mathcal{K}(\mathbf{x}_k, \mathbf{x}_j) - \mathbf{r}_1(\mathbf{x}_k)^\top (\mathbf{R}_1 + \mu \mathbf{I}_n)^{-1} \mathbf{r}_1(\mathbf{x}_j)) A_{1t}(\mathbf{x}_k, \boldsymbol{\theta}) \right. \\
&\quad \left. - \int_{\Omega} (\mathcal{K}(\mathbf{z}_1, \mathbf{x}_j) - \mathbf{r}_1(\mathbf{z}_1)^\top (\mathbf{R}_1 + \mu \mathbf{I}_n)^{-1} \mathbf{r}_1(\mathbf{x}_j)) A_{1t}(\mathbf{z}_1, \boldsymbol{\theta}_1) d\mathbf{z}_1 \right) \\
&\quad - \left( \int_{\Omega} A_{1t}(\mathbf{z}_1, \boldsymbol{\theta}_1) \left( \frac{1}{n} \sum_{k=1}^n (\mathcal{K}(\mathbf{z}_1, \mathbf{x}_k) - \mathbf{r}_1(\mathbf{z}_1)^\top (\mathbf{R}_1 + \mu \mathbf{I}_n)^{-1} \mathbf{r}_1(\mathbf{x}_k)) A_{1t}(\mathbf{x}_k, \boldsymbol{\theta}_1) \right. \right. \\
&\quad \left. \left. - \int_{\Omega} (\mathcal{K}(\mathbf{z}_1, \mathbf{z}_2) - \mathbf{r}_1(\mathbf{z}_1)^\top (\mathbf{R}_1 + \mu \mathbf{I}_n)^{-1} \mathbf{r}_1(\mathbf{z}_2)) A_{1t}(\mathbf{z}_2, \boldsymbol{\theta}_1) d\mathbf{z}_2 \right) d\mathbf{z}_1 \right).
\end{aligned}$$

Let

$$\begin{aligned}
\mathcal{F}_1 &= \left\{ h(\cdot) : h(\cdot) = \frac{1}{n} \sum_{k=1}^n (\mathcal{K}(\cdot, \mathbf{x}_k) - \mathbf{r}_1(\cdot)^\top (\mathbf{R}_1 + \mu \mathbf{I}_n)^{-1} \mathbf{r}_1(\mathbf{x}_k)) A_{1t}(\mathbf{x}_k, \boldsymbol{\theta}) \right. \\
&\quad \left. - \int_{\Omega} (\mathcal{K}(\cdot, \mathbf{z}_2) - \mathbf{r}_1(\cdot)^\top (\mathbf{R}_1 + \mu \mathbf{I}_n)^{-1} \mathbf{r}_1(\mathbf{z}_2)) A_{1t}(\mathbf{z}_2, \boldsymbol{\theta}) d\mathbf{z}_2, \boldsymbol{\theta} \in \Theta \right\}, \\
\mathcal{G}_1 &= \{g(\cdot) : g(\cdot) = A_{1t}(\cdot, \boldsymbol{\theta}), \boldsymbol{\theta} \in \Theta\}.
\end{aligned}$$

Thus,  $\mathbb{E}g(\boldsymbol{\theta})^2$  can be bounded by

$$\mathbb{E}g(\boldsymbol{\theta})^2 \leq \sup_{h \in \mathcal{F}_1, g \in \mathcal{G}_1} |(P_n - P)hg|.$$

Note that  $\mathbb{E}g(\boldsymbol{\theta})^2$  does not involve Gaussian process, which allows us to repeat the procedure in deriving (G.20). In order to do so, note that

$$\sup_{h \in \mathcal{F}_1} \|h(\cdot)\|_{L_\infty(\Omega)} \leq \sup_{h_1 \in \mathcal{F}_2, g \in \mathcal{G}_1} |(P_n - P)h_1g|,$$

where  $\mathcal{F}_2 = \{h_1(\cdot) : h_1(\cdot) = \mathcal{K}(\cdot, \mathbf{x}) - \mathbf{r}_1(\cdot)^\top(\mathbf{R}_1 + \mu\mathbf{I}_n)^{-1}\mathbf{r}_1(\mathbf{x}), \mathbf{x} \in \Omega\}$ . Clearly,  $\mathcal{F}_2 \subset \mathcal{N}_{\mathcal{K}}(\Omega)$ , and Lemma G.5 implies that

$$\sup_{h_1 \in \mathcal{F}_2} \|h_1(\cdot)\|_{L_\infty} = O_{\mathbb{P}}(n^{-(1-\frac{d}{2m_2})}).$$

Thus, repeating the procedure in deriving (G.20), we can obtain that

$$\sup_{h_1 \in \mathcal{F}_2, g \in \mathcal{G}_1} |(P_n - P)h_1g| = O_{\mathbb{P}}\left(n^{-(1-\frac{d}{2m_2})-\frac{1}{2}}\right). \quad (\text{G.49})$$

Applying the similar procedure to  $\sup_{h \in \mathcal{F}_1, g \in \mathcal{G}_1} |(P_n - P)hg|$ , we obtain that

$$\begin{aligned} \sup_{h \in \mathcal{F}_1, g \in \mathcal{G}_1} |(P_n - P)hg| &= O_{\mathbb{P}}\left(n^{-(1-\frac{d}{2m_2})(1-\frac{d}{2m_2})-\frac{1}{2}(1-\frac{d}{2m_2})}n^{-\frac{1}{2}}\right) \\ &= O_{\mathbb{P}}\left(n^{-1-\frac{(4m_2-d)(m_2-d)}{4m_2^2}}\right) = O_{\mathbb{P}}\left(n^{-1-\delta_0}\right). \end{aligned} \quad (\text{G.50})$$

Since  $m_2 > d$ , we have  $\delta_0 > 0$ . For the brevity of the proof, we omit the details of deriving (G.49) and (G.50) here. Thus, we obtain

$$\sigma_{\boldsymbol{\theta}}^2 = \sup_{\boldsymbol{\theta} \in \Theta} \mathbb{E}g(\boldsymbol{\theta})^2 = O_{\mathbb{P}}\left(n^{-1-\delta_0}\right).$$

The diameter  $D$  can be computed by

$$\begin{aligned} D^2 &= \sup_{\boldsymbol{\theta}_1, \boldsymbol{\theta}_2 \in \Theta} \mathfrak{d}(\boldsymbol{\theta}_1, \boldsymbol{\theta}_2)^2 \\ &\leq 2 \sup_{\boldsymbol{\theta}_1, \boldsymbol{\theta}_2 \in \Theta} \mathbb{E}g(\boldsymbol{\theta}_1)^2 + \mathbb{E}g(\boldsymbol{\theta}_2)^2 \\ &= O_{\mathbb{P}}\left(n^{-1-\delta_0}\right). \end{aligned}$$

It remains to bound  $\log N(\epsilon, T, \mathfrak{d})$ . By (G.47) and (G.48), we have

$$\begin{aligned} \mathfrak{d}(\boldsymbol{\theta}_1, \boldsymbol{\theta}_2)^2 &\leq \frac{2}{n^2} \sum_{j=1}^n \sum_{k=1}^n l(\mathbf{x}_k, \mathbf{x}_j) + 2 \int_{\Omega} \int_{\Omega} l(\mathbf{z}_1, \mathbf{z}_2) d\mathbf{z}_1 d\mathbf{z}_2 \\ &\leq C_2 \sup_{\mathbf{x} \in \Omega} |A_{1t}(\mathbf{x}, \boldsymbol{\theta}_1) - A_{1t}(\mathbf{x}, \boldsymbol{\theta}_2)|^2, \end{aligned} \quad (\text{G.51})$$

where the last inequality is because  $(\mathcal{K}(\mathbf{x}_k, \mathbf{x}_j) - \mathbf{r}_1(\mathbf{x}_k)^\top(\mathbf{R}_1 + \mu\mathbf{I}_n)^{-1}\mathbf{r}_1(\mathbf{x}_j)) \leq 1$  for all  $\mathbf{x}_k, \mathbf{x}_j \in \Omega$ , and

$$(A_{1t}(\mathbf{x}_k, \boldsymbol{\theta}_1) - A_{1t}(\mathbf{x}_k, \boldsymbol{\theta}_2))(A_{1t}(\mathbf{x}_j, \boldsymbol{\theta}_1) - A_{1t}(\mathbf{x}_j, \boldsymbol{\theta}_2)) \leq \sup_{\mathbf{x} \in \Omega} |A_{1t}(\mathbf{x}, \boldsymbol{\theta}_1) - A_{1t}(\mathbf{x}, \boldsymbol{\theta}_2)|^2.$$

The mean value theorem implies

$$\begin{aligned} |A_{1t}(\mathbf{x}, \boldsymbol{\theta}_1) - A_{1t}(\mathbf{x}, \boldsymbol{\theta}_2)| &= \left( \sum_{j=1}^{\infty} \frac{1}{\gamma_j} \int_{\Omega} \frac{\partial f_s(\mathbf{z}, \tilde{\boldsymbol{\theta}})}{\partial \theta_t \partial \boldsymbol{\theta}} \phi_j(\mathbf{z}) d\mathbf{z} \cdot \phi_j(\mathbf{x}) \right)^T (\boldsymbol{\theta}_1 - \boldsymbol{\theta}_2) \\ &\leq \left\| \sum_{j=1}^{\infty} \frac{1}{\gamma_j} \int_{\Omega} \frac{\partial f_s(\mathbf{z}, \tilde{\boldsymbol{\theta}})}{\partial \theta_t \partial \boldsymbol{\theta}} \phi_j(\mathbf{z}) d\mathbf{z} \cdot \phi_j(\mathbf{x}) \right\|_{L_2(\Omega)} \|\boldsymbol{\theta}_1 - \boldsymbol{\theta}_2\|_2, \end{aligned} \quad (\text{G.52})$$

where  $\tilde{\boldsymbol{\theta}}$  lies between  $\boldsymbol{\theta}_1$  and  $\boldsymbol{\theta}_2$ . Condition (C4') and Theorem 10.29 of Wendland (2004) gives us

$$\begin{aligned} &\sup_{\boldsymbol{\theta} \in \Theta} \left\| \sum_{j=1}^{\infty} \frac{1}{\gamma_j} \int_{\Omega} \frac{\partial f_s(\mathbf{z}, \tilde{\boldsymbol{\theta}})}{\partial \theta_{t_1} \partial \theta_{t_2}} \phi_j(\mathbf{z}) d\mathbf{z} \cdot \phi_j(\cdot) \right\|_{\mathcal{N}_{\mathcal{K}}(\Omega)}^2 \\ &= \sup_{\boldsymbol{\theta} \in \Theta} \sum_{j=1}^{\infty} \frac{1}{\gamma_j^2 \gamma_{\Psi, j}^{\beta_1}} \left( \int_{\Omega} \frac{\partial f_s(\mathbf{z}, \tilde{\boldsymbol{\theta}})}{\partial \theta_{t_1} \partial \theta_{t_2}} \phi_j(\mathbf{z}) d\mathbf{z} \right)^2 \leq C_3 \left\| \frac{\partial f_s(\mathbf{z}, \tilde{\boldsymbol{\theta}})}{\partial \theta_{t_1} \partial \theta_{t_2}} \right\|_{W^{2m+m_2}(\Omega)} \leq C_4, \end{aligned}$$

where  $\beta_1 = \frac{m_2}{\alpha}$ , and the last inequality is by Condition (C4') and the equivalence of  $\mathcal{N}_{\alpha}^{m/\alpha}(\Omega)$  and  $\mathcal{H}_m(\Omega)$ . The Sobolev embedding theorem implies that

$$\begin{aligned} &\left\| \sum_{j=1}^{\infty} \frac{1}{\gamma_j} \int_{\Omega} \frac{\partial f_s(\mathbf{z}, \tilde{\boldsymbol{\theta}})}{\partial \theta_{t_1} \partial \theta_{t_2}} \phi_j(\mathbf{z}) d\mathbf{z} \cdot \phi_j(\cdot) \right\|_{L_2(\Omega)} \\ &\leq C_5 \left\| \sum_{j=1}^{\infty} \frac{1}{\gamma_j} \int_{\Omega} \frac{\partial f_s(\mathbf{z}, \tilde{\boldsymbol{\theta}})}{\partial \theta_{t_1} \partial \theta_{t_2}} \phi_j(\mathbf{z}) d\mathbf{z} \cdot \phi_j(\cdot) \right\|_{W^{\alpha\beta_1}(\Omega)} \leq C_6, \end{aligned}$$

which, together with (G.51) and (G.52), implies

$$\mathfrak{d}(\boldsymbol{\theta}_1, \boldsymbol{\theta}_2)^2 \leq C_7 \|\boldsymbol{\theta}_1 - \boldsymbol{\theta}_2\|_2^2.$$

Therefore, the covering number is bounded above by

$$\log N(\epsilon, \Theta, \mathfrak{d}) \leq \log N\left(\frac{\epsilon}{C_7}, \Theta, \|\cdot\|_2\right). \quad (\text{G.53})$$

The right side of (G.53) is just the covering number of a Euclidean ball, which is well understood in the literature; See Lemma 4.1 of Pollard (1990). Thus, we have

$$\log N(\epsilon, \Theta, \mathfrak{d}) \leq C_8 \log \left(1 + \frac{C_7}{\epsilon}\right).$$

Therefore, the integral in Lemma G.6 can be computed by

$$\begin{aligned} \int_0^{D/2} \sqrt{\log N(\epsilon, \Theta, \mathfrak{d})} d\epsilon &\leq \int_0^{D/2} \sqrt{C_8 \log \left(1 + \frac{C_7}{\epsilon}\right)} d\epsilon \\ &\leq \left( \int_0^{D/2} d\epsilon \right)^{1/2} \left( \int_0^{D/2} C_8 \log \left(1 + \frac{C_7}{\epsilon}\right) d\epsilon \right)^{1/2} \\ &\leq C_9 D \sqrt{\log \left(\frac{1}{D}\right)}. \end{aligned}$$



Now we can apply Lemma G.6 and obtain

$$\sup_{\boldsymbol{\theta} \in \Theta} |g(\boldsymbol{\theta})| = O_{\mathbb{P}}(n^{-\frac{1-\delta_0}{2}} \log(n)) = o_{\mathbb{P}}(n^{-1/2}).$$

Therefore, we conclude that

$$Q_1 = 2 \int_{\Omega} \left( \widehat{f}_p(\mathbf{z}) - f_p(\mathbf{z}) \right) A_{1t}(\mathbf{z}, \widehat{\boldsymbol{\theta}}_S) d\mathbf{z} + o_{\mathbb{P}}(n^{-1/2}). \quad (\text{G.54})$$

(2) Consider  $Q_3$ . By the Cauchy-Schwarz inequality,

$$|Q_3| \leq 2 \frac{\mu}{n} \left\| \widehat{f}_p(\cdot) \right\|_{\mathcal{N}_{\mathcal{K}}(\Omega)} \left\| A_{1t}(\cdot, \widehat{\boldsymbol{\theta}}_S) \right\|_{\mathcal{N}_{\mathcal{K}}(\Omega)}. \quad (\text{G.55})$$

By (G.46), we have that  $\left\| A_{1t}(\cdot, \widehat{\boldsymbol{\theta}}_S) \right\|_{\mathcal{N}_{\mathcal{K}}(\Omega)} \leq C_{10}$ . Recall that

$$\widehat{f}_p(\mathbf{x}) = \mathbf{r}_1(\mathbf{x})^T (\mathbf{R}_1 + \mu \mathbf{I}_n)^{-1} \mathbf{y}^{(p)} = \mathbf{r}_1(\mathbf{x})^T (\mathbf{R}_1 + \mu \mathbf{I}_n)^{-1} \mathbf{F} + \mathbf{r}_1(\mathbf{x})^T (\mathbf{R}_1 + \mu \mathbf{I}_n)^{-1} \boldsymbol{\varepsilon},$$

where  $\mathbf{F} = (f_p(\mathbf{x}_1), \dots, f_p(\mathbf{x}_n))^T$  and  $\boldsymbol{\varepsilon} = (\varepsilon_1, \dots, \varepsilon_n)^T$ . The term  $\left\| \widehat{f}_p(\cdot) \right\|_{\mathcal{N}_{\mathcal{K}}(\Omega)}$  can be computed by

$$\left\| \widehat{f}_p(\cdot) \right\|_{\mathcal{N}_{\mathcal{K}}(\Omega)}^2 = (\mathbf{F} + \boldsymbol{\varepsilon})^T (\mathbf{R}_1 + \mu \mathbf{I}_n)^{-1} \mathbf{R}_1 (\mathbf{R}_1 + \mu \mathbf{I}_n)^{-1} (\mathbf{F} + \boldsymbol{\varepsilon}).$$

Since both  $\mathbf{F}$  and  $\boldsymbol{\varepsilon}$  are normally distributed, the expectation can be computed by

$$\begin{aligned} \mathbb{E} \left\| \widehat{f}_p(\cdot) \right\|_{\mathcal{N}_{\mathcal{K}}(\Omega)}^2 &= \mathbb{E} \text{tr} \left( (\mathbf{R}_1 + \mu \mathbf{I}_n)^{-1} \mathbf{R}_1 (\mathbf{R}_1 + \mu \mathbf{I}_n)^{-1} (\mathbf{F} + \boldsymbol{\varepsilon})(\mathbf{F} + \boldsymbol{\varepsilon})^T \right) \\ &= \text{tr} \left( (\mathbf{R}_1 + \mu \mathbf{I}_n)^{-1} \mathbf{R}_1 \right) \leq \text{tr} \mathbf{I}_n = n, \end{aligned}$$

and the variance can be bounded by

$$\begin{aligned} \text{Var}(\left\| \widehat{f}_p(\cdot) \right\|_{\mathcal{N}_{\mathcal{K}}(\Omega)}^2) &\leq \mathbb{E} \left( (\mathbf{F} + \boldsymbol{\varepsilon})^T (\mathbf{R}_1 + \mu \mathbf{I}_n)^{-1} \mathbf{R}_1 (\mathbf{R}_1 + \mu \mathbf{I}_n)^{-1} (\mathbf{F} + \boldsymbol{\varepsilon}) \right)^2 \\ &\leq \mathbb{E} \left( (\mathbf{F} + \boldsymbol{\varepsilon})^T (\mathbf{R}_1 + \mu \mathbf{I}_n)^{-1} (\mathbf{F} + \boldsymbol{\varepsilon}) \right)^2 \\ &= \mathbb{E} \left( \sum_{j=1}^n Z_j^2 \right)^2 \leq C_{11} n^2, \end{aligned}$$

where the last equality is because  $\mathbf{F} + \boldsymbol{\varepsilon}$  are normally distributed with mean zero and covariance  $\mathbf{R}_1 + \mu \mathbf{I}_n$ , and  $Z_j$ s are i.i.d standard normally distributed random variables. Thus, Chebyshev's inequality implies that

$$\left\| \widehat{f}_p(\cdot) \right\|_{\mathcal{N}_{\mathcal{K}}(\Omega)}^2 = \mathbb{E} \left\| \widehat{f}_p(\cdot) \right\|_{\mathcal{N}_{\mathcal{K}}(\Omega)}^2 + O_{\mathbb{P}}(\sqrt{\text{Var}(\left\| \widehat{f}_p(\cdot) \right\|_{\mathcal{N}_{\mathcal{K}}(\Omega)}^2)}) = O_{\mathbb{P}}(n). \quad (\text{G.56})$$

Plugging (G.56) into (G.55) leads to

$$|Q_3| = O_{\mathbb{P}}(n^{-1} n^{1/2}) = O_{\mathbb{P}}(n^{-1/2}). \quad (\text{G.57})$$

By combining (G.43),(G.44),(G.45), (G.54) and (G.57), we obtain that

$$(\mathbf{V} + \mathbf{E})(\widehat{\boldsymbol{\theta}}_S - \boldsymbol{\theta}_S^*) + \frac{2}{n} \sum_{k=1}^n \varepsilon_k A_1(\mathbf{x}_k) = O_{\mathbb{P}}(n^{-1/2}).$$

where each element in  $\mathbf{E}$  is  $o_{\mathbb{P}}(1)$  and

$$A_1(\cdot) = \sum_{j=1}^{\infty} \frac{1}{\gamma_j} \int_{\Omega} \frac{\partial f_s(\mathbf{z}, \boldsymbol{\theta}_S^*)}{\partial \boldsymbol{\theta}} \phi_j(\mathbf{z}) d\mathbf{z} \cdot \phi_j(\cdot) = (A_{11}(\cdot, \boldsymbol{\theta}_S^*), \dots, A_{1q}(\cdot, \boldsymbol{\theta}_S^*))^T.$$

Since  $\mathbf{E}$  converges to zero in probability, we have

$$\widehat{\boldsymbol{\theta}}_S - \boldsymbol{\theta}_S^* = -2\mathbf{V}^{-1} \left( \frac{1}{n} \sum_{k=1}^n \varepsilon_k A_1(\mathbf{x}_k, \boldsymbol{\theta}_S^*) \right) + O_{\mathbb{P}}(n^{-1/2}),$$

which finishes the proof. ■

## H Experimental Details and Additional Figures

### H.1 Uncertainty Quantification Details

In this subsection, we provide experimental details of uncertainty quantification in simulation studies. The key steps of uncertainty quantification are summarized in Algorithm 1.

#### H.1.1 Computation of Sample Variance of $\widehat{\boldsymbol{\theta}}$

In order to provide confidence intervals of the estimate  $\widehat{\boldsymbol{\theta}}$  for each trial and compute the average coverage rate, we need to numerically compute the asymptotic variance of  $\widehat{\boldsymbol{\theta}}$  as given in Theorem 3.2 and Theorem 4.2 based on each sample set, which requires approximations to  $\sigma^2, \mathbf{V}$  and  $\mathbf{W}$ .

We here take Sobolev calibration as an example. The asymptotic variance of  $\widehat{\boldsymbol{\theta}}_{L_2}$  and  $\widehat{\boldsymbol{\theta}}_{KO}$  can be calculated in a similar manner. First,  $\mathbf{V}$  can be approximated by  $\mathbf{V} := -\sum_{j=1}^{\infty} \frac{1}{\gamma_j} \frac{\partial^2}{\partial \boldsymbol{\theta} \partial \boldsymbol{\theta}^T} \left( \int_{\Omega} (f_p(\mathbf{z}) - f_s(\mathbf{z}, \boldsymbol{\theta}_S^*)) \phi_j(\mathbf{z}) d\mathbf{z} \right)^2 \approx -\frac{\partial^2}{\partial \boldsymbol{\theta} \partial \boldsymbol{\theta}^T} \|\mathcal{I}_{\mathcal{K}_m, \widetilde{\mathbf{X}}} (f_p(\cdot) - f_s(\cdot, \boldsymbol{\theta}_S^*))\|_{\mathcal{H}_m(\Omega)}^2 \approx -\frac{\partial^2}{\partial \boldsymbol{\theta} \partial \boldsymbol{\theta}^T} \|\mathcal{I}_{\mathcal{K}_m, \widetilde{\mathbf{X}}} (\widehat{f}_p(\cdot) - \widehat{f}_s(\cdot, \widehat{\boldsymbol{\theta}}_S))\|_{\mathcal{H}_m(\Omega)}^2$ , where the penultimate step is introduced in Section 2.2.3. For the computation of  $\mathbf{W}$ , we need to numerically calculate the eigenvalues and eigenfunctions of Matérn kernel, which can be achieved by Nyström method (Williams and Seeger, 2000). The details of approximation error and the number of truncations  $N$  can be found in Section H.1.3. Then we calculate

$$\begin{aligned} \mathbf{W} &:= \mathbb{E}(A_1(\mathbf{x})A_1(\mathbf{x})^T) = \sum_{j=1}^{\infty} \frac{1}{\gamma_j^2} \left( \int_{\Omega} \frac{\partial f_s(\mathbf{z}, \boldsymbol{\theta}_S^*)}{\partial \boldsymbol{\theta}} \phi_j(\mathbf{z}) d\mathbf{z} \right)^2 \\ &\approx \sum_{j=1}^N \frac{1}{\widetilde{\gamma}_j^2} \left( \int_{\Omega} \frac{\partial f_s(\mathbf{z}, \boldsymbol{\theta}_S^*)}{\partial \boldsymbol{\theta}} \widetilde{\phi}_j(\mathbf{z}) d\mathbf{z} \right)^2 \approx \sum_{j=1}^N \frac{1}{\widetilde{\gamma}_j^2} \left( \int_{\Omega} \frac{\partial \widehat{f}_s(\mathbf{z}, \widehat{\boldsymbol{\theta}}_S)}{\partial \boldsymbol{\theta}} \widetilde{\phi}_j(\mathbf{z}) d\mathbf{z} \right)^2, \end{aligned}$$

---

**Algorithm 1** Uncertainty Quantification for Sobolev Calibration
 

---

**Input:** Observations  $\{(\mathbf{x}_j, y_j^{(p)})\}_{j=1}^n$ , a design  $\widetilde{\mathbf{X}}$ , estimations  $\widehat{\boldsymbol{\theta}}_S$  and  $\widehat{\sigma}^2$ , approximations  $\widetilde{\gamma}_j$ ,  $\widetilde{\phi}_j$ ,  $\widehat{f}_s$ , parameters  $m, N, l$ .

Set  $\mathbf{V} \leftarrow -\frac{\partial^2}{\partial \boldsymbol{\theta} \partial \boldsymbol{\theta}^\top} \|\mathcal{I}_{\mathcal{K}_m, \widetilde{\mathbf{X}}}(\widehat{f}_p(\cdot) - \widehat{f}_s(\cdot, \widehat{\boldsymbol{\theta}}_S))\|_{\mathcal{H}_m(\Omega)}^2$ ;

$\mathbf{W} \leftarrow \sum_{j=1}^N \frac{1}{\widetilde{\gamma}_j^2} \left( \int_{\Omega} \frac{\partial \widehat{f}_s(\mathbf{z}, \widehat{\boldsymbol{\theta}}_S)}{\partial \boldsymbol{\theta}} \widetilde{\phi}_j(\mathbf{z}) d\mathbf{z} \right)^2$ ;

$\widehat{\sigma}_S^2 \leftarrow 4\widehat{\sigma}^2 \mathbf{V}^{-1} \mathbf{W} \mathbf{V}^{-1} / n$  (see Section H.1.1 for details).

**for**  $i \leftarrow 1$  to  $l$  **do**

1.  $\widehat{f}_{s,i}(\cdot) \leftarrow \widehat{f}_s(\cdot, \widehat{\boldsymbol{\theta}}_{S,i})$ , where  $\widehat{\boldsymbol{\theta}}_{S,i}$  is generated from Gaussian distribution  $\mathcal{N}(\widehat{\boldsymbol{\theta}}_S, \widehat{\sigma}_S^2)$ .
2. Use Gaussian process to estimate  $\delta(\cdot, \widehat{\boldsymbol{\theta}}_{S,i})$  based on samples  $\{(\mathbf{x}_j, y_j^{(p)} - \widehat{f}_{s,i}(\mathbf{x}_j))\}_{j=1}^n$ , and obtain the 95% upper bound  $\bar{\delta}_i(\cdot)$  and lower bound  $\underline{\delta}_i(\cdot)$ .

**end for**

Calculate the empirical 0.975 and 0.025 quantile  $\widehat{f}_s^{0.975}(\cdot)$  and  $\widehat{f}_s^{0.025}(\cdot)$  from  $\{\widehat{f}_{s,i}(\cdot)\}_{i=1}^l$ .

Calculate the empirical 0.975 and 0.025 quantile  $\widehat{f}_p^{0.975}(\cdot)$  and  $\widehat{f}_p^{0.025}(\cdot)$  from  $\{\widehat{f}_{s,i}(\cdot) + \bar{\delta}_i(\cdot)\}_{i=1}^l$  and  $\{\widehat{f}_{s,i}(\cdot) - \underline{\delta}_i(\cdot)\}_{i=1}^l$  respectively.

**Output:**

95% Confidence interval of  $\boldsymbol{\theta}_S^*$ :  $[\widehat{\boldsymbol{\theta}}_S - 1.96 \times \widehat{\sigma}_S, \widehat{\boldsymbol{\theta}}_S + 1.96 \times \widehat{\sigma}_S]$ ;

95% Point-wise confidence band of  $f_s(\cdot, \boldsymbol{\theta}_S^*)$ :  $[\widehat{f}_s^{0.025}(\cdot), \widehat{f}_s^{0.975}(\cdot)]$ ;

95% Point-wise confidence band of  $f_p(\cdot)$ :  $[\widehat{f}_p^{0.025}(\cdot), \widehat{f}_p^{0.975}(\cdot)]$ .

---

where  $\widetilde{\phi}_j$  and  $\widetilde{\gamma}_j$  are approximated eigenfunctions and eigenvalues, respectively. For the simplicity of computation, we assume that  $\sigma^2$  and  $f_s(\cdot)$  are known. If the true variance of random noise  $\sigma^2$  is unknown, in practice, it can be estimated by collecting physical experiments at some fixed points repeatedly. Note that since Example 2 considers  $f_p(\cdot)$  as a Gaussian process, the calculation procedures of each trial are based on a random sample path of  $f_p(\cdot)$ .

### H.1.2 Computation of Point-wise Confidence Band of $f_s(\cdot, \boldsymbol{\theta}_S^*)$ and $f_p(\cdot)$

Recall that we have  $\widehat{\boldsymbol{\theta}}$  follows Gaussian distribution asymptotically. After calculating the estimated asymptotic variance, a random sample set  $\{\widehat{\boldsymbol{\theta}}_1, \dots, \widehat{\boldsymbol{\theta}}_{100}\}$  can be generated by sampling 100 times from the Gaussian distribution  $\mathcal{N}(\widehat{\boldsymbol{\theta}}, \widehat{\sigma}^2)$ . Then we can plug  $\{\widehat{\boldsymbol{\theta}}_1, \dots, \widehat{\boldsymbol{\theta}}_{100}\}$  into  $\widehat{f}_s(\cdot, \boldsymbol{\theta})$  and obtain a function set  $\{\widehat{f}_{s,1}(\cdot), \dots, \widehat{f}_{s,100}(\cdot)\}$ , from which we can find the 0.025 and 0.975 sample quantiles and obtain the confidence band.

The computation of point-wise confidence band of  $f_p(\cdot)$  is in a similar manner, but we need to estimate the function  $\delta(\cdot, \widehat{\boldsymbol{\theta}})$  based on samples  $\{(\mathbf{x}_j, y_j^{(p)} - \widehat{f}_s(\mathbf{x}_j, \widehat{\boldsymbol{\theta}}))\}_{j=1}^n$ . The estimation error can lead to the bias of confidence interval, which can have some impact especially when the original variance is small. Therefore, to guarantee the validity of confidence interval, we need to ensure the estimation of  $\widehat{\delta}(\cdot, \widehat{\boldsymbol{\theta}})$  can cover  $\delta(\cdot, \widehat{\boldsymbol{\theta}})$ . Here we adopt the Gaussian process to estimate  $\delta(\cdot, \widehat{\boldsymbol{\theta}})$  together with 95% confidence region, and use upper bound and lower bound for the computation of 0.975 sample quantile and 0.025 sample quantile separately.

### H.1.3 Approximation Errors of Eigenvalues and Eigenfunctions

In this section, we provide some implementation details of Nyström method (Williams and Seeger, 2000) and the corresponding approximation errors.

Mercer’s theorem implies that

$$\Psi_m(\mathbf{s}, \mathbf{t}) = \sum_{j=1}^{\infty} \gamma_j \phi_j(\mathbf{s}) \phi_j(\mathbf{t}), \forall \mathbf{s}, \mathbf{t} \in \Omega,$$

where  $\gamma_j$  and  $\phi_j(\cdot)$  are the eigenvalues and eigenfunctions of  $\Psi_m(\cdot, \cdot)$  respectively. We approximate the first  $N$  eigenvalues and eigenfunctions, such that

$$\Psi_m(\mathbf{s}, \mathbf{t}) \approx \sum_{j=1}^N \tilde{\gamma}_j \tilde{\phi}_j(\mathbf{s}) \tilde{\phi}_j(\mathbf{t}), \forall \mathbf{s}, \mathbf{t} \in \Omega.$$

Note that empirically  $N$  should decrease with the increase of smoothness  $m$ , because the eigendecay rate of kernel  $\Psi_m(\cdot)$  would get faster. To empirically measure the approximation error, we first choose 1,000 equally spaced points from 0 to 1, denoted as  $\{s_j, j = 1, \dots, 1,000\}$ . Then we calculate  $\sum_{j=1}^{1,000} e(s_j)/1,000$ , where  $e(s) := |\Psi_m(s, s) - \sum_{j=1}^N \tilde{\gamma}_j \tilde{\phi}_j(s) \tilde{\phi}_j(s)|$ . Table H.1 summarizes truncation points  $N$  we choose and approximation errors corresponding to the smoothness  $m$ , and we can find that the approximation error is controlled below 0.05.

**Table H.1:** *Truncation points and approximation errors*

$m$	7/8	1	9/8	9/5	2
$N$	20	12	12	5	5
<i>Error</i>	0.0466	0.0303	0.0135	0.0038	0.0020

## H.2 Gaussian Process Details

To select the best  $\mu$  in (4.3), we randomly generate a data set with 300 samples, and divide 30% of samples as the validation set. During each round, a realization of  $f_p(\cdot)$  is generated and physical observations are attained based on this realization. The corresponding Sobolev calibration parameter is defined as in (2.4), where  $\mathcal{H}_m(\Omega)$  is the RKHS generated by  $\Psi_1(x)$ .

Note that  $\theta^*$  is a random variable, since each realization of  $f_p(\cdot)$  leads to different  $\theta^*$ . Therefore, we let  $d_k^2 = (\hat{\theta}_{Sk} - \theta_k^*)^2$ , where the subscript  $k$  defines each round of experiment, and then calculate the mean and standard deviation of  $d_k^2, k = 1, \dots, 500$ , to measure the performance of different methods.

## H.3 Additional Experiments

**Example H.1.** Suppose the physical experiment is  $f_p(x) = \exp(\pi x/5) \sin 2\pi x$ , for  $x \in \Omega = [0, 1]$ . The physical observations are given by  $y_j^{(p)} = f_p(x_j) + \varepsilon_j$ , with  $x_j \sim \text{Uniform}(0,1)$ ,

$\varepsilon_j \sim N(0, \sigma_\varepsilon^2)$  for  $j = 1, \dots, 200$ . We investigate two different  $\sigma_\varepsilon^2$  ( $\sigma_\varepsilon^2 = 0.05$  and  $\sigma_\varepsilon^2 = 0.1$ ) to evaluate the robustness of different methods under different information-noise ratio.

Suppose the computer experiment is

$$f_s(x, \theta) = f_p(x) - \sqrt{\theta^2 - \theta + 1} (\sin 2\pi\theta x + \exp(\pi\theta x/2)),$$

which is imperfect since  $\sqrt{\theta^2 - \theta + 1}$  is always positive. Therefore, the computer experiment cannot perfectly match the physical experiment. For the ease of computation, we assume the computer code is *cheap*. We follow Approach 2 to select function space  $\mathcal{H}_m(\Omega)$  and  $\mathcal{H}_{m_1}(\Omega)$  as the RKHS generated by Matérn kernel  $\Psi_1(x)$  and  $\Psi_2(x)$ , respectively. Since 0 (used in  $L_2$  calibration)  $< m < m_1$  (used in the frequentist KO calibration), we intuitively interpret the frequentist KO calibration and  $L_2$  calibration as using relatively smoother and less smooth kernels compared with Sobolev calibration, respectively. The tuning parameter  $\lambda$  in (2.5) of the regularized estimator  $\widehat{f}_p(x)$  is selected by the generalized cross validation (Wahba, 1990), and  $\theta_S^*$  in the Sobolev calibration is defined as in (2.4).

Figure H.1 plots the RKHS norm of the discrepancy function with respect to  $\theta \in [-1, 1]$ . Numerical optimization shows that  $\theta_S^* \approx -0.08$ . In Figure H.1(b), we interpret  $L_2$  calibration as an overfitting result because it only considers the best approximation in function value, and this sometimes can cause the computer model “wiggling”; see Example 1 for more details. In contrast, by specifying an over-smoothed kernel, KO is more conservative and may result in an inaccurate calibrated experiment. Sobolev calibrated experiment serves as a flexible intermediate version of  $L_2$  calibration and KO calibration, achieving a trade-off between the two methods, which further allows more potential in practical use.

Table H.2 summarizes the numerical experiment result. The mean value and the standard deviation (SD) are computed over 500 random simulations for the three methods. As shown in Table H.2, Sobolev calibration is accurate in calibration parameter estimation, which empirically verifies the theoretical results. The standard deviation of Sobolev calibration is relatively small, showing that our method is stable.

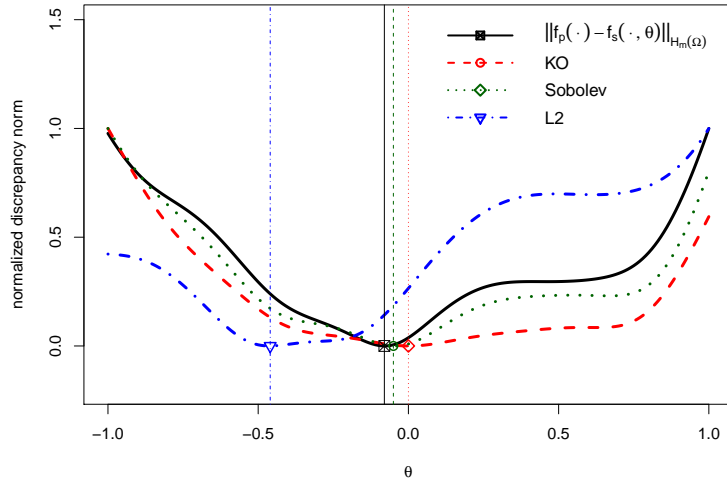
It is worth noting that the comparison of different methods is only valid on the specified settings applied to each method. Actually, since our proposed method is a generalization of other two methods, the main goal of the numerical experiment is to emphasize on the flexibility of Sobolev calibration and the merits it brings. Practitioners can select their own norm in the Sobolev calibration to reflect their preference on the function value approximation and function shape approximation.

**Table H.2:** *The mean and standard deviation (SD) of estimated calibration parameters for different methods in Example H.1, where  $\theta_S^*$  is -0.08.*

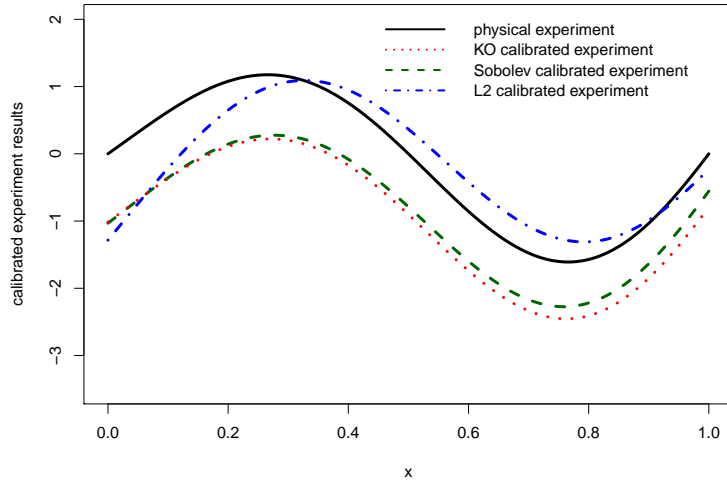
	$\sigma^2 = 0.05$		$\sigma^2 = 0.1$	
	Mean	SD	Mean	SD
Sobolev	-0.0606	0.0100	-0.0605	0.0135
$L_2$	-0.4572	0.0263	-0.4491	0.0493
KO	-0.0282	0.0178	-0.0280	0.0241

## H.4 Additional Tables and Figures in Numerical Studies

In this section, we list the figures of simulation studies owing to spatial confined. Figure H.1 is for Example H.1 in Section H.3; Figure H.2 and H.3 is for Example 1 in Section 5.1; Figure H.4 is for Example 2 in Section 5.1. Generally speaking, Figure H.1, Figure H.2 and Figure H.4 present the normalized discrepancy function and the calibrated experiment on three different settings; Figure H.3 is used for showing the flexibility of Sobolev calibration by specifying function space with different smoothness parameters. Figure H.5 is for the experiments in Section 5.1.2, which presents the calibrated computer experiments with different length-scale parameters. Figure H.6 is for the Ion Channel Example in Section 5.2.

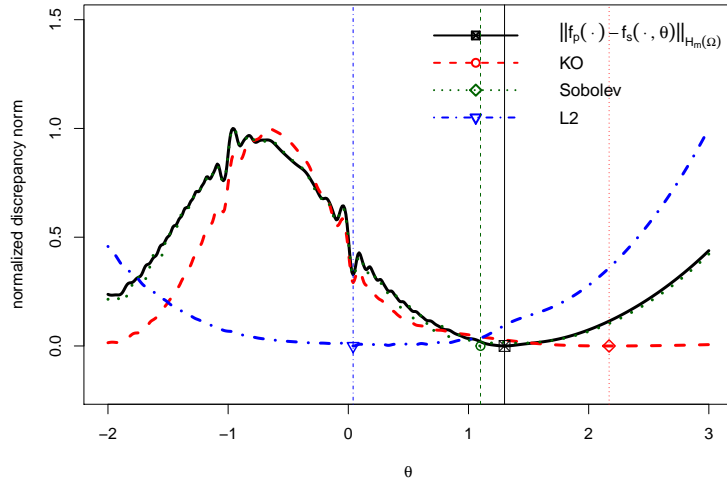


(a) Normalized model discrepancy

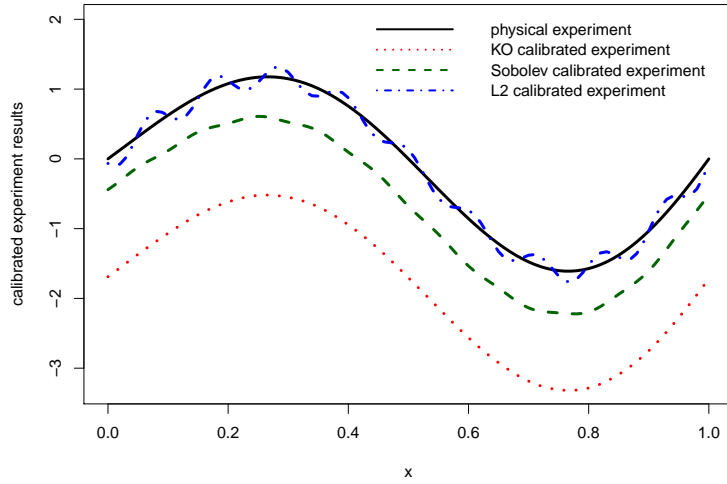


(b) Computer calibrated experiments

**Figure H.1:** Visualization of Example H.1 in the simulation studies. Panel (a) presents discrepancy measured by different normalized norms. The symbols (square, circle, triangle, etc.) together with vertical small dotted lines represent the minimizer of different norms, and the solid lines show  $\|f_p(\cdot) - f_s(\cdot, \theta)\|_{\mathcal{H}_m(\Omega)}$  and  $\theta_S^*$ . Panel (b) shows the calibrated computer models (in dotted lines) using the Sobolev calibration, the KO calibration, and the  $L_2$  calibration, respectively, together with the physical experiment (in solid line).



(a) Normalized model discrepancy



(b) Computer calibrated experiments

**Figure H.2:** Visualization of Example 1 in the simulation studies. Panel (a) presents discrepancy measured by different normalized norms. The symbols (square, circle, triangle, etc.) together with vertical small dotted lines represent the minimizer of different norms, and the solid lines show  $\|f_p(\cdot) - f_s(\cdot, \theta)\|_{\mathcal{H}_m(\Omega)}$  and  $\theta_S^*$ . Panel (b) shows the calibrated computer models (in dotted lines) using the Sobolev calibration, the KO calibration, and the  $L_2$  calibration, respectively, together with the physical experiment (in solid line).



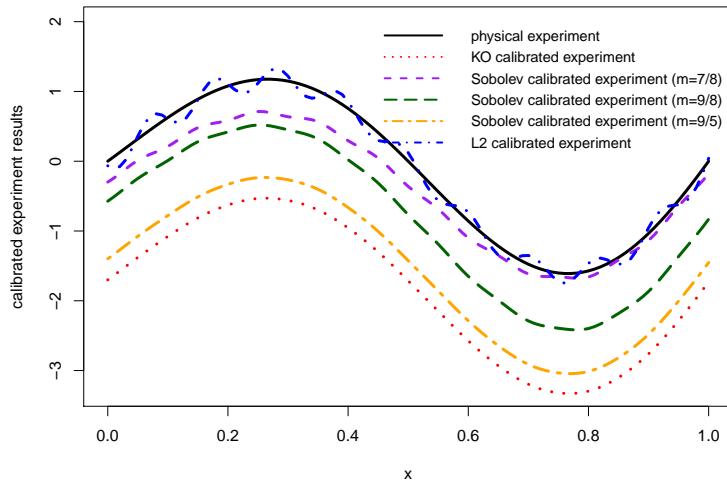
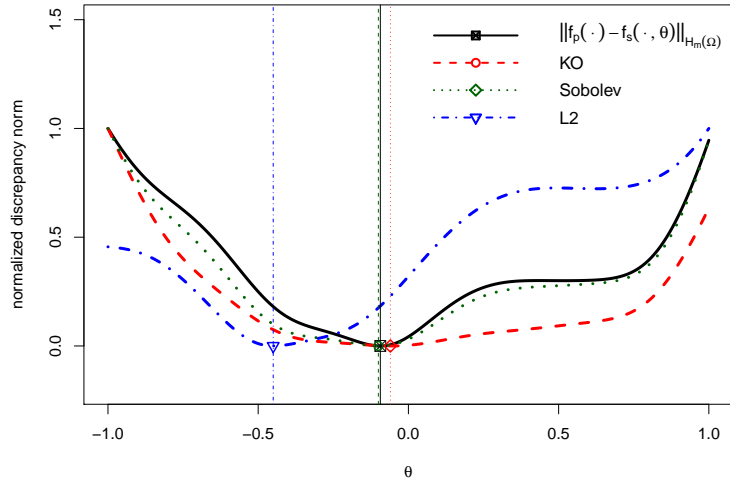
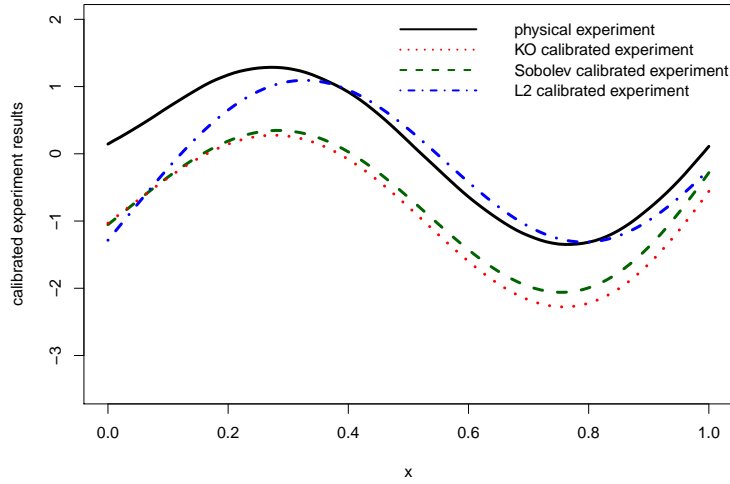


**Figure H.3:** Visualization of the calibrated computer models (in dotted lines) using the Sobolev calibration, the KO calibration, and the  $L_2$  calibration, respectively, together with the physical experiment (in solid line).



(a) Normalized model discrepancy



(b) Computer calibrated experiments

**Figure H.4:** Visualization of Example 2 in the simulation studies. Panel (a) presents one realization of discrepancy measured by different normalized norms (in dotted lines). Panel (b) shows one realization of the calibrated computer models (dotted lines) using the Sobolev calibration, the KO calibration, and the  $L_2$  calibration, respectively, and the physical experiment (solid line).

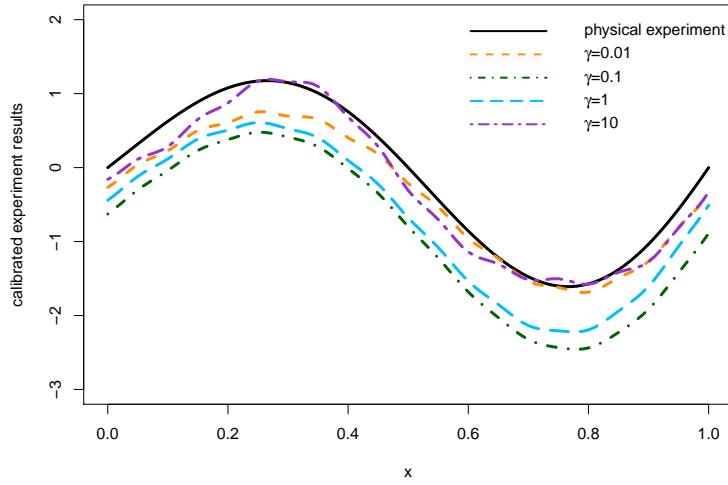


**Figure H.5:** Visualization of experiments in Section 5.1.2. The Sobolev calibration with length-scale parameters  $\gamma = 0.01, 0.1, 1, 10$  are presented in dotted lines, and the physical experiment is presented in a solid line.

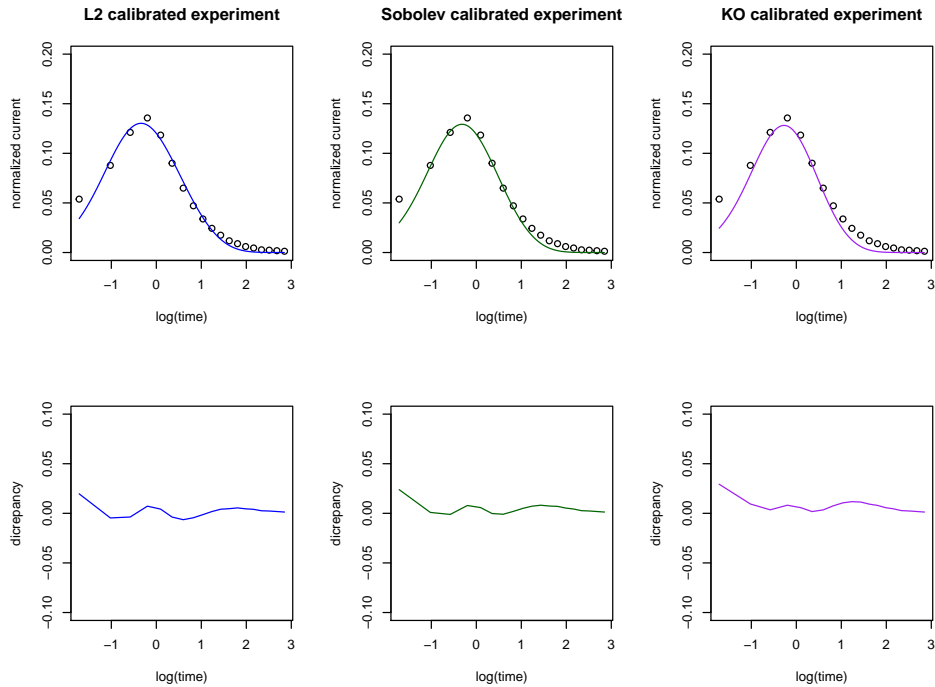


**Figure H.6:** Visualization of computer model calibration for the ion channel example. The top three panels show computer experiment with calibration parameter estimated by  $L_2$  calibration, Sobolev calibration, and KO calibration, respectively (in different colors), together with physical observations (circles); The bottom three panels show discrepancy between physical experiment and computer calibrated experiments with respect to logarithm of time.

## References

- Adams, R. A. and Fournier, J. J. (2003). *Sobolev Spaces*, volume 140. Academic Press.
- Adler, R. J. and Taylor, J. E. (2009). *Random Fields and Geometry*. Springer Science & Business Media.
- Almeida, A. and Samko, S. (2006). Characterization of Riesz and Bessel potentials on variable lebesgue spaces. *Journal of Function Spaces and Applications*, 4(2):113–144.
- Brezis, H. and Mironescu, P. (2019). Where Sobolev interacts with Gagliardo–Nirenberg. *Journal of Functional Analysis*, 277(8):2839–2864.
- Edmunds, D. E. and Triebel, H. (2008). *Function Spaces, Entropy Numbers, Differential Operators*, volume 120. Cambridge University Press.
- Fischer, S. and Steinwart, I. (2020). Sobolev norm learning rates for regularized least-squares algorithms. *Journal of Machine Learning Research*, 21:205–1.
- Gurka, P., Harjulehto, P., and Nekvinda, A. (2007). Bessel potential spaces with variable exponent. *Mathematical Inequalities and Applications*, 10(3):661.
- Kanagawa, M., Hennig, P., Sejdinovic, D., and Sriperumbudur, B. K. (2018). Gaussian processes and kernel methods: A review on connections and equivalences. *arXiv preprint arXiv:1807.02582*.
- Leoni, G. (2017). *A First Course in Sobolev Spaces*. American Mathematical Society.
- Lin, S.-B., Guo, X., and Zhou, D.-X. (2017). Distributed learning with regularized least squares. *The Journal of Machine Learning Research*, 18(1):3202–3232.
- Pollard, D. (1990). Empirical processes: theory and applications. In *NSF-CBMS Regional Conference Series in Probability and Statistics*, pages i–86. JSTOR.
- Steinwart, I. (2019). Convergence types and rates in generic Karhunen-Loève expansions with applications to sample path properties. *Potential Analysis*, 51(3):361–395.
- Steinwart, I. and Scovel, C. (2012). Mercer’s theorem on general domains: On the interaction between measures, kernels, and RKHSs. *Constructive Approximation*, 35(3):363–417.
- Tuo, R., Wang, Y., and Jeff Wu, C. (2020). On the improved rates of convergence for Matérn-type kernel ridge regression with application to calibration of computer models. *SIAM/ASA Journal on Uncertainty Quantification*, pages 1522–1547.
- Tuo, R. and Wu, C. (2014). A theoretical framework for calibration in computer models: Parametrization, estimation and convergence properties. *Technical Report*.
- Tuo, R. and Wu, C. (2015). Efficient calibration for imperfect computer. *The Annals of Statistics*, 43(6):2331–2352.
- van de Geer, S. (2000). *Empirical Processes in M-estimation*. Cambridge University Press.

- van de Geer, S. (2014). On the uniform convergence of empirical norms and inner products, with application to causal inference. *Electronic Journal of Statistics*, 8(1):543–574.
- Wang, W. (2021). On the inference of applying Gaussian process modeling to a deterministic function. *Electronic Journal of Statistics*, 15(2):5014–5066.
- Wang, W. and Jing, B.-Y. (2021). Convergence of gaussian process regression: Optimality, robustness, and relationship with kernel ridge regression. *arXiv preprint arXiv:2104.09778*.
- Wendland, H. (2004). *Scattered Data Approximation*, volume 17. Cambridge University Press.
- Williams, C. and Seeger, M. (2000). Using the nyström method to speed up kernel machines. *Advances in neural information processing systems*, 13.
- Xie, F. and Xu, Y. (2020). Bayesian projected calibration of computer models. *Journal of the American Statistical Association*, pages 1–18.